Faculdade de Engenharia da Universidade do Porto
Instituto de Ciências Biomédicas Abel Salazar

Instituto de Investigação e Inovação em Saúde

Two birds, one study: evaluating the therapeutic potential of amphibian ocellatin-PT4 and -PT9 peptides for application in leishmaniasis and neuroinflammation-related diseases

Anabela Durães de Sousa Moreira

Master's in Bioengineering

Supervisor: Alexandra Plácido, PhD
Co-supervisor: João Relvas, PhD

September 16, 2019

"Science cannot solve the ultimate mystery of nature. And that is because, in the last analysis, we ourselves are a part of the mystery that we are trying to solve."

Max Planck

Abstract

It is commonly said that the mankind will never surpass nature's ways. Despite ancient, the pursuit for therapeutic solutions in natural sources has been at the basis of the discovery of invaluable molecules that are still in use nowadays and may contribute, in the future, to the development of novel treatments where they are needed the most. Leishmaniasis, for instance, is a neglected tropical disease, for which the most effective solution is too expensive to be applied in the highly affected developing countries and the alternatives are often associated with the development of resistance mechanisms. In the spectral opposite of the world, the increase in life expectancy and consequent ageing of the population have resulted in a greater prevalence of chronic inflammatory and neurodegenerative diseases, for which effective therapies are also not available. In this scenario, the objective of the present thesis was to study two amphibian skin peptides, ocellatin-PT4 (oPT4) and ocellatin-PT9 (oPT9), to uncover i) their antileishmanial activity, and ii) their antioxidant and immunomodulatory activity in microglial cells for the potential application in neurological diseases, particularly in neuroinflammatory conditions.

Biocompatibility and haemolysis studies indicated that oPT4 and oPT9 are safe in human macrophages and erythrocytes. Mass spectrometry and circular dichroism studies, together with *in silico* analyses, revealed marked differences between the peptides in terms of amino acid composition, structure, charge, and amphipathicity, which had a direct influence on their bioactivity. oPT4 demonstrated antiparasitic activity in two distinct *Leishmania* species, which was associated to its increased positive charge and a stable amphipathic α-helix structure, two aspects that have been proven essential for membrane interaction and destabilisation. The lack of these elements in oPT9 may explain why it was devoid of any antileishmanial activity. Curiously, atomic force microscopy (AFM) studies in *Leishmania amazonensis* suggested that oPT4 probably has a complex mechanism of action, relying not only on membrane damage, but also on other toxic effects.

Conversely, in human microglia, oPT9 appears to have more interesting properties. As determined by fluorescence resonance energy transfer (FRET) microscopy, both peptides efficiently reduced the production of reactive species in lipopolysaccharide (LPS)-stimulated living microglial cells, but oPT9 had a more pronounced antioxidant effect. Moreover, only oPT9 was able to decrease microglial NF-κB pathway canonical activation after the same stimulus, which indicates that this peptide has a potential anti-inflammatory activity in microglia. How this peptide exerts such protective effects, however, is not known. Further mechanistic studies, gene and protein expression analyses, and the use of different *in vitro* models, will be required in order to disclose the mechanisms of action of oPT4 and oPT9.

Keywords: ocellatin peptides; bioprospecting; leishmaniasis; microglia; neuroinflammation

Resumo

Diz-se frequentemente que o ser humano nunca será capaz de ultrapassar as estratégias da natureza. Apesar de antiga, a procura por soluções terapêuticas em recursos naturais tem estado na base da descoberta de moléculas inestimáveis que estão ainda em uso hoje em dia e que podem contribuir, no futuro, para o desenvolvimento de novos tratamentos onde estes são mais precisos. A leishmaniose, por exemplo, é uma doença trópica negligenciada, para a qual a solução mais eficaz é demasiado dispendiosa para ser usada nos países desenvolvidos, extremamente afetados, e as alternativas estão muitas vezes associadas com o desenvolvimento de mecanismos de resistência. No extremo oposto do mundo, um aumento na esperança média de vida e o consequente envelhecimento da população resultaram numa maior prevalência de doenças crónicas inflamatórias e neurodegenerativas, para as quais terapias eficazes também não estão disponíveis. Perante este cenário, o objetivo da presente tese foi estudar dois péptidos provenientes da pele de anfíbios, ocelatina-PT4 (oPT4) e ocelatina-PT9 (oPT9), para determinar i) a sua atividade anti-parasítica em *Leishmania* e ii) o seu efeito antioxidante e imunomodulador em microglia para a potencial aplicação em doenças neurológicas, particularmente em condições neuroinflamatórias.

Estudos de biocompatibilidade e hemólise indicaram que os péptidos oPT4 e oPT9 não são tóxicos para macrófagos e eritrócitos humanos. Análises de espetrometria de massa e dicroísmo circular, juntamente com estudos *in silico*, revelaram grandes diferenças entre os dois péptidos relativamente à sua composição em aminoácidos, estrutura, carga e caráter anfipático, o que influenciou diretamente a sua bioatividade. O péptido oPT4 demonstrou atividade anti-parasítica em duas espécies de *Leishmania* distintas, o que foi atribuído à sua elevada carga positiva e a uma estrutura anfipática estável em α-hélice, dois aspetos que provaram ser essenciais para a interação com e destabilização de membranas celulares. A ausência destes elementos no péptido oPT9 poderão ser o motivo pelo qual este foi desprovido de qualquer atividade anti-parasítica. Curiosamente, estudos de microscopia de força atómica (AFM) em *Leishmania amazonensis* sugeriram que o péptido oPT4 tem um mecanismo de ação complexo, dependendo não só de danos membranares, mas também de outros efeitos tóxicos.

Em contrapartida, em células de microglia humana, o péptido oPT9 parece possuir propriedades mais interessantes. Tal como determinado por microscopia de transferência de energia de ressonância por fluorescência (FRET), ambos os péptidos reduziram a produção de espécies reativas em células vivas de microglia após estimulação com lipopolissacárido (LPS), mas o oPT9 teve um efeito antioxidante mais pronunciado. Para além disto, apenas este péptido foi capaz de diminuir a ativação canónica da via de sinalização do NF-κB após o mesmo estímulo, o que indica que poderá ter uma atividade

anti-inflamatória em microglia. Como o oPT9 exerce os referidos efeitos protetores, no entanto, não foi possível determinar. Estudos mecanísticos adicionais, análises de expressão génica e proteica e o uso de diferentes modelos *in vitro* serão necessários para revelar os mecanismos de ação dos péptidos oPT4 e oPT9.

Acknowledgements

First and foremost, I would like to thank Professor João Relvas for welcoming me into the Glial Cell Biology (GCB) research group and for his availability, support, and enthusiasm during this project.

I am very grateful to have had Dr. Alexandra Plácido, from GCB, Bio*prospectum*, and University of Porto's Faculty of Science (FCUP), as my supervisor. She was essential for the success of my thesis both at a professional level, due to her valuable scientific knowledge and guidance, and personally, because of her dedication, understanding, and support.

I also want to show my appreciation to the GCB group, particularly to Dr. Camila Portugal, Dr. Renato Socodato and Artur Rodrigues, for all their availability and assistance during this semester. They were always there when I needed help and never failed to offer me solutions for the obstacles I met, and for that I am extremely grateful.

Likewise, I want to thank Professor Ana Tomás, Maria Vieira, and Maria Inês Rocha from the Molecular Parasitology research group, for the collaboration in the parasitology studies. Their knowledge and experience in leishmaniasis, as well as their guidance during the experimental procedures, were pivotal for me to obtain the results I present herein. I further show my appreciation to Dr. Jaime Freitas, from the Microenvironments for New Therapies group, for performing the biocompatibility assays, and to Dr. Hugo Osório, from the i3S Proteomics unit, who carried the mass spectrometry analysis and was completely available to help me understand the technique and interpret the results. I also wish to acknowledge the support from i3S ALM, B_2Tech, and CCGen scientific platforms.

Moreover, I am very grateful for all the collaborations I was involved in with researchers from other institutions. Indeed, I want to thank Dr. Marcelo Bemquerer, from Embrapa Recursos e Biotecnologia (Brazil), for synthesising the peptides I worked with during this project, and to Dr. Daniel Carneiro, from NuPMIA (University of Brasília, Brazil), for performing the peptide purification and the radical-scavenging assays. I appreciate the collaboration with Dr. Peter Eaton, from FCUP, for all the precious help (and patience) during the AFM experiments and image analysis. In addition, I would like to thank Professor José Roberto Leite, for collecting human blood samples (provided by Hospital de São João) and guiding me through the haemolysis experiments. His knowledge on protein structural analysis, bioactivity of amphibian peptides, and *Leishmania* parasitology also provided invaluable insights on the work I have developed during this thesis.

Last, but not least, I want to show my appreciation to Dr. Inês Pinto and Dr. Andrea Cruz, from the International Iberian Nanotechnology Laboratory (INL), for receiving me in their lab and helping me perform the ELISA assay.

Quero agradecer à minha família, em particular os meus pais, sem os quais eu não teria chegado até aqui. Obrigada pelos sacrifícios que fizeram por mim, por me encorajarem sempre a ser persistente e corajosa, por me apoiarem incondicionalmente, e por acreditarem em mim independentemente das circunstâncias, principalmente quando eu deixo de acreditar.

À Raquel: pela lealdade inabalável com que me acompanha há tantos anos, pelo apoio indispensável em todas as más alturas, por nunca me deixar duvidar de mim própria, e por celebrar comigo as minhas vitórias como se fossem também dela. Como não podia deixar de ser, também esta minha conquista é tua. Obrigada pelos lanches, pelos litros de chá, pelas *playlists*, pelo sexto sentido que adivinha quando preciso de ajuda, enfim, por teres sido uma constante, a melhor constante, na minha vida.

Um obrigada gigante à Inês, a pessoa mais talentosa e dedicada que alguma vez conheci, pela presença e apoio constantes, pela paciência e, acima de tudo, pela amizade. Eu sei que isto é cliché, mas foste verdadeiramente o melhor que a FEUP me trouxe. Não queria ter tido mais ninguém ao meu lado durante as minhas crises depois de qualquer aula relacionada com eletricidade, nas serenatas, nas contaminações e muito menos nos passeios de reboque. Obrigada por programares sempre por mim.

Agradeço também, do fundo do meu coração, aos meus amigos de Bioengenharia, por me terem acompanhado durante todo este tempo e por terem sido uma fonte inesgotável de apoio e carinho num dos períodos mais difíceis da minha vida.

Finalmente, não posso deixar de agradecer à Dra. Beatriz Gonçalves, que me deixou uma marca indelével ao ajudar-me a reencontrar a minha motivação, a minha confiança e a minha resiliência.

Table of Contents

Table of Figures

List of Tables

List of Abbreviations

ABTS	2,2-azino-bis(3-ethylbenzothiazoline-6-sulphonic acid)
ACN	Acetonitrile
AD	Alzheimer's disease
AFM	Atomic force microscopy
AIDS	Acquired immunodeficiency syndrome
ALS	Amyotrophic lateral sclerosis
AMP	Antimicrobial peptide
Aβ	Amyloid β
BLAST	Basic local alignment search tool
BMDM	Bone marrow-derived macrophages
BZTS	4-nitrobenzaldehyde thiosemicarbazone
CC_{50}	Half maximal cytotoxic concentration
CD	Circular dichroism
CFP	Cyan fluorescent protein
CL	Cutaneous leishmaniasis
CNS	Central nervous system
DAMP	Damage-associated molecular pattern
DIC	1,3-diisopropylcarbodiimide
DMF	Dimethylformamide
DMSO	Dimethylsulfoxide
DPPH	2,2-diphenyl-1-picrylhydrazyl
ELISA	Enzyme-linked immunosorbent assay
ER	Endoplasmic reticulum
ESI	Electrospray ionisation
FA	Formaldehyde
FADH	Reduced flavin adenine nucleotide
FBSi	Heat-inactivated foetal bovine serum
FMNH	Reduced flavin mononucleotide
FRET	Fluorescence resonance energy transfer
HIV	Human immunodeficiency virus
HPLC	High performance liquid chromatography
HSP	Heat shock protein
IC_{50}	Half maximal inhibitory concentration
IFNγ	γ-interferon
IL	Interleukin
iNOS	Inducible nitric oxide synthase
IκBα	NF-κB inhibitor α
L-AMB	Liposomal amphotericin B
LC	Liquid chromatography
LCI	Live cell imaging
LPG	Lipophosphoglycan
LPS	Lipopolysaccharide
MA	Meglumine antimoniate

MBC	Minimum bactericidal concentration
MCM	Microglia-conditioned medium
MIC	Minimum inhibitory concentration
ML	Mucocutaneous leishmaniasis
MP	Maximum parsimony
MS	Mass spectrometry
MS/MS	Tandem mass spectrometry
MSA	Multiple sequence alignment
MTT	3-(4,5-dimethylthiazol-2-yl)-2,5-diphenyltetrazolium bromide
NADH	Reduced nicotinamide adenine dinucleotide
NADPH	Reduced nicotinamide adenine dinucleotide phosphate
NCBI	US National Center for Biotechnology Information
NF-κB	Nuclear factor κ-light-chain-enhancer of activated B cells
nNOS	Neuronal nitric oxide synthase
NO	Nitric oxide
NOS	Nitric oxide synthase
NTD	Neglected tropical disease
oPT1-8	Ocellatins-PT1 to -PT8
PAMP	Pathogen-associated molecular pattern
PBMC	Peripheral blood mononuclear cell
PBS	Phosphate-buffered saline
PD	Parkinson's disease
PRR	Pattern recognition receptor
PTM	Post-translational modification
RBC	Red blood cell
RNS	Reactive nitrogen species
ROS	Reactive oxygen species
RP-HPLC	Reversed-phase high performance liquid chromatography
RT	Room temperature
RT-qPCR	Reverse transcription quantitative polymerase chain reaction
SCI	Spinal cord injury
SD	Standard deviation
SEM	Scanning electron microscopy/Standard error of the mean
SSG	Sodium stibogluconate
TFE	2,2,2-trifluoroethanol
TGFβ	Transforming growth factor β
TLR	Toll-like receptor
TNF	Tumour necrosis factor
US	United States
VL	Visceral leishmaniasis
WHO	World Health Organization
YFP	Yellow fluorescent protein

Introduction

A. The Discovery of Ocellatins: Searching Nature for Answers

A.1. The concept of bioprospecting

Earth's biodiversity is astonishing. There are uncountable species of microorganisms, plants and animals, each one of them with exquisite features that make them unique. Indeed, there are a few species with capabilities that us, human beings, cannot reproduce: what makes turtles able to live for hundreds of years? How does a salamander regenerate the entirety of an amputated limb? Could we translate these phenomena into human biology?

Naturally, the answer to these questions is often very complex and hard to obtain, and there is still quite a lot of mysteries in nature that remain unsolved. However, we seem to have been looking for natural solutions since a very early stage of our history. People from past times often searched nature for products with properties of interest, like the ability of healing wounds or ameliorating a given condition. This concept of bioprospecting (see Glossary) is at the inception of several traditional medicine practices, where plant-derived substances are still widely applied as homemade remedies [1]. In fact, these people found that such organisms frequently contained a wide variety of products that could help relieve pain and improve their quality of life, without any insights on the mechanism of action of these substances [2].

Nevertheless, natural products are not used only in a traditional context, and a few examples of how exploring our surroundings may result in great discoveries can be given. Salicylic acid, commonly known as aspirin, was derived from salicin, a glycoside present in numerous plant species of the genera *Salix* and *Populus* [2]. Perhaps the most well-known (and successful) case is, however, that of penicillin. In 1928, Alexander Fleming and his secretions from the fungus *Penicillium notatum* [3] initiated what is now called "the antibiotic era", when he realized that these secretions inhibited the growth of a number of bacterial species. This fortuitous discovery was an important hallmark in the treatment of countless infections, and its consequences were so remarkable that penicillin is still broadly utilized today.

Many other examples can be further described to emphasize the potential of bioprospecting. Paclitaxel (Taxol), for instance, a well-known anticancer drug, was obtained from the *Taxus brevifolia* yew tree [4]. However, the interest in biodiversity as a source of valuable compounds has been decaying over the last years. Considering how the process of isolating and characterizing a new substance from a living organism can be complex, expensive, and time-consuming, it would be inevitable for this disinterest in natural products

to occur. Automated, artificial synthesis of small molecules has become dominant in a large portion of the pharmaceutical industry [2], and the development of computational tools related to data mining, high-throughput, and *in silico* screening methods greatly improved the search for new drug targets [5, 6]. Computational analysis revolutionised drug discovery and design, allowing the selection of lead compounds with the appropriate physicochemical properties, half-life times, target specificity, and pharmacokinetic/pharmacodynamic parameters [6].

Nonetheless, this does not mean that nature has nothing else to offer. As recently noted by R. P. Borris, «in biology, what's old is new again» [7]. A considerable fraction of the world, mainly in Asian countries (China, Japan), still makes use of natural therapies [7]. Furthermore, despite the enormous computational drug screening and testing capabilities, current scientific and pharmaceutical research has been unable to answer a number of major health issues of the twenty-first century, of which antibiotic resistance is an important example [8]. A few parasitic diseases, including malaria, filariasis, trypanomiasis, and leishmaniasis, are also in need of new therapeutic solutions [2].

Hence, perhaps it is time to look around and search for answers in our natural environment. Conveniently, performing this task nowadays is considerably easier than in the past, since we can take advantage of innovative and sensitive techniques such as high performance liquid chromatography (HPLC), mass spectrometry (MS), and tandem mass spectrometry (MS/MS) to effectively and rapidly analyse natural extracts and secretions [7]. It was precisely this principle that drove this dissertation project, as detailed in the next sections.

A.2. Amphibian skin secretions as a valuable source of active compounds

Searching for molecules with therapeutic potential in amphibians might not seem intuitive at a first glance, taking into account that bioprospecting has been carried mainly in microorganisms (bacteria, fungi), plants, and marine species [1, 7]. However, they present several characteristics that make them potential sources of a myriad of interesting compounds. This project will be focused on the products of amphibian skin secretions.

Amphibians are, in principle, very susceptible to their surrounding conditions, since they possess an exposed, permeable skin that must be kept moist for their physiological functions to occur. Being poikilotherms, their body temperature adjusts depending on the temperature of their surroundings. In addition, most of these animals typically inhabit humid territories, which are particularly adequate for the growth of potentially pathogenic microorganisms. Yet, amphibians are part of the biota of every continent on the planet (except Antarctica), meaning they can be found in all kinds of environments and conditions (Fig. 1) [9]. This capability of persisting and growing in such diverse circumstances reveals that these organisms had to adapt physiologically and morphologically, modulating their biochemical responses and

behaviour to survive in each condition [9]. Another interesting aspect about amphibians is that they are at the interface of aquatic-terrestrial habitats. In evolutionary terms, they bridge the gap between water and land [10]. What kind of adaptive responses allowed this habitat flexibility?

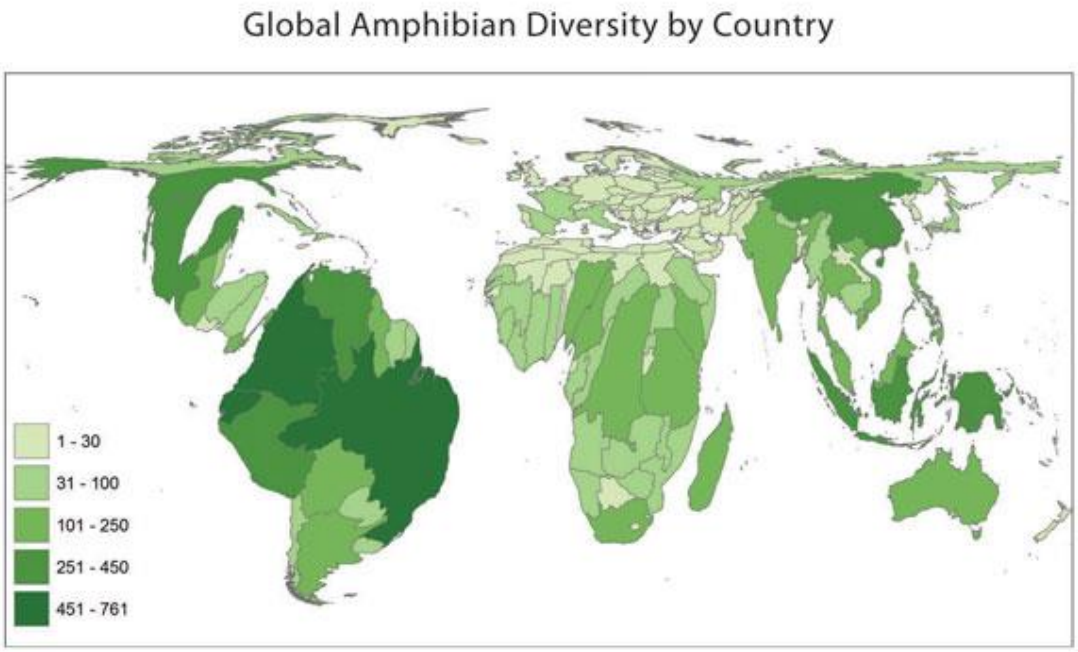

Figure 1 – Cartogram representing global amphibian distribution (data from 2013). It is possible to observe that the countries located on the north hemisphere lose relevance, while central and southern locations possess most of the world's amphibian diversity. Brazil, Colombia, and Ecuador contain the highest numbers of different species. Cartogram and information retrieved from [11].

Amphibian skin secretions play a very important role in the survival of these animals to external threats, like pathogens and predators, and they are produced in mucous or granular glands. Mucous glands mostly secrete substances that help keep amphibian skin moist, making it suitable for cutaneous respiration, protecting it from mechanical lesions, hindering water loss, and physically trapping potentially harmful microorganisms. In turn, granular glands are activated by stress or injury, releasing toxins and other active molecules that participate in defence responses [9, 12]. These active molecules are extremely versatile, ranging from biogenic amines and alkaloids to bufotoxins and peptides (oligo/polypeptides and proteins) [9]. Importantly, their versatility is not limited to their chemical nature, but it also applies to their biological effects, comprising antimicrobial, anti-diabetic, cardiotonic, immunomodulatory, and neurotoxic properties (consult references [10, 13] for extensive reviews on the subject).

In particular, peptides and proteins isolated from several amphibian species have demonstrated interesting assets (see references [10], [14] and [15] for further details). The first relevant peptide class to be discovered and fully characterised was that of magainins, isolated from the African clawed toad *Xenopus laevis* in 1987 [16, 17]. Magainins had broad-

spectrum antimicrobial activity, hampering the growth of several Gram-positive and Gram-negative bacteria, fungi, and inducing osmotic lysis in protozoa [17]. Since then, a lot of research has been directed to identifying other antimicrobial peptides (AMPs) in amphibian skin secretions. While being extremely variable in terms of amino acid composition, lacking conserved motifs that could prove essential to this antimicrobial activity, there are a few structural characteristics shared by these peptides: i) normally, they are cationic (+1 to +6 charges at a physiological pH); ii) their length varies from 8 to 48 amino acids; iii) they present a high content in hydrophobic residues; iv) they tend to form an amphipathic α-helix in membrane-mimetic conditions [14, 18-20].

Although the mechanism of action of amphibian AMPs has not been fully uncovered, it is thought to be independent of cell surface receptors, relying instead on the direct interaction with the plasma membrane and consequent cell lysis. This makes them more attractive than regular antibiotics, since it is harder for microorganisms to develop resistance pathways [19, 21, 22]. The positive net charge promotes their interaction with negatively charged membranes [23, 24], explaining why their action is often selective towards bacteria rather than zwitterionic mammalian cell membranes, and the amphipathic α-helix is essential for the process of cell lysis to occur [25, 26].

Antimicrobial activity is, however, far from being the only function of these peptides. Several other properties have been identified, and these are summarized in Table 1, together with a few examples per category. It is possible to conclude that their action is not restricted to microorganisms, since they can also target virus, tumour cells, and act as immunomodulatory, insulin-releasing, and spermicidal agents, among other effects. Thus, these peptides have a huge potential of application in a wide variety of scientific areas and health conditions, presenting themselves as truly multifunctional, versatile compounds.

Importantly, the isolation of amphibian skin peptides can be performed without sacrificing or harming the animals, which is particularly relevant in a time on Earth's history where so many species are endangered. In 1992, Tyler *et al.* [27] developed a non-invasive method based on mild transdermal electric stimulation. This procedure causes the holocrine release of the skin granular glands' content, allowing the collection of both peptides and mRNA [28]. Additionally, it is possible to extract samples from the same animals over time, because the content of the glands is replenished within a few weeks [27]. Of note, samples obtained through this method are also not contaminated with other peptides from the animal's blood or dissected skin [29]. An alternative but more invasive strategy for collecting these secretions is norepinephrine stimulation *via* injection of this hormone into the animals' dorsal lymph sacs [28, 30-32].

This dissertation project focused on two amphibian skin peptides that belong to the class of the ocellatins. These will be described in further detail in the next section.

Table 1 – Properties of amphibian skin peptides.

Property	Peptide	Species	References
Antimicrobial	Bombinin	*Bombina variegata*	[33]
	Magainins	*Xenopus laevis*	[16, 17]
	Dermaseptin	*Phyllomedusa sauvagii*	[34]
	Brevinins	*Rana brevipoda porsa*	[35]
	Ranatuerins	*Rana catesbeiana*	[36]
	Esculentins	*Rana esculenta*	[37]
Antiviral	Brevinin-1	*Rana brevipoda porsa*	[35, 38]
	Caerin 1.1	*Litorea caerulea*	[39-41]
	Caerin 1.9	*Litoria chloris*	[39, 42]
	Maculatin 1.1	*Litoria genimaculata*	[39, 43]
	Urumin	*Hydrophylax bahuvistara*	[44]
Cytotoxic/antitumoral	Magainin-2	*Xenopus laevis*	[16, 17, 45, 46]
	Dermaseptins B2 and B3	*Phyllomedusa bicolor*	[47]
	Dermaseptins PD-1 and PD-2	*Pachymedusa dacnicolor*	[48]
	Pentadactylin	*Leptodactylus labyrinthicus*	[49]
	Peptide XT-7	*Silurana tropicalis*	[50]
Spermicidal	Magainin-A	Synthetic (derived from magainin-2)	[26, 51-53]
	Dermaseptin-S4 and derivatives	Synthetic (derived from dermaseptin)	[54-56]
Immunomodulatory	Frenatins 2.1S and 2.2S	*Sphaenorhynchus lacteus*	[57]
	Tigerinin-1R	*Hoplobatrachus rugulosus*	[58, 59]
	Tigerinin-1V	*Lithobates vaillanti*	[59, 60]
	Tigerinin-1M	*Xenopus muelleri*	[59, 61]
	Plasticin-L1	*Leptodactylus laticeps*	[62, 63]
Insulinotropic	Amolopin	*Amolops loloensis*	[64]
	Hymenochirin-1B	*Hymenochirus boettgeri*	[65, 66]
	Esculentins 1 and 1B	*Rana saharica*	[67]

A.3. Amphibian ocellatin peptides: state-of-the-art

Ocellatins owe their name to the first species from which they were isolated, the South American frog *Leptodactylus ocellatus*, in 2004 [68]. Ocellatins-1, -2 and -3 were first explored as AMPs, demonstrating inhibitory activity against an *E. coli* strain and haemolytic properties in human erythrocytes. Since then, a great variety of ocellatin peptides have been isolated, characterized, and studied in several different scenarios. A summary of all ocellatins identified until the present moment can be consulted in Table 2, with the respective peptide sequences and species from which they were first obtained.

Shortly after the isolation and characterization of ocellatins-1 to -3, four other peptides were discovered and named fallaxin [69], pentadactylin [70], laticeptin [71], and syphaxin [72], after the species from which they were retrieved (*L. fallax*, *L. pentadactylus*, *L. laticeps*, and *L. syphax*, respectively). These peptides are active preferentially against Gram-negative bacteria and present low haemolytic activity in human red blood cells (RBCs). The authors hypothesized that this specific toxicity towards Gram-negative bacteria is due to the lack of peptide amphipathicity and ability to form well-structured α-helices, which are essential for the interaction with both Gram-positive bacteria and the erythrocytic membrane [73]. Of note, since these peptides presented a large similarity to the previously identified ocellatins, J. Michael Conlon (2008) [74] proposed a new nomenclature, therefore replacing the term “fallaxin” for “ocellatin-F1”, “pentadactylin” for “ocellatin-P1”, laticeptin for “ocellatin-L1”, and “syphaxin” for “ocellatin-S1”.

Following these discoveries, Nascimento *et al.* (2008) [75] identified ocellatin-4. Similarly to ocellatins-1, -2 and -3, ocellatin-4 has haemolytic activity. Its nearly neutral charge at pH 7.0 (-0.0012) probably contributes to its weak antimicrobial activity, presenting a relatively high minimum inhibitory concentration (MIC) of 64 µg/mL against *E. coli* (Gram-negative) and *Staphylococcus aureus* (Gram-positive) bacteria. Likewise, ocellatins-V1, -V2 and -V3 [76] and ocellatins-5 and -6 [77] have relatively low inhibitory activities against both these bacterial species, possibly owing to their low amphipathicity and cationicity.

Considering this information, it is clear that ocellatin peptides have mainly been explored in terms of antimicrobial potential, but it was not long until other properties were investigated. In 2009, Conlon *et al.* [62] published a study in which a novel peptide termed ocellatin-L2, which differs from ocellatin-L1 in just one amino acid position (Asn^{23} → Asp), demonstrated insulinotropic properties in rat pancreatic β-cells (BRIN-BD11 cell line) at relatively low concentrations (3 µM). Nonetheless, other studies from the same research group showed that other amphibian peptides, named phylloseptin-L2 [78], pseudin-2 [79-81], and a Lys^{18} analogue of pseudin-2 [80] were even more potent at stimulating insulin release in this cell line (see Table 1 for more examples of amphibian insulinotropic peptides).

Table 2 – Information on the sequences and species of each ocellatin peptide isolated and characterized until the present date.

Ocellatin	Sequence	C-terminal amidation	Species	Reference
1	GVVDILKGAGKDLLAHLVGKISEKV	Yes	*Leptodactylus ocellatus*	[68]
2	GVLDIFKDAAKQILAHAAEKQI			
3	GVLDILKNAAKNILAHAAEQI			
4	GLLDFVTGVGKDIFAQLIKQI			[82]
5	AVLDILKDVGKGLLSHFMEKV			[77]
6	AVLDFIKAAGKGLVTNIMEKVG			
PT1	GVFDIIKDAGKQLVAHAMGKIAEKV	Yes	*Leptodactylus pustulatus*	[83]
PT2	GVFDIIKDAGKQLVAHATGKIAEKV			
PT3	GVIDIIKGAGKDLIAHAIGKLAEKV			
PT4	GVFDIIKGAGKQLIAHAMGKIAEKV			
PT5	GVFDIIKDAGRQLVAHAMGKIAEKV			
PT6	GVFDIIKGAGKQLIAHAMEKIAEKVGLNKDGN	No		
PT7	GVFDIIKGAGKQLIAHAMGKIAEKVGLNKDGN			
PT8	GVFDIIKGAGKQLIARAMGKIAEKVGLNKDGN			
PT9	GVVDLLQGAAKDLAGH			This work
L1	GVVDILKGAAKDLAGHLATKVMNKL	Yes	*Leptodactylus laticeps*	[71]
L2	GVVDILKGAAKDLAGHLATKVMDKL			[62]
V1	GVVDILKGAGKDLLAHALSKLSEKV	Yes	*Leptodactylus validus*	[76]
V2	GVLDILKGAGKDLLAHALSKISEKV			
V3	GVLDILTGAGKDLLAHALSKLSEKV			
F1	GVVDILKGAAKDIAGHLASKVMNKL	Yes	*Leptodactylus fallax*	[69]
P1	GLLDTLKGAAKNVVGSLASKVMEKL	Yes	*Leptodactylus pentadactylus*	[70]
S1	GVLDILKGAAKDLAGHVATKVINKI	Yes	*Leptodactylus syphax*	[72]
K1	GVVDILKGAAKDLAGHLASKVMNKI	Yes	*Leptodactylus knudseni*	[84]
LB1	GVVDILKGAAKDIAGHLASKVM	Yes	*Leptodactylus labyrinthicus*	[85]
LB2	GVVDILKGAAKDIAGHLASKVMN			

Furthermore, studies performed with ocellatin-P1 (former *pentadactylin*) have shown that this peptide is cytotoxic to murine melanoma B16F10 cells in a dose-dependent manner [49], affecting cell viability, morphology, and proliferation. Alterations in membrane and DNA integrity, mitochondrial membrane potential, and the ability to arrest tumour cell cycle indicate that ocellatin-P1 causes tumour cell death by apoptosis. Presumably, its positive +3 charge at a physiological pH[1] may facilitate the interaction with the tumour cell membranes, generally more negatively charged than healthy cells [86, 87], although its mechanism of action is yet to be uncovered. Of note, the peptide +3 charge is maintained for more acidic pH values (around 6.0), characteristic of the tumour microenvironment [88-90]. Nevertheless, this is not a targeted effect, since the peptide also reduced the viability of human fibroblasts, meaning the therapeutic application of ocellatin-P1 would probably require the use of strategies to reduce cytotoxicity in healthy cells, as suggested by the authors.

Recently, two other molecules were obtained from *L. labyrinthicus* and named ocellatins-LB1 and -LB2 [85]. Their antimicrobial potential was compared to that of ocellatin-F1 in various species, including Gram-negative (*E. coli*, *Aggregatibacter actinomycetemcomitans*) and Gram-positive (*S. aureus*, *Streptococcus sanguinis*) bacteria, as well as two *Candida* species (*C. albicans* and *C. lusitaneae*). Both ocellatins-LB1 and -LB2 had weak antimicrobial activity, although ocellatin-LB1 was more potent than -LB2. In turn, ocellatin-F1 had the strongest antimicrobial effect against *A. actinomycetemcomitans*, *S. aureus*, and *C. lusitaneae*. None of the three peptides was, however, active against *S. sanguinis*.

One could find intriguing the fact that almost all the peptides described so far have such weak antimicrobial properties, questioning whether they really play a role as a host-defence mechanism. There are several hypotheses that have been proposed to explain these results. Conlon [91] suggested that these peptides may not have stronger antimicrobial action due to the symbiotic microorganisms that inhabit the amphibian skin, allowing their permanence and survival in that environment. Another possibility was raised by Leite *et al*. [77], who proposed that such peptides may act synergistically, potentiating their individual effects as a whole in the amphibian skin.

In 2015, Marani *et al.* [83] isolated eight brand-new ocellatin peptides from the frog *Leptodactylus pustulatus* (Fig. 2), which were named **ocellatins-PT1 to -PT8** (oPT1 to oPT8). All the peptides showed no toxicity towards human erythrocytes nor murine NIH-3T3 fibroblasts, but, excluding oPT2, they were all active against *E. coli*, although with relatively low potency. The most effective peptides were oPT4, oPT7, and oPT8, with a MIC of 200 µg/mL. These three compounds also inhibited the growth of *S. choleraesuis*, with a MIC of

[1] This prediction was performed using PepCalc.com online software.

800 µg/mL. oPT4 and oPT8 demonstrated inhibitory activity for *K. pneumoniae*, while oPT7 and oPT8 were active against *S. aureus*, all with a MIC of 800 µg/mL.

Figure 2 – Male, adult specimen of the frog *Leptodactylus pustulatus*. Photo credits: J. R. Leite.

Nevertheless, it is possible to conclude that none of these peptides is very potent as an antibacterial agent, despite showing bacterial growth inhibitory activity when present in high concentrations. The authors attribute the variations in antibacterial action between the peptides to differences in their amino acid composition and peptide structure. Concerning Gram-negative bacteria, oPT4, oPT7, and oPT8 probably have a more pronounced effect due to an increased positive charge and isoelectric point, both of which facilitate the interaction with the negatively charged lipopolysaccharide (LPS) from these bacterial cell membranes. As mentioned earlier, the mechanism of action in Gram-positive bacteria (such as *S. aureus*) needs to rely on more than their surface charge, implying that oPT7 and oPT8 possibly have amphipathic, helix-forming properties that are not characteristic of the other ocellatins from this class.

Ocellatins-PT2 to -PT6 were also investigated in terms of antibacterial potential in *Pseudomonas aeruginosa* [92]. In this case, the most promising peptide was oPT3. Interestingly, oPT3 was active against several strains of this bacterium, but it had higher potency against multidrug-resistant strains. Furthermore, it acted synergistically with ceftazidime and ciprofloxacin, two antibiotics commonly used to treat infections with *P. aeruginosa*, also in multidrug-resistant strains. The authors theorised that oPT3 may increase the bacterial cell membrane permeability, facilitating the uptake of the antibiotics and, thus, potentiating their action. Moreover, oPT3 had deleterious effects on 48h mature *P. aeruginosa* biofilms, decreasing their metabolic activity and promoting a modest disaggregation.

Importantly, ocellatins-PT have not only been tested in prokaryotic cells, but their antimicrobial activity was also assessed in eukaryotic models, namely *Leishmania infantum* parasites. This will be explored in **section B.1.3**.

B. Unlocking the Potential of Ocellatin Peptides

B.1. Leishmaniasis: a neglected tropical disease

Leishmaniasis is a parasitic, vector-borne disease caused by more than 20 species of the genus *Leishmania*. It is transmitted to mammals by infected female sand-flies from the genera *Phlebotomus* in the old world (Europe, Asia, Africa) and *Lutzomyia* in the new world (America) [93]. Hence, leishmaniasis can be found all over the planet except in Australia, Antarctica, and the Pacific Islands [94], and it has three main kinds of clinical manifestation: cutaneous leishmaniasis (CL), mucocutaneous leishmaniasis (ML), and visceral leishmaniasis (VL), where the latter is the most severe form of the disease and can be fatal when untreated [95]. Furthermore, depending on the parasite species, a few CL cases evolve to more aggressive lesions and symptoms, resulting in disseminated leishmaniasis, diffused leishmaniasis, or leishmaniasis recidivans [96].

Importantly, the World Health Organization (WHO) has considered leishmaniasis a neglected tropical disease (NTD), together with 19 other maladies, including leprosy, trypanosomiasis, and schistosomiasis. NTDs affect over one billion people and represent a huge burden in the economy of developing countries, which have a higher incidence of these pathologies [97]. According to the WHO, in 2017, 94% of the newly reported cases were located in only seven countries: Brazil, Ethiopia, India, Kenya, Somalia, South Sudan, and Sudan [98]. For this reason, it has been proven difficult to gather precise epidemiological data on leishmaniasis [94]. Nevertheless, it is estimated that about 700 000 to 1 million new cases and 26 000 to 65 000 deaths occur every year [95], making leishmaniasis one of the leading causes of death by a parasitic disease, second only to malaria [94]. Poor housing and hygiene conditions, the lack of financial resources, and a fragile immune system are important risk factors for the development of leishmaniasis [95].

Additionally, there are several factors that may contribute to spread the disease to other areas of the world, including not only environmental aspects like climate change, deforestation, and urbanisation, but also traveling, military operations, and immigration from endemic countries [94, 99].

B.1.1. Etiopathology

Leishmaniasis is considered predominantly zoonotic, having parasite reservoirs in a great variety of mammalian hosts, including rodents and canines. However, anthroponotic transmission can also occur, namely with *Leishmania donovani* and *L. tropica* species [94, 96]. In general, the transmission of *Leishmania* parasites to mammalian hosts occurs *via* the bite of infected female sand-flies, which release these microorganisms in a promastigote (flagellated) form (Fig. 3). The promastigotes are phagocytosed by immune cells, such as

neutrophils, macrophages, and dendritic cells, where they lose their flagella and become amastigotes. The amastigotes multiply by binary fission and are then able to infect other cells in different regions of the body. When a new sand-fly takes a blood meal from an infected individual, it ingests the amastigotes, and these migrate to the proboscis of the fly and become ready to reinitiate the cycle [94]. Of note, transmission of *Leishmania* parasites can also be carried through blood transfusions [100] and organ transplants [101, 102], the use of infected needles by patients co-infected with the human immunodeficiency virus (HIV) [103], laboratory incidents [104], and congenitally [105], although these occurrences are relatively rare.

B.1.2. Leishmaniasis clinical presentations and treatment

The clinical manifestations of leishmaniasis are highly variable, ranging from asymptomatic to fatal outcomes [94]. This highly depends on the species of the infecting parasite and on the vector, but also on individual characteristics like the host's age, immune defences, nutritional status, and genetic background [106-108]. Comprehensive reviews on the different types of leishmaniasis caused by *Leishmania* spp. can be found in the references [96, 109, 110]. The present work will focus on VL and CL.

Visceral leishmaniasis

VL, also known as kala-azar leishmaniasis, is the deadliest form of this disease. Because it does not result in external symptoms (for example, skin or mucosal lesions) like other types of leishmaniasis, VL is often more difficult to diagnose and treat [111]. VL can be caused by *L. donovani* and *L. infantum* (synonym of *L. chagasi*) infections. While *L. donovani* primarily infects humans, being transmitted among them *via* the sand-fly vectors, the main reservoir of *L. infantum* are domestic dogs [112]; hence, the transmission of *L. infantum* parasites is mainly zoonotic.

Of note, immunocompetent carriers of these parasites generally do not manifest the disease. VL is mainly an opportunistic pathology that appears in immunocompromised or immunosuppressed individuals [113, 114], explaining why this disease is often found in patients infected with HIV. HIV and *Leishmania* co-infections have been reported in Europe (Portugal, Spain, France, Italy), Africa, and Latin America, mainly in Brazil [93, 115]. Importantly, both *Leishmania* parasites and HIV infect cells from the monocytic lineage, which allows them to interact and potentiate each other's pathogenic effects. As a consequence, HIV infection increases the chances of developing leishmaniasis from 100 to 2300 times, and VL also aggravates the effects of HIV [115, 116]. Non-HIV immunosuppressed patients, such as those under chemotherapy or immunosuppressants, are also at a higher risk of developing clinical VL [114].

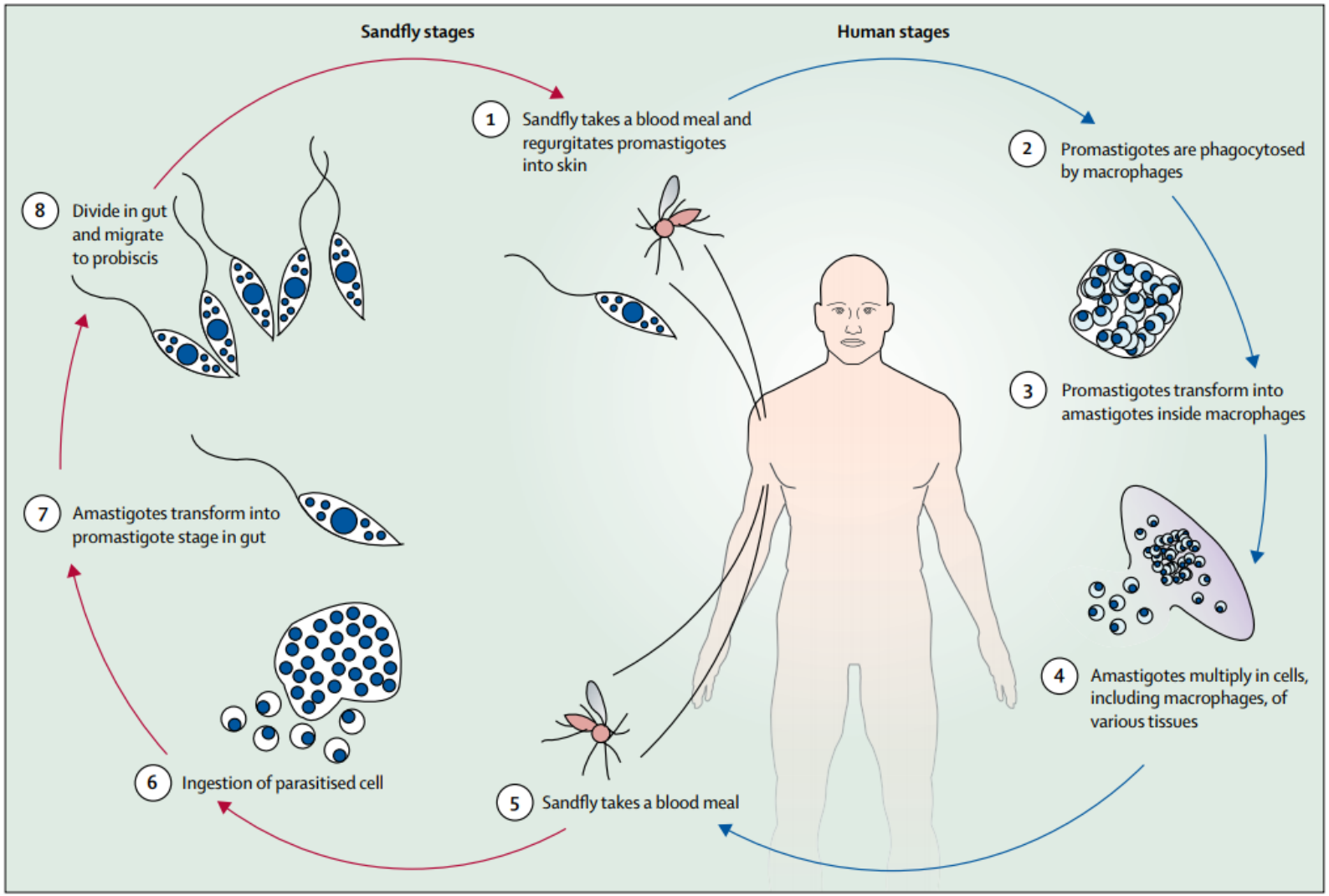

Figure 3 – Lifecycle of *Leishmania* parasites. Retrieved from [96].

VL symptoms are variable, but normally include persistent fever, abdominal pain, vomiting, diarrhoea, and anaemia. When the disease progresses for at least a few weeks, it is also possible to observe weight loss and splenomegaly. Ultimately, when untreated, VL is fatal, frequently due to secondary bacterial infections, severe anaemia, or haemorrhages. VL can also result in post kala-azar dermal leishmaniasis, characterised by skin lesions that range from mild to severe [96, 117].

Treatment

Since leishmaniasis affects mostly developing countries, often characterised by extreme poverty, not many treatment options have yet been provided by pharmaceutical companies, for which the economic return on developing such therapies is very low [118]. As a consequence, current treatment of VL relies on mainly four different options: liposomal amphotericin B (L-AMB), pentavalent antimonial drugs (namely sodium stibogluconate (SSG) and meglumine antimoniate (MA)), miltefosine, and paromomycin [93]. Due to its high effectiveness and safety, L-AMB is used as a first-line therapy in regions where treatment is not cost-limited, namely Southern Europe [119]. It is also the only drug approved by the United States (US) Food and Drug Administration (FDA) for VL treatment [93]. In most countries affected by this illness, however, antimonial drugs have been the standard treatment. Alas, these are far from ideal, since the treatment is longstanding, painful, and frequently associated with high rates of toxicity and development of resistance [119-122].

Miltefosine, a phosphocholine analogue, is the only drug for the treatment of leishmaniasis that is administered orally. It was shown to be more effective than injectable antimonial drugs in clinical trials and subsequently approved for the treatment of both VL and CL. In spite of this, greater costs than those anticipated made it unaffordable for most people living with this disease, limiting their access to alternative therapies [118]. In addition, it was found that miltefosine is embryo- and fetotoxic [123], precluding its use by pregnant women; it is also associated with severe side effects [124] and a few concerns regarding its efficiency rate have been raised as well, mostly in children [125].

Lastly, bioprospecting allowed the identification and isolation of paromomycin, an aminoglycoside broad-spectrum antibiotic derived from *Streptomyces* spp. [119]. Paromomycin is usually administered concomitantly with SSG in a combined therapy approach, which is more effective than treatment with the antimonial drug or the antibiotic alone [126-128]. This antibiotic is relatively safe and affordable, but it should be used consciously in order to avoid the development of resistance mechanisms [119].

Cutaneous leishmaniasis

Although they are not as life-threatening as VL, both CL and ML are very limiting forms of leishmaniasis, since they are associated with disfiguring, often painful skin and mucosal

lesions [94]. The extension of these lesions is greatly dependent on the *Leishmania* infecting species. Normally, multiple wounds result from different bites and no systemic effects are observable [96], but a lymphatic spread of the infection can occur [129].

Generally, such lesions start as a papule that progresses over time (weeks to months) to an ulcerating nodule. In many cases, like those resulting from *L. tropica* and *L. major* infections, these wounds are self-healing, but they result in permanent scars that lead to the stigmatisation of the individuals suffering from this pathology [96, 130]. Infection by other species, like *L. aethiopica*, *L. braziliensis,* and *L. guyanensis*, originates more severe lesions that can evolve to ML. Likewise, *L. amazonensis* and *L. mexicana* are not only able to cause CL, but also diffused and disseminated CL.

Of note, *Leishmania* parasites may persist in these wounds even after treatment and cicatrisation, potentially causing a disease relapse during a period of immunosuppression [94].

Treatment

A great part of CL lesions will self-heal in a period of 2-15 months [131]. Ergo, the application of a certain treatment will be prompted by the need of accelerating healing or minimising scarring and avoiding potential dissemination through the lymphatic nodes or progression to ML. Additionally, patients can be treated when they show multiple or large lesions, or when the wounds are located in sensitive areas like the face or joints [96].

Therapeutic strategies are different for simple and complex CL, a nomenclature used to distinguish the CL cases that cannot evolve to ML from those that can, respectively. Accordingly, in simple, non-self-healing CL, treatments should normally be local, while complex CL requires a systemic approach [132]. In general, CL local treatment resorts to intralesional antimonial injections, thermotherapy, cryotherapy, or topical treatments with paromomycin. Combined therapies with SSG or MA injections and cryotherapy were proven more effective than either in monotherapy [133-135]. Regarding CL systemic therapies, the approaches are similar to those used to treat VL. Systemic administration of antimonial drugs [136] and miltefosine [137], for instance, are effective against CL, and studies indicate that L-AMB may also be adequate for the treatment of this disease [138-140].

B.1.3. The need for new therapies: where do ocellatin-PT peptides fit in?

There has not been any major development concerning novel antileishmanial treatments for over a decade. Strategies regarding the already existing molecules, like different lipid formulations of amphotericin B and combined therapies, provide alternatives that, despite having increased safety and efficacy, are still far from ideal. Intravenous infusions, used for L-AMB and antimonial drugs [93], are not only time-consuming and uncomfortable, but they also require medical care facilities that can accommodate patients regularly and for long

periods of time. Unfortunately, such facilities are most commonly not available in developing countries, adding in another difficulty to the already costly treatments (the cost of L-AMB, for instance, is referred to throughout the literature as “prohibitively expensive”). Although miltefosine can be administered orally, the development of parasite resistance and the associated high costs forced its use mainly in combined therapy with other drugs [96, 118, 141], defeating this purpose. The remaining treatment options are also associated with resistance mechanisms and loss of effectiveness over time, often culminating in refractory disease. It is, therefore, imperative to work on new solutions for leishmaniasis.

Preventing disease spreading and limiting the number of cases is pivotal too. Using bed-nets drenched in insecticide and appropriate insect-repellents and clothing, for example, may hinder transmission of the parasites through the sand-fly vectors [142, 143]. Minimising the infection of domestic animals, namely dogs, would also help decrease parasite transmission [144].

Ocellatins-PT as antileishmanial peptides

A large number of AMPs obtained from insects, plants, amphibians, and mammals have already demonstrated antileishmanial potential, as reviewed in [145] and [146]. Interestingly, this antimicrobial activity is not limited to *Leishmania*, since a few AMPs were toxic against other protozoa, including *Trypanosoma* and *Plasmodium* spp. Recently, ocellatin-PT peptides were tested in *L. infantum* parasites, both in promastigote and axenic amastigote forms [147]. In general, all of them were active against *L. infantum* promastigotes, apart from oPT2. The most effective peptide, in this case, was oPT4, with a half maximal inhibitory concentration (IC_{50}) of 9.8 µM. In addition, oPT4 and oPT6 had an inhibitory activity against the axenic amastigotes of this parasite, with IC_{50} values of 28.9 and 19.8 µM, respectively. This demonstrates the leishmanicidal potential of ocellatins-PT, although further tests in other *Leishmania* species will clarify whether this is a broad-spectrum inhibitory activity or species-specific. Moreover, biocompatibility tests in other cell types and, naturally, *in vivo* tests will be important to truly determine if ocellatins-PT can be applied as an antileishmanial therapy. A few of these answers have already been answered during this project, as detailed in **section C**.

B.2. Inflammation in homeostasis and disease of the central nervous system

B.2.1. Inflammation as a homeostatic restorative response

The notion of homeostasis emerged in the second half of the 19th century, when Claude Bernard proposed that our cells constantly respond towards maintaining the uniformity of their internal environment (*milieu intérieur*) [148]. The term *homeostasis*, however, was only

created in the 20th century by Walter Cannon [149], who affirmed that all physiological variables are kept within a well-defined range [150]. This need of maintaining internal constancy and stability independently of external factors governs all our biological processes, in a dynamic equilibrium that preserves the integrity and well-functioning of all living beings.

Importantly, our body is capable of sensing external and internal variations that may interfere with this homeostatic state. Such biological sensors include endocrine cells and sensory neurons (mainly nociceptors), which detect systemic alterations like body temperature, blood pressure, osmolarity, and concentrations of O_2 and CO_2. In terms of intracellular homeostasis, there are signalling proteins capable of recognising inappropriate protein folding, production of reactive oxygen species (ROS), and nutrient distribution [151]. Naturally, one of the most important sensors of deleterious insults and changes in the human body is our immune system. Tissue-resident macrophages and mast cells, for instance, also act as biological sensors, identifying threats like pathogenic agents, toxins, and xenobiotics. This recognition of noxious substances or microorganisms can be performed either directly, using pattern recognition receptors (PRRs) present at the cell surface, or indirectly, due to toxic effects like cell death and tissue damage [152]. Inevitably, it is usually followed by the cascade of events that characterises an inflammatory response: briefly, there is a release of pro-inflammatory cytokines (tumour necrosis factor α (TNFα), interleukin (IL)-1β, IL-6) and chemokines (CCL2, CXCL8) that act as signals in the surrounding tissue, promoting the activation of immune cells, with the migration of leukocytes (e.g. neutrophils) and leakage of plasma into the site of injury. Depending on the proportions of this inflammatory response, systemic reactions may also occur, with the release of C-reactive protein, prostaglandins, and other pro-inflammatory stimuli [152]. Remarkably, the ultimate goal of all these players is to eradicate the threat, repair tissue damage, and return the organism back to its homeostatic state.

B.2.2. The double-edged sword of inflammation: when the cure becomes the disease

Curiously, inflammation seems to be comparable to a double-edged sword: while it is crucial to fight infections and re-establish tissue integrity after an injury, it can be highly detrimental when it becomes chronic. In fact, chronic inflammation underlies a very wide range of pathologies, including diabetes, cancer, atherosclerosis, and pulmonary diseases, affecting millions of people worldwide [153].

A very substantial field that is intimately related with chronic inflammation is that of neurodegenerative diseases. Alzheimer's disease (AD), Parkinson's disease (PD), and multiple sclerosis, despite the differences between their onset mechanisms, are all characterised by a persistent immune activation that results in neuroinflammation. Glial cells, mainly microglia, are major contributors for this inflammatory response in the central

nervous system (CNS) [154]. Accordingly, microglial cells will be one of the focus of the present work.

Microglial actions during CNS homeostasis and pathogenesis

For a long time, research on brain disease, particularly on neurodegeneration, has been "neurocentric", focusing essentially on neuronal damage and neurological defects [155]. However, growing evidence indicates that glial cells – astrocytes, microglia, and oligodendrocytes – play fundamental roles not only in maintaining brain homeostasis, but also in the pathogenesis of several diseases. As a matter of fact, and contrarily to the old belief that these cells were merely "brain glue" (hence the Greek-derived word *glia*), they are becoming established as a key component of the brain, even though their participation in both the maintenance of normal cerebral function and neurological diseases is still not very well characterised [156].

Microglia, in particular, are the cerebral resident macrophages and, thus, an important immune component of the CNS [157]. They represent up to 10% of the total number of glial cells in the adult brain, and they are originated very early in development from myeloid precursors in the yolk sac [158-160]. Their role, however, comprises way more than immune defence responses; indeed, these cells are extremely versatile and multifunctional. Importantly, even though they share many features with peripheral macrophages, microglial cells acquire distinct properties that give them a unique identity [158, 160, 161].

Microglia are responsible for a wide variety of functions in the CNS (Fig. 4), including communication with other cells (namely astrocytes and neurons), specific elimination of synapses (synaptic stripping or pruning), phagocytosis, and the secretion of molecules like cytokines, chemokines, growth factors, ROS, and reactive nitrogen species (RNS) [157, 162, 163]. Under pathological circumstances, microglia clear cell debris and phagocyte dead or compromised cells, participating in repair and reorganization processes that occur after an insult has taken place [164, 165]. Considering this broad range of physiological functions, it should not be surprising that microglial cells are associated with virtually all CNS pathologies [163].

Microglia phenotypic plasticity

Traditionally, it is said that two main states can be adopted by microglial cells. When in a "resting" state, microglia have a small cell body and are extensively ramified, using these motile cellular processes to scan the surrounding environment and functioning as brain surveillants [166]. When a threatening factor is detected, these cells become "activated", and their cell shape is altered – they assume a more amoeboid form, with a larger soma. This phenotype is not only capable of performing phagocytosis, but also of releasing immune mediators and other kinds of signalling molecules [157, 163]. In recent years, however,

microglial phenotypic characteristics have been proven to be a lot more complex than the simple dichotomy of a “resting” versus an “activated” state [167], and this terminology is increasingly being abandoned by the scientific community. In fact, microglia are never truly “resting”, since even under homeostatic conditions they are highly active and responsible for a great number of functions, as mentioned above. Thus, as proposed by Burda and Sofroniew [168], the term “reactive” will be used to distinguish healthy, homeostatic microglial activation from the response of these cells to infection or injury.

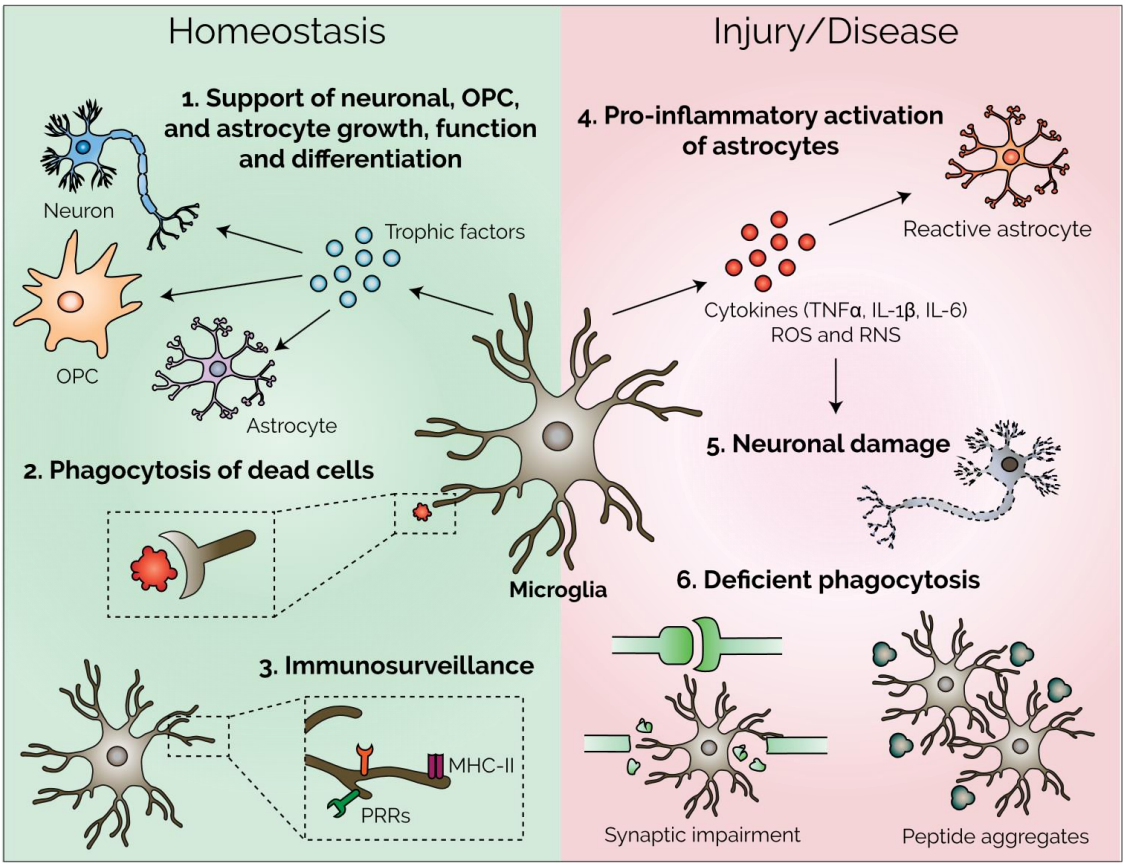

Figure 4 – Microglial functions and responses in central nervous system (CNS) homeostasis and disease (based on [160, 169]). **1.** Under homeostatic conditions, microglial cells secrete several trophic factors that support the correct function and growth of other cell types, including neurons, astrocytes, and oligodendrocyte progenitor cells (OPCs). **2.** Microglia are also capable of phagocytosis, participating in the removal of compromised cells or cell debris. **3.** Microglial cells are responsible for CNS immunosurveillance. To this end, they express pattern recognition receptors (PRRs) for the detection of potential insults (*e.g.* intracellular products indicative of cell damage, bacterial or viral components) and molecules of the class II major histocompatibility complex (MHC-II), which allow them to function as antigen-presenting cells. **4.** Upon injury or during disease pathogenesis, there is a reactive gliosis characterised by the constant pro-inflammatory activation of glial cells. Microglia secrete cytokines, chemokines, and reactive species, which activate astrocytes, and this sustained pro-inflammatory environment causes neuronal damage (**5**). **6.** In many pathological conditions, the phagocytic activity of microglia is also dysregulated, resulting in deleterious responses that lead to the elimination of synapses and accumulation of peptide aggregates that underlie numerous neurological diseases.

In accordance to this binary approach, two main opposite phenotypes have been typically described for macrophages and microglial cells: the M1 and M2 phenotypes (classically and alternatively activated phenotypes, respectively) [170]. M1 microglia were considered pro-inflammatory and characterised by the release of cytokines like IL-1β, IL-6, and TNFα, chemokines like CCL2, and the expression of enzymes related to the production of ROS and RNS (NADPH oxidase, nitric oxide synthase (NOS)) [167, 171], creating an overall inflammatory milieu. On the opposite direction were the anti-inflammatory M2 microglia, capable of secreting cytokines like IL-10 and transforming growth factor β (TGFβ), growth factors, among other mediators that are associated with tissue repair and healing [157, 171].

This characterization, however, was mostly done in *in vitro* systems that do not replicate the much more complex environment that surrounds macrophages and microglia within a living organism. Nowadays, it is thought that these cells can assume phenotypes situated anywhere between both the described extremes, often having simultaneous expression of markers that belong to the M1 and the M2 types. This strongly depends on the microenvironment and the external factors detected and processed by the cells [157, 171].

Microglia in neuroinflammation and neurological diseases

Microglial inflammatory responses can be triggered due to infection or sterile tissue damage. Microglia express at their surfaces PRRs, which are able to sense either pathogen- or damage-associated molecular patterns (PAMPs or DAMPs, respectively) [172]. Some of these PRRs include Toll-like receptors (TLRs), the mannose receptor CD206, C-type lectins, and scavenger receptors, which are then able to recognize both substances coming from compromised cells (DAMPs, like intracellular proteins and nucleic acids) and pathogen-linked compounds (PAMPs, like LPS or viral components) [173, 174]. Upon detection of such insults, microglia suffer alterations in gene and protein expression, due to the activation of signalling pathways that result in the production of pro-inflammatory cytokines and chemokines, initiating an adequate inflammatory response [175]. A classic example of such a signalling pathway is that of the nuclear factor κ-light-chain-enhancer of activated B cells (NF-κB) family, which not only controls the expression of pro-inflammatory mediators, but is also involved in cell survival, proliferation, and differentiation [176]. In addition, microglial cells undergo cytoskeletal rearrangements that facilitate their migration towards the site of injury and improve their phagocytic capability [174, 177].

Notwithstanding, although acute microglial reactivity and inflammatory responses are fundamental to recover homeostasis in the presence of a certain threat, chronic neuroinflammation compromises the integrity of the CNS by causing cell damage, oxidative stress and, hence, neurotoxicity [172]. The features of this toxic neuroinflammation include sustained activation of glial cells (reactive gliosis), with the constant production of

inflammatory cytokines and chemokines, loss of integrity and leakage of the blood-brain barrier, infiltration of peripheral immune cells, and oedema, to name just a few [175].

The substantial role of microglial cells in CNS pathogenesis becomes, perhaps, more evident when we realise how they are involved in such a wide variety of diseases (for a comprehensive review, see [178]). In AD, microglia are able to degrade amyloid β (Aβ) peptides, not only by means of internalization and phagocytosis, but also through the release of proteolytic enzymes that locally degrade these aggregates [171]. However, there is a constant pathological activation of these cells that causes the release of neurotoxic mediators like cytokines, chemokines, and ROS/RNS, hence contributing for the aggravation of the disease [178-180]. Similarly, in PD, the release of pathological α-synuclein activates microglia towards the production of IL-1β, IL-6, TNFα, γ-interferon (IFNγ), inducible NOS (iNOS), and ROS [181]. Still in the field of neurodegeneration, reactive microglia also play a detrimental role in multiple sclerosis and amyotrophic lateral sclerosis (ALS). Likewise, they are important players in modulating the disease progression of mechanical CNS damage, like that involved in spinal cord injury (SCI) and traumatic brain injury [178].

Interestingly, neuroinflammation has not only been implicated in physical CNS damage, but also in psychiatric disorders. Relatively recent studies indicate that microglial loss of function, due to excessive pathological activation or senescence, can be a risk factor for the development of depression [182, 183]. Furthermore, a chronic subclinical inflammation involving both the gut and the CNS appears to underlie the pathophysiology of autism [178]. As a matter of fact, the brain of patients diagnosed with autism spectrum disorder is characterised by microglial and astrocytic reactivity, a pro-inflammatory cytokine expression profile, and aberrant NF-κB activity [184-186].

All the presented evidence supports the idea that microglia are fundamental components of the CNS, responsible for a multitude of functions that preserve its integrity and homeostatic state, but can become highly detrimental when these physiological responses are dysregulated, representing an important feature of brain diseases. Nevertheless, and even though a great progress has been made in the last few years towards clarifying the function of glial cells in the healthy and afflicted CNS, no glia-targeted drugs are yet available on the market [187]. Naturally, the process of drug screening and development is typically complex, time-consuming and often unfruitful, and one can only expect this to be aggravated by the complexity of the CNS and its highly multifactorial diseases. Hence, in the context of neuroinflammation, it seems reasonable to affirm that new therapies must tackle not only microglial cells, but also other brain and immune components, such as astrocytes and mast cells, shifting their destructive, pro-inflammatory actions towards a more anti-inflammatory, healing response that promotes tissue repair and homeostatic recovery. Of note, progression from the currently limited treatments to effective, disease-directed therapies can only be

achieved once the extensive networks of cellular communication and biochemical and physiological mechanisms are taken into consideration.

B.2.3. The immunomodulatory potential of amphibian peptides

In the previous sections, it became clear that amphibian peptides have a wide spectrum of biological activities and potentialities of application in many different areas. Is it possible that they can also be used as anti-inflammatory agents? If so, they would possibly emerge as therapeutic molecules for a broad range of pathologies, including the neurologic diseases abovementioned. This hypothesis has already been explored in a number of studies that evaluated the effect of amphibian peptides in immune cells, including peripheral mononuclear blood cells (PBMCs), macrophages, and microglia.

Popovic *et al*. [188], for example, explored five frog-skin derived peptides for their therapeutic potential in acne vulgaris, a chronic skin condition caused by infection with *Propionibacterium acnes* and characterised by an exacerbated inflammatory response [189]. All peptides inhibited the growth of a reference strain and clinical isolates of *P. acnes* with MICs ranging from 3 to 50 μM, where [D4k]ascaphin-8 was the most potent peptide. Interestingly, they also demonstrated immunomodulatory properties in human PBMCs: all peptides significantly reduced the release of TNFα from these cells after concanavalin A (ConA) stimulation. Furthermore, [D4k]ascaphin-8 and brevinin-2GU were able to decrease the production of IFNγ by unstimulated PBMCs, in concentrations as low as 1 μg/mL. Two other peptides involved in the study, [T5k]temporin-DRa and B2RP-ERa, enhanced anti-inflammatory cytokine (TGFβ, IL-4, IL-10) release both by unstimulated and ConA-treated PBMCs. The authors suggest that the potency of [D4k]ascaphin-8 and [T5k]temporin-DRa in inhibiting *P. acnes* growth and immunomodulating PBMCs towards an anti-inflammatory action may reveal a therapeutic role for these peptides in the treatment of acne vulgaris.

Treatment of human PBMCs with an analogue of hymenochirin-1B, a peptide isolated from *Hymenochirus boettgeri* with broad-spectrum antimicrobial activity, improved IL-4 and IL-10 production in unstimulated cells (peptide concentration – 10 μg/mL). In ConA-stimulated cells, this analogue had a more complex effect, since it increased the levels of both IL-10 (anti-inflammatory) and IFNγ (pro-inflammatory). However, it did not have any influence on the production of the pro-inflammatory cytokines IL-17 and TNFα [190].

Moreover, three members from the family of tigerinins, namely tigerinins-1R, -1V, and 1M (see Table 1), were able to increase the release of IL-10 from unstimulated and LPS-treated murine peritoneal macrophages at a concentration of 20 μg/mL. They also enhanced the production of IL-6 in these cells, but they had no effects on the release of IL-12 and IL-23. Curiously, in murine spleen-derived mononuclear cells, the production of IL-10 was improved by the three peptides, with tigerinins-1V and -1M further suppressing the secretion of IFNγ. Finally, all three tigerinins significantly increased IL-10 production by unstimulated and LPS-

treated human PBMCs [59]. Additionally, in a recent study by Cao *et al.* [191], cathelicidin-OA1, a peptide obtained from the skin of *Odorrana andersonii*, showed immunomodulatory and wound-healing properties, both in *in vitro* (human keratinocytes and skin fibroblasts) and *in vivo* lesion models.

Granted, the presented results demonstrate interesting immunomodulatory properties associated with amphibian peptides, but not a lot of studies has already been performed on CNS cell types or directed to brain/spinal cord diseases. Nonetheless, recent work by Barbosa *et al.* [192] on a peptide isolated from *Physalaemus nattereri* and named antioxidin-I shows that there is a potential neurological application of these molecules. Antioxidin-I protected both murine fibroblasts from menadione-induced oxidative damage and human microglial cells from hypoxia-driven ROS generation, thus demonstrating a protective effect of this peptide against oxidative stress.

Additionally, unpublished (already submitted) work by Sousa *et al.* studies the effect of two ocellatin peptides, termed ocellatin-K1(1-16) and ocellatin-K1(1-21), both in *in vitro* neuronal and microglial cell models and in a mouse model. The two peptides were able to reduce the production of ROS and NF-κB pathway activation in living microglia. The incubation of murine hippocampal neurons with microglia-conditioned medium (MCM) after treatment with LPS and LPS in the presence of both ocellatins showed a protective action of both peptides, resulting in lower levels of oxidative stress in these cells. Furthermore, the hippocampi of mice treated with ocellatins-K1(1-16) and -K1(1-21) had higher activity of superoxide dismutase and increased amounts of glutathione, further accentuating their antioxidant potential. Treatment of mice with both these peptides also reduced the levels of hippocampal nitrite and malondialdehyde, additional indicators of oxidative and nitrosative stress.

C. Aims and Work Description

Motivation

This project was driven by the broad spectrum of biological activity offered by amphibian peptides, particularly ocellatins, considering the current need for new therapeutic solutions against a myriad of diseases and conditions that affect millions of people worldwide, representing a huge global economic burden. Even though they are, naturally, completely distinct, leishmaniasis and neurological diseases both fall into this group. Leishmaniasis is an NTD, affecting mostly developing countries that cannot afford efficient treatments for their population. Most of the available solutions are associated with nefarious side effects and the development of resistance mechanisms, and they require specialised facilities and personnel for intravenous administration. From another perspective, in a world where life expectancy keeps rising concomitantly with the lowering of fertility rates, chronic diseases, like dementia

and neurodegenerative conditions, will tend to prevail [193]. Additionally, traumatic CNS injuries, like SCI, cause highly limiting lesions, often resulting in paraplegia and tetraplegia, for which there has yet to be a cure [194]. Consistently, neurodegenerative, traumatic, and psychiatric diseases have been associated with chronic inflammation and reactive gliosis, suggesting that immunomodulatory agents capable of shifting this exacerbated inflammatory activity to a healthy, repairing response will likely slow down disease progression and restrict tissue and cellular damage.

General and specific aims

The general aim of this thesis was to contribute to the fields of leishmanial and neurological diseases by studying two members of the ocellatin peptide family, **ocellatins-PT4** and **-PT9**, in terms of **structure**, **biocompatibility**, **antileishmanial activity**, and **antioxidant** and **immunomodulatory properties in microglial cells**. The details on each one of these objectives can be consulted in Table 3.

Table 3 – Specific aims of the presented master thesis.

General aims	Specific aims
Structural characterisation of oPT4 and oPT9	• Mass spectrometry (MS) coupled to liquid chromatography (LC) and tandem mass spectrometry (MS/MS); • Phylogenetic analysis to compare the sequence and amino acid composition of oPT4 and oPT9 with other ocellatin peptides; • *In silico* predictions of peptide physicochemical properties and secondary/tertiary structure; • Experimental determination of oPT4 and oPT9 secondary structure: circular dichroism (CD) in the presence of trifluoroethanol (TFE) and LPS.
Biocompatibility assessment	• Treatment of human monocyte-derived macrophages and a human microglial cell line (CHME3/HMC3[b]) with oPT4 and oPT9, followed by a cell-viability assay;

[b] CHME3 and HMC3 cells are two existing designations of the same cell line.

	• Haemolytic activity assessment in human erythrocytes.
Antileishmanial activity	• Treatment of *Leishmania infantum* and *Leishmania amazonensis* promastigotes with oPT4 and oPT9, followed by cell-viability assays; • Atomic force microscopy (AFM) imaging of *L. amazonensis* promastigotes treated with both peptides.
Antioxidant and immunomodulatory activity in microglia	• Assessment of the antioxidant potential of oPT4 and oPT9 in ABTS and DPPH radical-scavenging assays; • Evaluation of the antioxidant effect of oPT4 and oPT9 on living HMC3 microglial cells *via* fluorescence-resonance energy transfer (FRET) microscopy; • Assessment of the immunomodulatory effect of oPT4 and oPT9 regarding: i) NF-kB pathway activation in living microglial cells by fluorescence microscopy; ii) microglial TNFα production by an enzyme-linked immunosorbent assay (ELISA); iii) microglial NO production by a Griess nitrite colorimetric assay.

Complementary analyses

These studies were complemented with antimicrobial assays on reference Gram-positive and Gram-negative bacterial strains (*S. aureus* and *E. coli*, respectively).

Materials & Methods

A. Structural Analysis

A.1. Peptide synthesis and purification

oPT4 synthesis

The synthesis of the amidated oPT4 was carried out manually, with a standard Fmoc (N-(9-fluorenyl)methoxycarbonyl) chemistry [195] starting from a Rink-amide-MBHA (4-methylbenzhydrylamine) resin (0.59 mmol/g, Peptides International). Fmoc-protected amino acids (Peptides International) were used in four-fold molar excess relative to the nominal scale of synthesis (1.2 mmol). Couplings were performed with 1,3-diisopropylcarbodiimide/ethyl 2-cyano-2-(hydroxyimino) acetate (DIC/Oxyma® [196]) in N,N-dimethylformamide (DMF) for 2–3 h. Side chain protected groups were tert-butyl for serine, and Boc for lysine and tryptophan. Amino group deprotections were conducted by 4-methylpiperidine/DMF (1:4, v:v) for 20–30 min. Removal of side chain protection and cleavage of the peptide from the resin were performed by the use of 10.0 mL trifluoroacetic acid (TFA):H_2O:tioanisol:ethanodithiol:triisopropylsilane (86:5.0:5.0:2.5:1.0, v:v:v:v:v) with addition of 1 g phenol for 90 min at room temperature (RT) under shaking.

After solvent evaporation under nitrogen, the peptide was precipitated by addition of cold diisopropyl ether, collected by filtration and washed four times with the same solvent. Extraction was performed with 200 mL H_2O:acetonitrile (ACN) (1:1, v:v) and crude peptide was lyophilized.

oPT9 synthesis

oPT9 was synthesised using a Fmoc solid-phase method [197] with Wang resin for non-amidated peptides. This synthesis was performed from the C-terminal to the N-terminal residues. Fmoc group deprotection reactions were conducted with a solution of 20% 4-methylpiperidine in DMF for 20-30 minutes (two stages of 10-15 minutes). Coupling for peptide bond formation was carried with DIC and Oxyma or [benzotriazole-1-yloxy(dimethylamino)methylidene]-dimethylazanium tetrafluoroborate (TBTU) and *N,N'*-diisopropylethylamine (DIEA) in DMF for 1-2 hours. Ninhydrin reaction was used to monitor deprotection and coupling stages [197, 198].

After each of these stages, the resin was washed three times with methanol or 2-propanol and DMF, alternately. Once the synthesis was complete, the final reaction of deprotection and release of the peptide from the resin was carried as described for oPT4, for 2h at RT. After precipitation of the crude material with diisopropyl ether and 4-6 washes with the same

solvent, the peptide was collected by filtration in a porous plate funnel, extracted with water or aqueous solution of ACN and lyophilized.

Purification

Peptides were purified by reversed-phase chromatography (RP-HPLC) and characterized by mass spectroscopy (matrix assisted laser desorption/ionisation time-of-flight mass spectrometry, MALDI-TOF) and analytical RP-HPLC. oPT4 and oPT9 sample purity was >98.5% and >95.2%, respectively. The chromatograms are available in **Appendix A**.

A.2. Mass spectrometry (electrospray ionisation (ESI)-LC-MS) and tandem mass spectrometry (MS/MS)

Peptide identification was performed by RP-HPLC-MS and MS/MS. This equipment is composed by an Ultimate™ 3000 liquid chromatography (LC) system coupled to a Q-Exactive™ Hybrid Quadrupole-Orbitrap™ mass spectrometer (Thermo Fisher Scientific). oPT4 and oPT9 samples were loaded onto a trapping cartridge (Acclaim PepMap C18 100Å, 5 mm x 300 µm I.D., Thermo Fisher Scientific) in a mobile phase of 2% ACN, 0.1% formaldehyde (FA) at 30 µL/min. After 1 min loading, the trap column was switched in-line to a 15 cm by 150 µm inner diameter EASY-Spray column (ES806, PepMap RSLC, C18, 2 µm, Thermo Fisher Scientific) at 1.2 µL/min. Separation was generated by mixing A: 0.1% FA, and B: 80% ACN, with the following gradient: 0.5 min (2.5% B to 15% B), 5.5 min (15% B to 30% B), 1 min (30% B to 99% B), 1 min (99% B). Data acquisition was controlled by Xcalibur 4.0 and Tune 2.9 software (Thermo Fisher Scientific).

The mass spectrometer was operated in data-dependent (dd) positive acquisition mode alternating between a full scan (*m/z* 380-1580) and higher-energy collision dissociation (HCD) MS/MS. Electrospray ionization (ESI) spray voltage was 1.9 kV. Global settings: use lock masses best (*m/z* 445.12003), lock mass injection Full MS, chrom. peak width (FWHM) 15s. Full scan settings: 70k resolution (*m/z* 200), AGC target 3e6, maximum injection time 50 ms. MS2 settings: microscans 1, resolution 35k (*m/z* 200), isolation window 2.0 *m/z*, isolation offset 0.0 m/z, spectrum data type profile.

Theoretical predictions of peptide fragmentation (see **Appendix B**) were performed using Protein Prospector 5.22.1 (University of California, San Francisco, USA). The raw data was processed using Proteome Discoverer 2.2.0.388 software (Thermo Fisher Scientific) and searched against the provided peptide sequence. The Sequest HT search engine was used for peptide identification. The ion mass tolerance was 10 ppm for precursor ions and 0.02 Da/0.2 Da for oPT4/oPT9 fragment ions, respectively. Peptide confidence was set to high. The processing node peptide to spectrum matches (PSM) validator was enabled with the maximum delta Cn setting at 0.05.

A.3. Phylogenetic analysis

A phylogenetic analysis of all ocellatin peptide sequences was performed using MEGA X software [199]. After gathering all peptide sequences on a FASTA file, a multiple sequence alignment (MSA) was carried with a ClustalW algorithm. The MSA was then used to construct a phylogenetic tree, using the maximum parsimony (MP) statistical method with 500 bootstrap replications. The percentage of identity between ocellatin peptide sequences was calculated using the peptide basic local alignment search tool (BLASTP) provided by the US National Center for Biotechnology Information (NCBI).

A.4. *In silico* studies for peptide physicochemical properties and structure predictions

oPT4 and oPT9 sequence analysis and secondary structure prediction were performed using PEP-FOLD3 online software [200]. Schiffer and Edmundson wheel projections [201] were obtained with HeliQuest [202], which was also used to determine peptide hydrophobic moments. Other physicochemical parameters, namely the theoretical molecular weight, isoelectric point and charge at physiological pH (7.0), were calculated using the PepCalc website [203].

A.5. Circular dichroism (CD)

oPT4 and oPT9 structure in the presence of 2,2,2-trifluoroethanol (TFE). Both peptides were tested at a concentration of 100 µM with increasing concentrations of TFE (0, 10, 20 and 40% v/v) in Milli-Q water. Polarized light absorbance was measured using a JASCO J-815 CD spectrometer (JASCO Corp.), between the wavelengths of 190 and 260 nm, with a cell path length of 1 mm. The analysis was performed under a nitrogen flow of 8 L/hour and at a temperature of 20 °C. Data was acquired with a scan speed of 50 nm/min, a response time of 1s and a bandwidth of 1 nm.

oPT4 and oPT9 structure in the presence of* E. coli *LPS. This experiment was performed with increasing LPS:peptide mass ratios in Milli-Q water. Peptide concentration was kept at 150 µg/mL, and LPS (Sigma-Aldrich) concentrations were 200 µg/mL, 400 µg/mL and 600 µg/mL. A spectrum of LPS alone was recorded and subtracted to the peptide spectra. The parameters of the analysis were the same as the previous experiment.

Time-course experiments in the presence of LPS. oPT4 and oPT9 (150 µg/mL) were incubated with LPS (600 µg/mL) for 30 min, and spectra were recorded at the timepoints of 0, 5, 10, 20 and 30 min.

Molar ellipticity determination. Peptide molar ellipticity was calculated using the following relationship:

$$[\theta] = \frac{\theta \times MW}{10 \times L \times C}$$

Where [θ] is the molar ellipticity (in degrees (deg).cm^2.dmol^{-1}), θ is the measured ellipticity (in millidegrees, mdeg), *MW* is the peptide molecular weight (in g.mol^{-1}), *L* is the cell pathlength (in cm), and *C* is the peptide concentration (in g/L).

B. Radical-scavenging activity assessment

2,2-azino-bis(3-ethylbenzothiazoline-6-sulphonic acid) (ABTS) assay. ABTS (7 mM) was mixed with potassium persulfide (2.45 mM) for 12-16h in the dark (RT) to originate the radical cation ABTS$^+$. This solution was then diluted in water for a final absorbance of 0.70 at 734 nm. Aliquots (10 µL) of oPT4 and oPT9 (both at 0.25, 0.50, 1.00, and 2.00 mg/mL) diluted in phosphate-buffered saline (PBS) were mixed with ABTS$^+$ solution (190 µL), and the absorbance was read after incubating the reaction for 6 min. The scavenging ability (%) of each peptide was compared to that of Trolox (6-hydroxy-2,5,7,8-tetramethylchroman-2-carboxylic acid) solutions at different concentrations (8–64 µg/mL). The experiment was performed once, and samples were prepared in triplicates. Results were expressed as mg of Trolox equivalent per mg of peptide.

2,2-diphenyl-1-picrylhydrazyl (DPPH) assay. A solution of DPPH$^\bullet$ in methanol (60 µM) was prepared with an absorbance of 0.60 at 515 nm. Aliquots (20 µL) of oPT4 and oPT9 (both at 0.25, 0.50, 1.00, and 2.00 mg/mL) diluted in PBS were mixed with DPPH ethanolic solution (180 µL) and kept in the dark for 30 min at 25 °C, after which their absorbances were measured. The scavenging ability (%) of each peptide was compared to that of Trolox solutions at different concentrations (2–64 µg/mL). The experiment was performed once, and samples were prepared in triplicates. Results were expressed as mg of Trolox equivalent per mg of peptide.

C. Biological activity assessment

C.1. Biocompatibility studies

C.1.1. Cell culture conditions

Human PBMCs. Human PBMCs were isolated from buffy coats of healthy blood donors from the immuno-haemotherapy Department of Hospital de São João (Porto, Portugal) by centrifugation over Lymphoprep (Axis-Shield), and monocytes were further purified by magnetic cell sorting using CD14 microbeads (Miltenyi Biotec). The ethics committee granted approval for the study and all volunteers gave their informed consent. Monocyte-derived macrophages were generated in RPMI 1640 (supplemented with 10% foetal calf serum, 2 mM L-glutamine, 100 U/mL penicillin and 100 µg/mL streptomycin). “M1” macrophages were

obtained by differentiation of monocytes with macrophage colony-stimulating factor (M-CSF, 50 ng/mL) for 7 days.

Human microglia. The HMC3 human microglial cell line was developed in 1995 after the transfection of human primary embryonic microglial cells with the SV40 large T antigen [204], and it has already been used as a valid model to study the responses of microglia in several distinct studies (extensively reviewed in [205]). HMC3 cells were kept in DMEM (1x) with high glucose, GlutaMAX™ supplement and pyruvate (Gibco® Life Technologies, Thermo Fisher Scientific), supplemented with 10% heat inactivated foetal bovine serum (FBSi, Gibco® Life Technologies, Thermo Fisher Scientific), 100 U/mL penicillin, and 100 µg/mL streptomycin (Pen/Strep, Gibco® Life Technologies, Thermo Fisher Scientific), at 37 °C, 95% air/5% CO_2.

C.1.2. Cell viability assessment

Resazurin assay. Cell viability was determined by measuring total cellular metabolic activity using the reduction of resazurin to the fluorescent resorufin. Briefly, following the 24h exposure to each peptide (concentrations: 0.1, 1, 10, and 100 µM), 8 µL of a 400 µM resazurin solution was added to each well. After 4h of incubation in the dark (37°C, 95% air/5% CO_2), fluorescence was measured at λ_{ex} = 530 nm and λ_{em} = 590 nm, using a Synergy Mx microplate reader coupled with Gen5 software v1.11 (BioTek). All exposures were performed in triplicate.

C.2. oPT9 haemolytic activity assessment

Human RBC isolation and incubation with oPT9. Blood samples (type O) were provided by Hospital de São João. To isolate RBCs, the whole blood was centrifuged (3600 rpm, 15 min, RT), the supernatant and leukocyte phases were removed, and erythrocytes were washed with PBS. These steps were repeated two to three times. RBCs were then resuspended in PBS and transferred to clean eppendorf tubes, where they were incubated with increasing concentrations of oPT9 (0-200 µM) for 1h at 37 °C. PBS and 0.1% Triton X-100 (Sigma Aldrich) were used as negative and positive controls, respectively.

Haemolysis assessment. The RBC suspensions were centrifuged (3600 rpm, 15 min, RT) and the supernatant was collected for absorbance measurements at 595 nm, using a Synergy 2 microplate reader coupled with Gen5 software (Biotek). The experiment was performed once, and samples were prepared in triplicates. Percentage of haemolysis was calculated as follows:

$$\%\, haemolysis = \frac{Abs_{sample} - Abs_{NC}}{Abs_{PC} - Abs_{NC}} \times 100$$

Where Abs_{NC} and Abs_{PC} are the absorbances of the negative and positive controls, respectively.

C.3. Antimicrobial assays

The MIC of oPT4 and oPT9 was determined using the broth microdilution method in cation-adjusted Mueller-Hinton broth (MHB2 – Sigma-Aldrich), according to the recommendations of the Clinical and Laboratory Standards Institute (CLSI, 2012), against two reference strains, *E. coli* ATCC 25922 and *S. aureus* ATCC 29213. Briefly, peptide stock solutions of 10 mg/mL were prepared in water and then two-fold dilutions were made in a microtiter plate, in order to achieve in-test concentrations ranging from 1 to 1024 µg/mL. Ciprofloxacin in the concentration range of 0.001 to 1 µg/mL was used as control antibiotic in the experiment. A bacterial inoculum was prepared in MHB2 and standardized to obtain a concentration of 5×10^5 colony-forming units (CFU)/mL in each inoculated well of the microtiter plate. The MIC was defined as the lowest concentration of the peptide that inhibited visible bacterial growth. The minimum bactericidal concentration (MBC) was determined by spreading 10 µL from the wells showing no visible growth on MH plates, which were further incubated for 24h at 37 °C. The lowest concentration at which no bacterial growth occurred on MH plates was defined as the MBC.

C.4. Antileishmanial assays

Leishmania *cell cultures.* *Leishmania infantum* (strain MHOM/MA/67/ITMAP263) and *L. amazonensis* (strain MHOM/BR/LTB0016) parasites were obtained from infected mice organs by amastigote to promastigote differentiation. To this end, homogenates of infected organs were cultured at 25 °C in complete Schneider's medium (Schneider's medium (Sigma-Aldrich) supplemented with 10% FBSi, 100 U/mL penicillin and 100 µg/mL streptomycin, 5 mg/mL Phenol Red and 5 mM HEPES sodium salt pH 7.4 (Sigma-Aldrich)). *L. infantum* promastigotes were kept in culture at 25 °C in RPMI 1640 GlutaMAX™-I (Gibco® Life Technologies, Thermo Fisher Scientific) medium supplemented with 10% FBSi, 50 U/mL penicillin and 50 µg/mL streptomycin and 5 mM HEPES sodium salt pH 7.4. *L. amazonensis* promastigotes were maintained in complete Schneider's medium. The culture medium of *L. infantum* and *L. amazonensis* parasites was replaced by fresh medium 7 and 5 days before the experiment, respectively.

Incubation of* Leishmania *promastigotes with oPT4 and oPT9. *L. infantum* and *L. amazonensis* promastigotes were seeded in complete RPMI and Schneider's medium, respectively, at a cell density of 3×10^5 parasites per well, and incubated with increasing peptide concentrations (0-512 µg/mL) for 24h at 25 °C. Samples were prepared in triplicates.

Cell viability assessment. After this period, parasitic cell viability was assessed *via* a resazurin assay, in which 20 µL of a resazurin solution (320 µg/mL) were added to each well. Resorufin fluorescence was measured after a 3h (for *L. amazonensis*) and a 24h (for *L. infantum*) incubation (25 °C in the dark), using a Synergy Mx or Synergy 2 microplate reader

coupled with Gen5 software. Analysis parameters: λ_{ex} = 530/540 nm and λ_{em} = 590/620 nm, respectively. Results were analysed using GraphPad Prism 6 software, which allowed the calculation of IC_{50} values for both peptides.

Atomic force microscopy (AFM): *Sample fixation. L. amazonensis* promastigotes treated with 0, 256, and 512 µg/mL of oPT4 were centrifuged (3000 rpm, 3 min, RT), resuspended in fixative buffer (2.5% glutaraldehyde in 100 mM sodium (Na)-cacodylate buffer, pH 7.4), and deposited onto poly-L-lysine (PLL)-coated glass coverslips in a 24-multiwell plate. After a 2h incubation (RT, 1h with no agitation + 1h with very gentle agitation), the coverslips were washed with 100 mM Na-cacodylate buffer pH 7.4 for 5 min. Following a final wash with ultra-pure water (5 min), the coverslips were blotted, inserted in dry wells, and left to dry overnight in a laminar flow chamber. Samples were prepared in duplicates.

AFM: *Imaging.* A TT-ATM microscope (ATM Workshop) was used for imaging in vibrating mode, with a scanner of 50 x 50 x 17 µm. ACT probes (AppNano) with frequencies of approximately 300 kHz were used. Images were displayed and processed with Gwyddion software.

C.5. Evaluation of oPT4 and oPT9 antioxidant and immunomodulatory potential in microglia

C.5.1. FRET and fluorescence microscopy analysis

Microglial cell transfection. HMC3 cells were plated in 35 mm µ-Dish plates (ibidi) and kept in culture for two days. Transfection was carried using jetPRIME® transfection reagent (Polyplus Transfection), according to the manufacturer's instructions. Two different DNA probes were used: HSP-FRET ROS-sensitive probe [206, 207] and miRFP703-IκBα probe [208]. After transfection, cells were incubated at 37 °C, 95% air/5% CO_2 for at least 18h before the microscopy analysis, to allow protein expression.

Treatment of microglia with oPT4 and oPT9 peptides in the presence of* E. coli *LPS and live cell imaging (LCI). The imaging timeline can be visualized in Fig. 5. Peptide and LPS solutions at 100 µM and 1 µg/mL, respectively, were prepared in Hank's balanced salt solution (HBSS, 1x) with Ca^{2+}/Mg^{2+}. A DMI6000 microscope (Leica Microsystems) was used to perform FRET and fluorescence LCI, coupled with LASX software (Leica Microsystems). The excitation light source was a mercury metal halide bulb integrated with an EL6000 light attenuator. An external filter wheel with dichroic cubes (CG1 440/520) allowing the detection of cyan fluorescent protein (CFP, BP 427/10) and yellow fluorescent protein (YFP, BP 504/12) was used for HSP-FRET probe, while the signal from miRFP703-IκBα probe was observed using an Y5 filter (excitation: 590-650; BS: 660; emission: 662-738). Cells were visualized using a HCX PlanApo 63× 1.3NA glycerol immersion objective. Images were acquired with an exposure time of 200 milliseconds and a 2 × 2 binning using a Hamamatsu

FLASH4.0 camera. A small stage temperature controller (ibidi) was used to maintain the plate temperature at 37 °C. The time-lapse images were exported as 16-bit TIFF images and subsequently processed and analysed with Fiji (Image J) software, as described in [209-211].

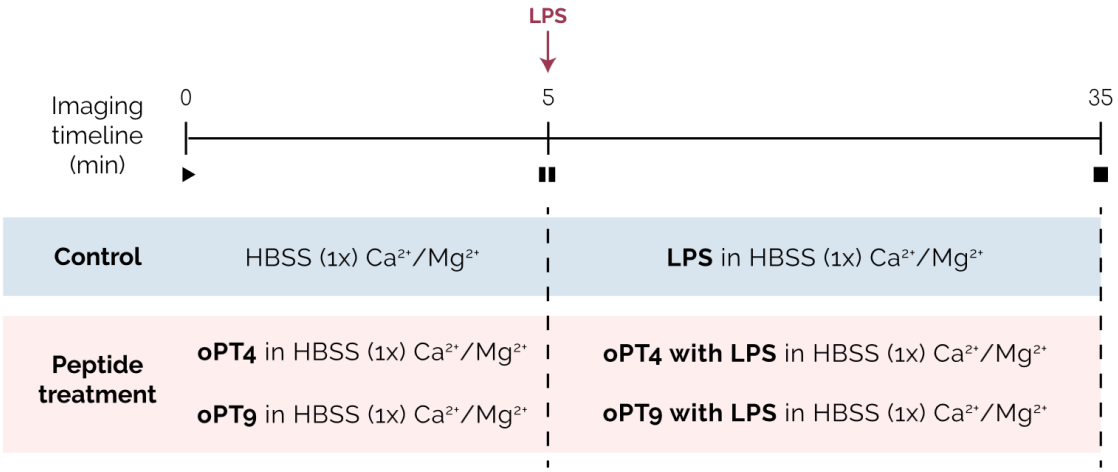

Figure 5 – Live-cell imaging (LCI) conditions. A **baseline** (control) imaging was performed for 5 min in the absence or presence of each peptide (100 µM), after which LPS (1 µg/mL) was added to the plate. The response to this pro-inflammatory stimulus is recorded for an additional 30 min (total LCI duration = 35 min). Cells were kept in HBSS buffer with Ca^{2+} and Mg^{2+} throughout the LCI.

C.5.2. Quantification of TNFα in the supernatant of LPS-stimulated microglia treated with oPT4 and oPT9

Treatment of human microglial cells with oPT4 and oPT9 in the absence or presence of LPS. HMC3 cells were plated in 6-multiwell plates and pre-incubated with oPT4 and oPT9 (25 µM and 50 µM) for 30 min at 37 °C, 95% air/5% CO_2. After this period, cells were incubated in the presence or absence of *E. coli* LPS (500 ng/mL) for 24h at 37 °C, 95% air/5% CO_2. Microglia-conditioned medium (MCM) was then collected, centrifuged (10 000g, 10 min, 4 °C) and stored at -80 °C until the next experiments.

TNFα detection* via *ELISA. A human TNFα ELISA kit (Human TNF-α ELISA Ready-SET-Go!, eBioscience) was used to quantify the cytokine levels in the previously obtained MCM. Protocol was performed according to the manufacturer's instructions. Absorbance at 450 nm was measured using a Synergy H1 microplate reader coupled with Gen5 software (BioTek). TNFα concentrations were expressed in pg/mL.

C.5.3. Griess nitrite colorimetric assay: evaluation of nitrite production in the supernatant of LPS-stimulated microglia treated with oPT4 and oPT9

Treatment of human microglial cells with LPS and both peptides (only at 25 µM) and subsequent MCM collection was carried as detailed in **section C.5.2**. Nitrite quantification was performed using a Griess colorimetric assay. Griess reagent was obtained by mixing sulphanilamide at 1% in 5% ortho-phosphoric acid (H_3PO_4) and 0.1% N-(1-naphthyl)ethylenediamine in Milli-Q water at a 1:1 proportion. A sodium nitrite ($NaNO_2$) stock solution at 1 mM was prepared in Milli-Q water, after which a 50 µM solution was prepared in culture medium. Serial 1:2 dilutions of this solution were made in culture medium in order to build a standard calibration curve. 170 µL of each standard (in duplicate) and MCM sample (in triplicate) were plated in a 96-multiwell plate, to which 170 µL of Griess reagent were subsequently added. After an incubation of 30 min in the dark (RT), absorbance at 550 nm was read using a Synergy 2 microplate reader coupled with Gen5 software. The nitrite concentration in each sample was extrapolated from the standard $NaNO_2$ curve and expressed in µM.

C.6. Statistical analysis

All experimental results are expressed as mean ± standard deviation (SD) or mean ± standard error of the mean (SEM). The number of independent experiments and the controls used in each case are indicated on the legend of every respective table or figure. Statistical analysis and graph construction was performed using GraphPad Prism 6 software or Microsoft Excel. Results were tested for normality using D'Agostino-Pearson normality test, and, since in none of the experiments a Gaussian distribution was observed, the non-parametric Kruskal-Wallis test followed by the Dunn's multiple comparisons test were applied. A p-value (P) inferior to 0.05 was considered statistically significant.

Results & Discussion

A. oPT4 AND oPT9 STRUCTURAL ANALYSIS

A.1. Mass spectrometry and tandem mass spectrometry

In order to confirm the identity of the peptide samples as oPT4 and oPT9, ESI-LC-MS and MS/MS studies were performed to determine their sequence and molecular weight. According to the monoisotopic mass theoretical predictions (**Appendix B,** Figs. B.1. and B.2.), the chromatographic fractions containing oPT4 and oPT9 were eluted at 9.58 and 5.78 minutes, respectively. The partial chromatograms containing the corresponding peaks can be observed in Figs. B.3A and B.4A. oPT4 and oPT9 MS spectra relative to these fractions are represented in Figs. B.3B and B.4B.

Observing Table 4, it is possible to conclude that the MS/MS analysis provided a confirmation of both peptide sequences (see Figs. B.7. and B.8. for further details), thus validating them as oPT4 and oPT9, and that the monoisotopic masses obtained experimentally are coincident with the theoretical predictions. Importantly, the monoisotopic mass of oPT4 is consistent with a post-translational modification (PTM), namely a C-terminal amidation, implying that it was synthesised in agreement with previous studies [83, 92, 147]: using ProteinProspector software [212], one can calculate the theoretical monoisotopic mass of oPT4 without the C-terminal amidation (2594.48507). Subtracting the experimental monoisotopic mass (2593.49887) to this value, we obtain a difference of -0.986, which is, indeed, typical of a C-terminal amidation [213]. On the opposite, oPT9 does not appear to contain any PTMs.

Table 4 – oPT4 and oPT9 monoisotopic mass and sequence information, as confirmed by MS and MS/MS, respectively. $[M+H]^+$ – monoisotopic mass; PTMs – post-translational modifications.

Peptide	oPT4	oPT9
Sequence	GVFDIIKGAGKQLIAHAMGKIAEKV	GVVDLLQGAAKDLAGH
PTMs	C-terminal amidation	-
Estimated $[M+H]^+$	2593.50	1563.85
Experimental $[M+H]^+$	2593.50	1563.89

Moreover, considering oPT4's chromatogram (Fig. B.3A), it appears that this sample is very homogeneous, since one can observe a single, well-defined peak with a relative abundance of 100% at 9.58 min. This homogeneity is consistent with the degree of purity (>98.5%) estimated for oPT4 after purification by RP-HPLC, and the longer retention time,

compared to that of oPT9, indicates a higher peptide hydrophobicity. Relevantly, longer retention times have also been correlated with increased amphipathicity [82]. In oPT4's mass spectrum, it is possible to conclude that this peptide generated ions mainly with charges of +3, +4 and +5. Zooming in on the ions with a +3 charge (Fig. B.5.) and comparing their m/z ratios with the theoretical predictions, we can easily see that they coincide with a precision of 0.01, which is typical for this type of analysis [214].

In turn, in oPT9's chromatogram, there is a visible heterogeneity, with several fractions being eluted at distinct times. Using the theoretical m/z ratio predictions, it was possible to identify the fraction at 5.78 minutes as the one containing oPT9. The peptide's mass spectrum reveals that oPT9's ionisation resulted mainly in +2, +3 and +4-charged ions. Similarly to what was observed with oPT4, focusing on the ions with a +3 charge (Fig. B.5.), the respective m/z ratios are in accordance to the theoretical predictions.

Considering the entirety of oPT9's chromatogram, the most abundant fraction was eluted at 5.87 minutes, but its m/z ratios do not correspond to those of oPT9 (Fig. B.6), indicating the presence of distinct substances in this sample. Interestingly, this substance ionises with +2 and +3 charges, which could indicate that it corresponds to another peptide [215]. This could be the result of: i) the contamination of the oPT9 sample with another unknown substance, or ii) impurities introduced in the sample during peptide synthesis [216, 217]. Additionally, several peaks with lower intensity could be observed in oPT9's chromatogram. Nevertheless, since oPT9 was purified by RP-HPLC with a purity of >95.2% (**Appendix A**), we excluded a major contamination with another peptide, reason why we decided that this sample was suitable for using in the next experiments.

A.2. Peptide sequence and phylogeny studies

Since there are yet no studies available with oPT9, it may prove useful to compare its sequence to that of the other ocellatins described so far and locate it phylogenetically in this family. Towards this goal, an MSA of all ocellatin peptide sequences was performed and can be consulted in Table 5. This MSA was further used to construct a phylogenetic tree, which is displayed in Fig. 6.

Considering the MSA, even though the similarity between the sequences is evident, there is only one conserved amino acid position: the aspartate (D) in position 4. Additionally, in the longest ocellatin peptides (ocellatin 6 and oPT6 to oPT8), the final amino acids (GLNKDGN) are also conserved. According to Conlon *et al*. [71], this suggests that, despite having a common ancestor, as indicated by the similarity between the different peptide sequences, the evolutionary pressure to maintain conserved amino acid motives was weak. Hence, this supports the hypothesis that these peptides do not play a crucial role in the survival of amphibians, potentially participating in other biological processes.

Table 5 – Multiple sequence alignment (MSA) of all ocellatin peptide sequences. oPT4 and oPT9 are highlighted in yellow. Conserved positions are highlighted in green.

Ocellatin-PT1	**G**	**V**	**F**	**D**	**I**	**I**	**K**	**D**	**A**	**G**	**K**	**Q**	**L**	**V**	**A**	**H**	**A**	**M**	**G**	**K**	**I**	**A**	**E**	**K**	**V**	**-**	**-**	**-**	**-**	**-**	**-**	**-**
Ocellatin-PT2	G	V	F	D	I	I	K	D	A	G	K	Q	L	V	A	H	A	T	G	K	I	A	E	K	V	-	-	-	-	-	-	-
Ocellatin-PT3	G	V	I	D	I	I	K	G	A	G	K	D	L	I	A	H	A	I	G	K	L	A	E	K	V	-	-	-	-	-	-	-
Ocellatin-PT4	G	V	F	D	I	I	K	G	A	G	K	Q	L	I	A	H	A	M	G	K	I	A	E	K	V	-	-	-	-	-	-	-
Ocellatin-PT5	G	V	F	D	I	I	K	D	A	G	R	Q	L	V	A	H	A	M	G	K	I	A	E	K	V	-	-	-	-	-	-	-
Ocellatin-PT6	G	V	F	D	I	I	K	G	A	G	K	Q	L	I	A	H	A	M	E	K	I	A	E	K	V	G	L	N	K	D	G	N
Ocellatin-PT7	G	V	F	D	I	I	K	G	A	G	K	Q	L	I	A	H	A	M	G	K	I	A	E	K	V	G	L	N	K	D	G	N
Ocellatin-PT8	G	V	F	D	I	I	K	G	A	G	K	Q	L	I	A	R	A	M	G	K	I	A	E	K	V	G	L	N	K	D	G	N
Ocellatin-PT9	G	V	V	D	L	L	Q	G	A	A	K	D	L	A	G	H	-	-	-	-	-	-	-	-	-	-	-	-	-	-	-	-
Ocellatin-1	G	V	V	D	I	L	K	G	A	G	K	D	L	L	A	H	L	V	G	K	I	S	E	K	V	-	-	-	-	-	-	-
Ocellatin-2	G	V	L	D	I	F	K	D	A	A	K	Q	I	L	A	H	A	A	E	K	-	-	-	Q	I	-	-	-	-	-	-	-
Ocellatin-3	G	V	L	D	I	L	K	N	A	A	K	N	I	L	A	H	A	A	E	-	-	-	-	Q	I	-	-	-	-	-	-	-
Ocellatin-4	G	L	L	D	F	V	T	G	V	G	K	D	I	F	A	Q	L	I	K	Q	I	-	-	-	-	-	-	-	-	-	-	-
Ocellatin-5	A	V	L	D	I	L	K	D	V	G	K	G	L	L	S	H	F	M	-	-	-	-	E	K	V	-	-	-	-	-	-	-
Ocellatin-6	A	V	L	D	F	I	K	A	A	G	K	G	L	V	T	N	I	M	-	-	-	-	E	K	V	G	-	-	-	-	-	-
Ocellatin-L1	G	V	V	D	I	L	K	G	A	A	K	D	L	A	G	H	L	A	T	K	V	M	N	K	L	-	-	-	-	-	-	-
Ocellatin-L2	G	V	V	D	I	L	K	G	A	A	K	D	L	A	G	H	L	A	T	K	V	M	D	K	L	-	-	-	-	-	-	-
Ocellatin-V1	G	V	V	D	I	L	K	G	A	G	K	D	L	L	A	H	A	L	S	K	L	S	E	K	V	-	-	-	-	-	-	-
Ocellatin-V2	G	V	L	D	I	L	K	G	A	G	K	D	L	L	A	H	A	L	S	K	I	S	E	K	V	-	-	-	-	-	-	-
Ocellatin-V3	G	V	L	D	I	L	T	G	A	G	K	D	L	L	A	H	A	L	S	K	L	S	E	K	V	-	-	-	-	-	-	-
Ocellatin-F	G	V	V	D	I	L	K	G	A	A	K	D	I	A	G	H	L	A	S	K	V	M	N	K	L	-	-	-	-	-	-	-
Ocellatin-P	G	L	L	D	T	L	K	G	A	A	K	N	V	V	G	S	L	A	S	K	V	M	E	K	L	-	-	-	-	-	-	-
Ocellatin-S	G	V	L	D	I	L	K	G	A	A	K	D	L	A	G	H	V	A	T	K	V	I	N	K	I	-	-	-	-	-	-	-
Ocellatin-K1	G	V	V	D	I	L	K	G	A	A	K	D	L	A	G	H	L	A	S	K	V	M	N	K	I	-	-	-	-	-	-	-
Ocellatin-LB1	G	V	V	D	I	L	K	G	A	A	K	D	I	A	G	H	L	A	S	K	V	M	-	-	-	-	-	-	-	-	-	-
Ocellatin-LB2	G	V	V	D	I	L	K	G	A	A	K	D	I	A	G	H	L	A	S	K	V	M	N	-	-	-	-	-	-	-	-	-

Curiously, the sequence of oPT9 stands out from the remaining ocellatins-PT, which are all quite similar. In fact, if we observe the phylogenetic tree represented in Fig. 6, it is possible to conclude that all ocellatins-PT form a cluster (as previously pointed out in [83]), with the exception of oPT9. Using the BLASTP tool provided by NCBI, oPT3 is the peptide which sequence is most similar to oPT9 (56.25%), followed by oPT8 (53.85%) and oPT4, oPT6 and oPT7 (50%). Notwithstanding, and as expected from the phylogenetic tree data, oPT9 was quite similar to other ocellatin peptide sequences: this peptide shared 87.5% of identity with ocellatins-K1, -L1 and -L2. Ocellatin-F and -S were also closer to oPT9, with identity percentages of 81.25%.

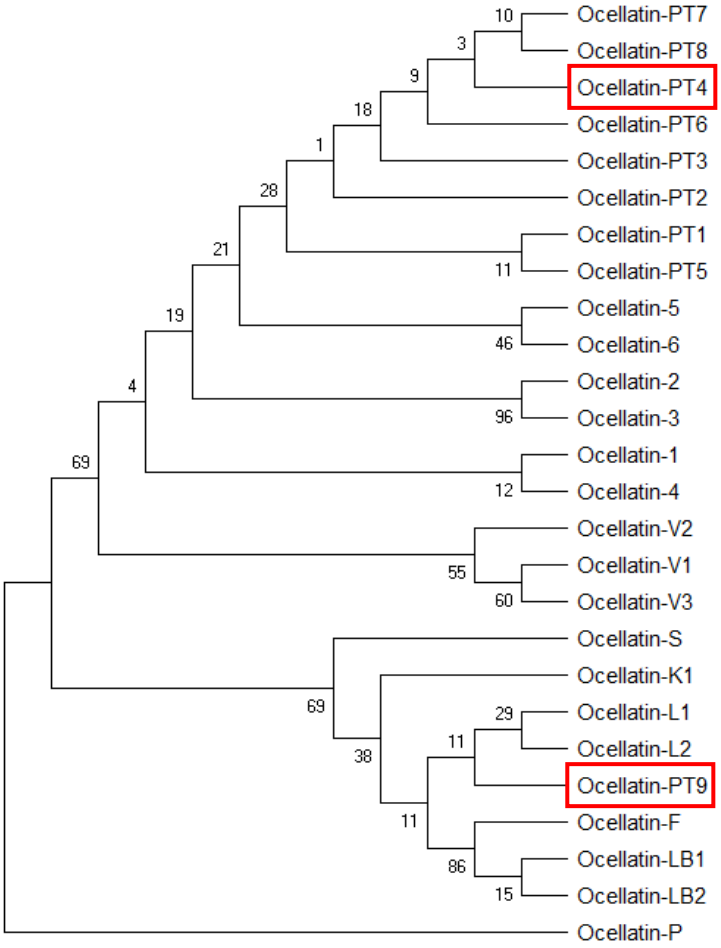

Figure 6 – Maximum parsimony (MP) phylogenetic tree of all ocellatin peptides. The ocellatins used in this work are highlighted within red boxes.

However, it should be taken into account that the shorter length of oPT9 compared to the remaining ocellatins-PT and the absence of a C-terminal amidation suggest that it probably corresponds to a truncated form of a longer peptide, making it difficult to uncover the phylogenetic relationship it holds with the ocellatin peptide class.

Furthermore, Leite Jr. *et al.* [77] noted that the N-terminal region of ocellatin peptides is more conserved than the C-terminal amino acids, limiting the accuracy of this analysis even further. Hence, such inferences regarding phylogenetic relationships should, preferentially, be based not only on sequence information, but also on ribosomal RNA (rRNA) and DNA information, as well as morphological and ecological characteristics of each species involved in the analysis [77].

A.3. *In silico* predictions of peptide structure and physicochemical properties

Peptide structure and physicochemical properties can highly influence their interaction with biological systems. As such, many open-source programs with powerful and versatile software can be consulted nowadays to construct *in silico* models of peptide secondary structure and to predict important physicochemical parameters, including isoelectric points and hydrophobic moments.

Accordingly, a computational analysis of oPT4 and oPT9 sequences was performed, in order to collect valuable information that may help explain their effects at a biological level. The theoretical molecular weight, isoelectric point, net charge at pH 7.0, hydrophobicity, and hydrophobic moment of each peptide can be consulted in Table 6. In Fig. 7, it is possible to observe the models of oPT4 and oPT9 secondary structure, as well as Schiffer and Edmundson wheel projections of both peptides.

Table 6 – Physicochemical information for oPT4 and oPT9. MW – molecular weight; μ_H – hydrophobic moment; pI – isoelectric point.

Peptide	**oPT4**		**oPT9**
MW (Da)	2594.13		1563.75
pI	10.7		5.04
Net charge at pH 7.0	+3.1		-0.9
Hydrophobicity	0.406		0.366
μ_H	**oPT4(1-9)**	**oPT4(11-23)**	**oPT9(2-15)**
	0.560	0.398	0.517

Starting with the *in silico* secondary structure models (Fig. 7A), it is possible to observe that both peptides tend to assume an α-helical structure. oPT4 is composed of two α-helices: the first is formed by the residues Val^2 to Gly^8, while the amino acids Lys^{11} to Glu^{23} make up the last α-helix. The model for oPT9 indicates that this peptide is characterised by a single α-helix that spans the positions Val^2 to Gly^{15}.

Regarding the physicochemical characterization of both peptides, it is already clear that they have very different properties. Both the isoelectric point and the hydrophobicity index are higher for oPT4: this peptide is, therefore, more hydrophobic than oPT9, and it has a considerable positive charge (+3.1) at a physiological pH. Of note, oPT4 is C-terminally amidated, and, thus, it contains an extra amine group that can be protonated, contributing to this overall positive charge. oPT9 has a low negative charge (-0.9) at pH 7.0, indicating that the two ocellatins will potentially have very distinct biological effects.

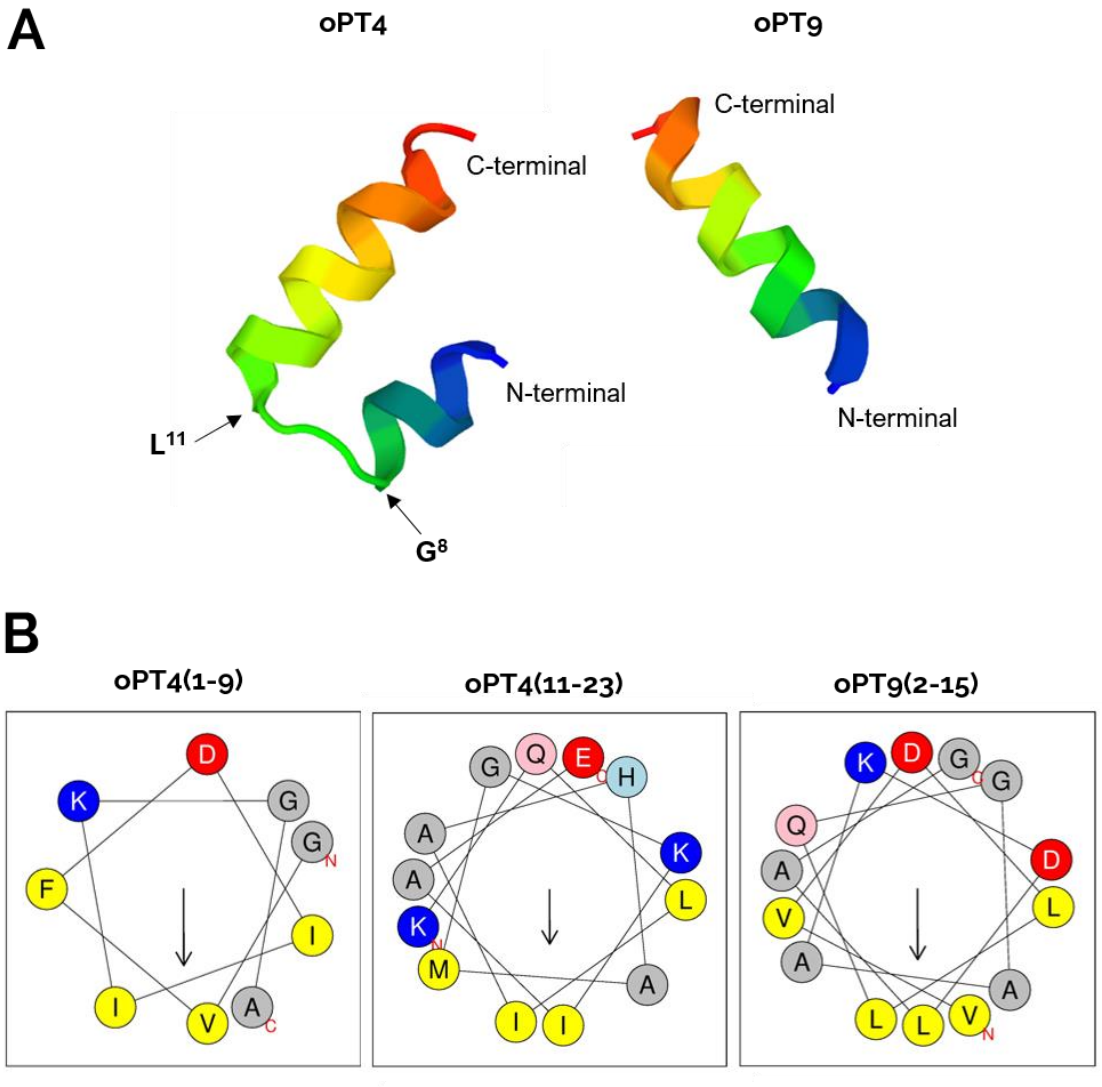

Figure 7 – **A)** *In silico* models of oPT4 and oPT9 secondary structure. **B)** Schiffer and Edmundson wheel projections of the α-helical portions of oPT4 and oPT9. Amino acid colour code: **red** – acid; **dark**/**light blue** – basic; **yellow** – hydrophobic; **pink** – polar, uncharged; **grey** – Gly/Ala.

As a measurement of peptide amphipathicity, the hydrophobic moments (μ_H) of the α-helical portions of oPT4 and oPT9 were also calculated[c]. It is possible to observe that the two oPT4 helixes have distinct μ_H values, and that these are in the same order of magnitude than the hydrophobic moment of oPT9. LC-MS studies indicated, however, that oPT4 is not only more hydrophobic, but also more amphipathic than oPT9, due to a higher retention time in the RP-HPLC. Nonetheless, one should take into account the peptide tertiary structure that originates from the interactions between the amino acid side chains that compose oPT4 and oPT9. Thus, the global amphipathicity and structure of both peptides will possibly depend on the properties of the solvent and change in the presence of cell membranes with different chemical compositions.

Peptide wheel projections can be visualised in Fig. 7B. These projections, popularised by Schiffer and Edmundson [201], are two-dimensional representations of peptide helical structures that allow their visualisation from the same axis around which the helix grows [218]. To this end, each residue is placed on the perimeter of a circle/spiral with a periodicity of 100° between different residues, achieving the typical 3.6 residues per turn that characterise an α-helix [201]. Thus, with wheel projections, it is easy to observe the distribution of amino acids in the helix, facilitating, for instance, the identification of hydrophobic or hydrophilic clusters and potential hydrogen bond formation [201, 218]. Indeed, observing the wheel projection for the α-helical portion of oPT9, one can conclude that there is a hydrophobic cluster composed of alanine, valine, and leucine residues, while a more hydrophilic face containing charged amino acids (aspartate, lysine) can also be observed. In the wheel projections of both oPT4 helixes, hydrophobic and hydrophilic groups are also observable; nevertheless, in the second α-helix, there is a lysine (K) residue interrupting the hydrophobic face, which may account for the lower μ_H value compared to that of the first helix.

Interestingly, a similar analysis performed by Marani *et al*. [83] revealed that, while the hydrophobic cluster is relatively conserved among ocellatin peptides, the hydrophilic residues are more variable. This implies that such differences in the peptide hydrophilic portion may account for the distinct antimicrobial potential and biological activity [71, 72, 76].

A.4. Circular dichroism analysis

The secondary structure of oPT4 and oPT9 was assessed experimentally by CD analysis. The results can be consulted in Fig. 8. Starting with the studies in TFE (Fig. 8A), it is possible to observe that oPT4 spectra are similar to those published previously [147]. In water and for low concentrations of TFE (10%), oPT4 presents low molar ellipticity, mainly from 210 nm

[c] Even though the first α-helix of oPT4 spans the positions 2 to 8, due to a software limitation, the wheel projection and the hydrophobic moment were calculated for the positions 1 to 9.

on, and a minimum at around 200 nm, demonstrating a random coil conformation [219, 220]. However, for concentrations of TFE of 20 and 40%, oPT4 assumes a more defined secondary structure. At 40% TFE, the molar ellipticity of oPT4 reaches a maximal value at a wavelength of 192 nm and a minimal value at 207 nm; furthermore, we can observe an inflexion near 220 nm. This is typical of α-helical conformations [221], corroborating the theoretical predictions.

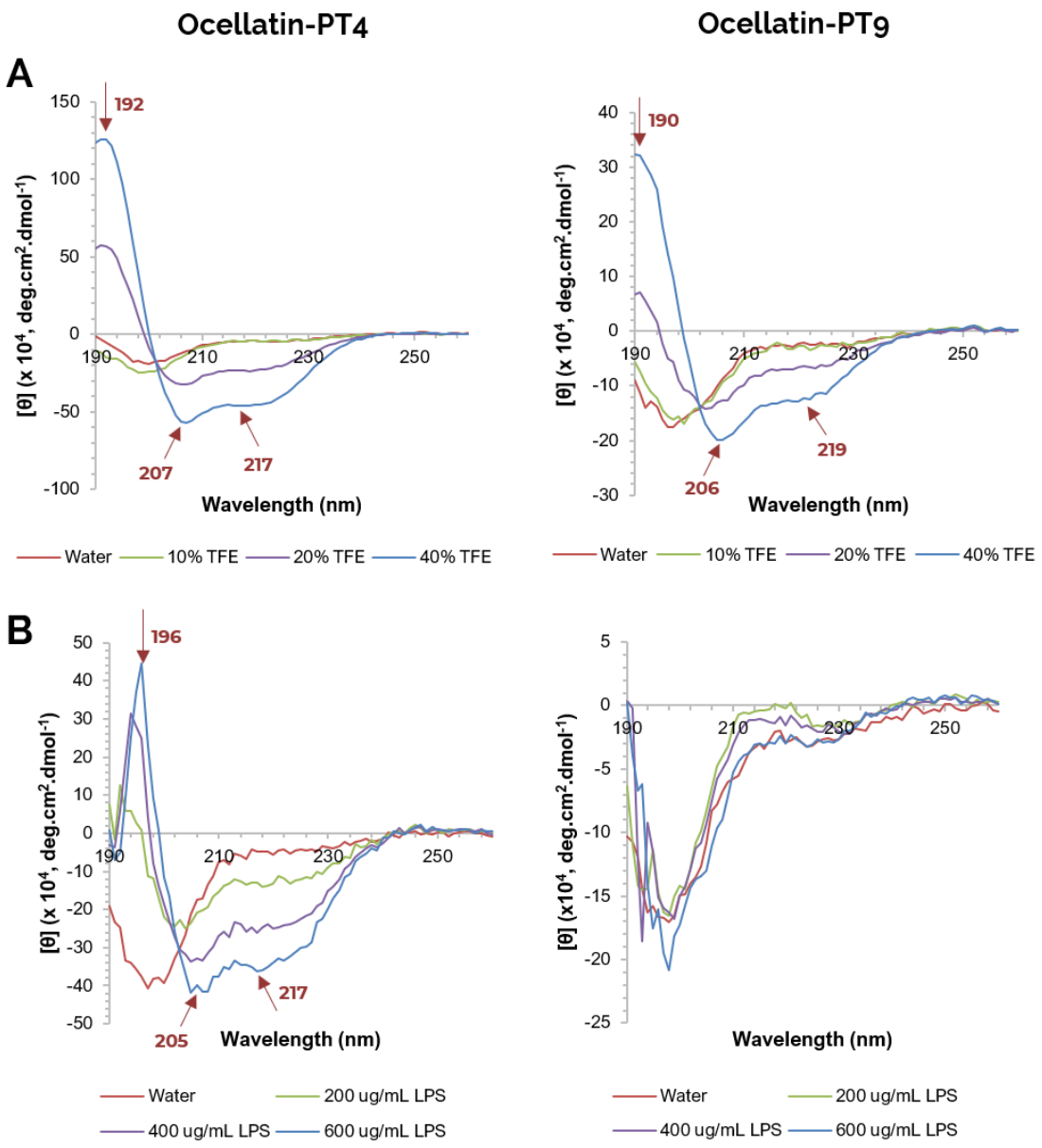

Figure 8 – Circular dichroism spectra of oPT4 and oPT9 in the presence of increasing concentrations of trifluoroethanol (TFE) (**A**) and lipopolysaccharide (LPS) (**B**). Peptide concentration for TFE and LPS studies was 100 μM and 150 μg/mL, respectively. [θ] – molar ellipticity.

Similarly to oPT4, oPT9 presents a random coil structure when dissolved in water or 10% TFE, but it assumes a defined α-helical conformation when in higher concentrations of this solvent, which is also in agreement with the *in silico* model. Of note, the observed [θ] values are lower than those observed for oPT4. This may be explained by the fact that, according to the theoretical predictions, oPT4 is composed of two α-helixes, while oPT9 has a single helix spanning its length. Because the α-helical structure is less extensive in oPT9, it can result in lower ellipticity values.

Since one of the main objectives of this project was treating microglial cells with both peptides in the presence of LPS, we assessed whether it could induce any modifications on the secondary structure of oPT4 and oPT9. However, at the LPS concentration used in microglial assays (1 µg/mL), it would probably be very difficult to detect any interactions between this molecule and the peptides. Therefore, we assessed the secondary structure of oPT4 and oPT9 in aqueous solutions with three different concentrations of LPS: 200, 400, and 600 µg/mL (Fig. 8B). It is possible to conclude that the structure of oPT9 is not greatly altered in the presence of any LPS concentration, while oPT4 tends to form α-helical structures even at the lowest LPS concentration tested (200 µg/mL).

Additionally, a time-course experiment was performed, in which both ocellatins were incubated with LPS for 30 minutes. CD spectra were recorded at 5, 10, 20 and 30 minutes of incubation, but they showed no major alterations in the peptide structure, both for oPT4 and oPT9 (Appendix C, Fig. C.1.).

These results reveal that oPT4 and oPT9 may behave differently when contacting with biological membranes. In fact, the interaction of oPT4 with LPS was expected, since this peptide has demonstrated antimicrobial activity against a plethora of Gram-negative bacterial species, namely *Escherichia coli*, *Klebsiella pneumoniae*, and *Salmonella choleraesuis* [83]. It is well-known that the cell wall of Gram-negative bacteria contains an outer membrane mainly formed by LPS, while this exterior layer is absent from the cell wall of Gram-positive bacteria [222]. Therefore, oPT4's ability to interact with LPS may explain its antibacterial activity against Gram-negative strains.

Conversely, oPT9 does not seem to interact with LPS. These differences between both peptides can probably be explained due to their different amino acid composition and physicochemical properties: as displayed in Table 6, oPT4's net charge at pH 7.0 is positive (+3.1), while oPT9 has a low negative charge (-0.9) in these conditions. Since LPS is also negatively charged, it should easily interact electrostatically with oPT4, but not with oPT9.

B. Radical-scavenging activity assessment

As summed up by Barbosa *et al*. [192], the radical-scavenging activity of a peptide depends on its amino acid composition and sequence, structure, and hydrophobicity. Studies indicate that shorter peptides, with 2-10 amino acids, present greater antioxidant activity than larger polypeptides [223]. The presence of aromatic residues, like tryptophan (W), tyrosine (Y), and phenylalanine (F), has also been associated to increased antioxidant properties, due to their ability of accommodating unpaired electrons in resonance structures [224, 225] after donating either protons (hydrogen atom transfer, HAT) or electrons (single electron transfer, SET) [226]. Cysteine (C) and histidine (H) can also participate in such reactions and provide antioxidant properties. Likewise, antioxidant peptides normally have a high content in hydrophobic amino acids [227]. Proline (P) was important for the antioxidant activity of a peptide derived from soy bean [228].

The radical-scavenging activity of oPT4 and oPT9 was assessed by two *in vitro* colorimetric assays: the ABTS and the DPPH assay. Both are based on the same principle: when in their radical forms, $ABTS^{+}$ and $DPPH^{\bullet}$ form blue-green and violet solutions, respectively, with absorption maxima at 734 and 515 nm. Upon reduction by an antioxidant molecule, they become the non-radicals ABTS and DPPH, the corresponding solutions turn colourless and yellow, and the light absorption at those wavelengths decreases [229, 230]. The antioxidant potential of oPT4 and oPT9 was compared to that of Trolox in different concentrations, and glutathione, a well-known endogenous antioxidant [231], was used as a positive control. The results can be visualised in Table 7.

Table 7 – Antioxidant activity of oPT4 and oPT9 compared to that of glutathione in two radical-scavenging assays. Results are expressed as mg of Trolox equivalent per mg of peptide (mean ± SD, triplicate measurements, N = 1). ABTS - 2,2-azino-bis(3-ethylbenzothiazoline-6-sulphonic acid; DPPH - 2,2-diphenyl-1-picrylhydrazyl.

Peptide	***In vitro* antioxidant activity (Trolox-eq/mg peptide)**	
	ABTS assay	**DPPH assay**
Glutathione	1.911 ± 0.003	0.829 ± 0.005
oPT4	0.011 ± 0.000	0.000 ± 0.000
oPT9	0.027 ± 0.001	0.000 ± 0.000

It is possible to conclude that none of the peptides had a detectable radical-scavenging activity in the DPPH assay, while a residual antioxidant potential could be measured in the ABTS test. Nevertheless, glutathione antioxidant activity was greatly superior to that of both peptides, indicating that neither oPT4 or oPT9 are capable of neutralising radical species.

Taking into account the amino acid composition and sequence of both peptides, these results were expected: there are no aromatic, cysteine, or proline residues in either of the peptides, and the hydrophobic amino acids correspond only to about 50% of the total sequence. Both oPT4 and oPT9 have a histidine residue in position 16 (His^{16}), but their length, mainly in the case of oPT4, may also contribute to the very weak radical-scavenging activity.

C. Biological assays

C.1. Biocompatibility assessment

When exploring a new molecule or formulation for a therapeutic or cosmetic application, it is essential to perform biocompatibility studies to determine its safety profile and uncover eventual detrimental effects in living cells and tissues [232]. *In vitro* assays can be used as first-line cytotoxicity studies, and there is a wide range of techniques available, including dye exclusion, fluorometric, colorimetric, and luminometric assays, which can evaluate parameters like cell metabolic activity and viability, membrane integrity, ATP and co-enzyme production [233]. The reduction of Alamar Blue (resazurin) dye has been extensively used in cytotoxicity assays as an indicator of the cellular reducing potential and viability. The principle of this assay is simple: when resazurin is reduced, originating resorufin, it changes from a blue, non-fluorescent state to a bright pink solution capable of emitting fluorescence at 590 nm after excitation at 530-560 nm. This reduction can be carried by co-enzymes like NAD(P)H, FADH, FMNH, and mitochondrial and cytoplasmic reductases [234]. Importantly, Alamar Blue has been used preferentially to MTT (3-(4,5-dimethylthiazol-2-yl)-2,5-diphenyltetrazolium bromide), since it is not cytotoxic [235].

The biocompatibility of oPT4 and oPT9 was evaluated in human monocyte-derived macrophages and microglia. After incubation with 0.1 to 100 µM of each peptide for 24h, an Alamar Blue assay was used as strategy to measure cell viability.

Human monocyte-derived macrophages

Observing Fig. 9, it is possible to conclude that none of the peptides had statistically significant effects on macrophage metabolic activity in the range of concentrations tested, although oPT9-treated cells tend to show lower levels of resazurin reduction compared to oPT4 treatment. This indicates that oPT9 may have a more pronounced cytotoxic effect than oPT4. Interestingly, for both peptides, cell viability appears to increase with higher peptide concentrations – in the case of oPT4, it largely exceeds basal levels, reaching up to almost 150% (139.7% ± 17.4%). Even though these differences are not significant, this may imply that oPT4 and oPT9 stimulate cellular metabolic activity, and this stimulation seems to be dose-dependent. Such an increased cell metabolism can be a consequence of a stress

response triggered by the presence of the peptides, but further investigation should be conducted in order to evaluate this hypothesis.

Human microglial cells (HMC3 cell line)

The cell viability of human microglia treated with oPT4 and oPT9 was also measured and quantified in Fig. 10. Observing the histogram, it is possible to conclude that microglial cells responded differently than macrophages to the presence of the peptides. While the treatment of these cells with oPT4 did not majorly affect cell viability, the 24h incubation with oPT9 appears to have caused harmful effects, mainly at a concentration of 100 µM. In this case, there was a reduction of resorufin fluorescence of nearly 50% compared to control (untreated) cells, potentially indicating that microglial cells are more sensitive to oPT9 treatment than macrophages. Of note, and contrarily to the macrophage biocompatibility assay, this experiment was only performed once (N = 1), which precludes a proper statistical analysis of the results: repeating the assay is pivotal so as to clarify if oPT9 is, in fact, toxic for microglial cells. It would also be interesting to use intermediate concentrations between 10 and 100 µM to build a dose-response curve, from which it would be possible to determine the maximum safe concentration of the peptide.

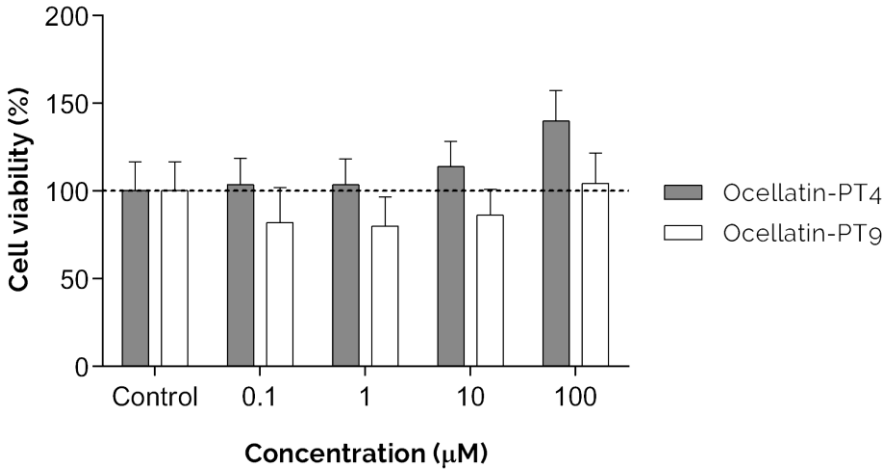

Figure 9 – Biocompatibility studies of oPT4 and oPT9 in human macrophages. Untreated cells were used as negative control. Results are presented as mean ± SEM (N = 3).

Surprisingly, these preliminary results seem to support the hypothesis that oPT9 is more cytotoxic than oPT4, despite being negatively charged and less amphipathic, interacting, in principle, with the zwitterionic cell membranes to a lesser extent. In addition, oPT4 has a C-terminal amidation, which is thought to stabilise the peptide α-helix conformation and partially protect against the activity of endopeptidases [146] – but oPT9 does not have such modification. In this case, it is evident that the properties that drive peptide toxicity against a certain cell type are multifactorial, relying on more than electrostatic interactions. Possibly,

oPT9's shorter length, compared to that of oPT4, may allow the peptide to cross the membrane and result in its internalisation. Thus, if confirmed by additional experiments, its deleterious effect may originate not exclusively from membrane destabilisation, but also from the activation of cellular stress pathways, both due to the engagement of cell surface receptors or cytoplasmic mediators.

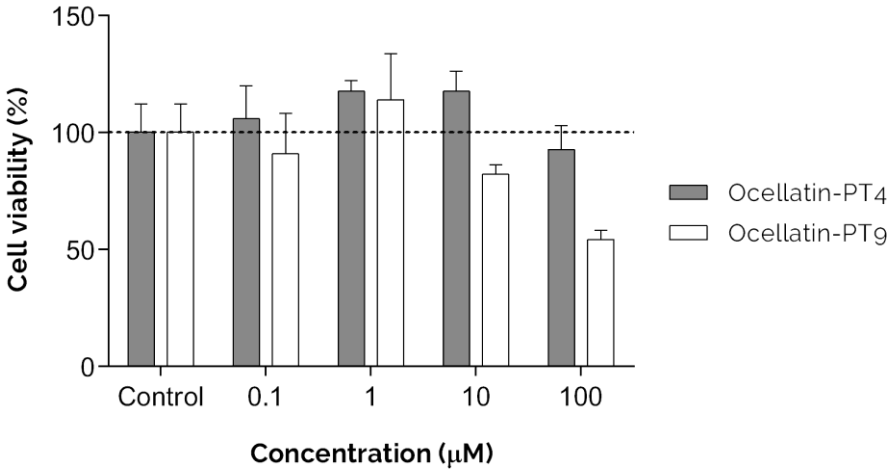

Figure 10 – Biocompatibility studies of oPT4 and oPT9 in human microglial cells. Untreated cells were used as negative control. Results are presented as mean ± SD from triplicate measurements (N = 1).

Unlike oPT9, the cytotoxic potential of oPT4 had already been tested in other cell types. In the study that reported, for the first time, the isolation and characterization of ocellatins PT1-PT8, Marani *et al.* [83] evaluated the toxicity induced by these peptides in a murine fibroblast cell line (NIH-3T3). None of the peptides showed significant effects on fibroblast cell viability compared to untreated cells. Moreover, Oliveira *et al.* [147] studied the effect of ocellatins PT1-PT8 in murine BMDMs. Interestingly, all peptides had 50% cytotoxicity concentrations (CC_{50}) superior to 150 µM, except for oPT4, for which the CC_{50} was 101.5 µM. Conversely, the results obtained in this work indicate that, at a concentration of 100 µM, oPT4 does not have a deleterious effect in human macrophage or microglia metabolic activity.

As a suggestion for future experiments, studies with a wider range of peptide concentrations can be conducted, in order to determine the values of CC_{50} for both oPT4 and oPT9 in both the human cell types tested. Moreover, resazurin and MTT-based assays present one important limitation: they rely on metabolic activity as an indicator of cell viability [236] and, therefore, provide no direct information on cell death or proliferation. Thus, it can be interesting to evaluate other parameters like membrane integrity and activation of apoptotic pathways. Accordingly, the cytotoxicity caused by oPT4 and oPT9 can be assessed

in more detail using several other markers, namely lactate dehydrogenase (LDH) leakage, utilized to evaluate membrane integrity and necrosis [237-239], and caspase-3/7 activity, which is widely used as an apoptotic marker [239]. Cell viability information can be complemented using live/dead assays, with fluorescent dyes that selectively permeate live and compromised cells [240]. It should also be taken into account that cytotoxic effects cannot be excluded for higher concentrations of peptide (*i.e.*, >100 µM) or longer incubation periods (*e.g.* 48h or 72h).

Furthermore, clarifying whether oPT4 and oPT9 are internalised by cells or act at a plasma membrane level can be achieved by coupling each peptide to a fluorescent probe and monitoring with flow cytometry or microscopy studies [241, 242].

C.2. oPT9 haemolytic activity assessment

The development of a novel therapeutic compound also involves the assessment of its haemolytic activity, that is, the ability to lyse RBCs, since it will most likely be in contact with these cells in the blood stream when administered to a patient. In previous studies [83], oPT4 demonstrated low haemolytic activity ((4.29 ± 0.23)%) up to a concentration of 308 µM (800 µg/mL), despite its positive charge and increased amphipathicity. Among the ocellatin-PT peptide family, the most haemolytic peptides were oPT7 and oPT8, with percentages of haemolysis of (13.72 ± 1.39)% and (8.09 ± 0.52)% at ~240 µM (800 µg/mL). Both these peptides have a length of 32 amino acids and a positive charge at a physiological pH (oPT7: +2.1; oPT8: +3.0). Therefore, there are two fundamental differences between oPT4 and these two peptides: the length (25 vs 32 amino acids) and the C-terminal amidation, which is absent from oPT7 and oPT8. Curiously, even though oPT4 and oPT8 have an increased positive charge, it was oPT7 that had the highest haemolytic activity. This becomes even more interesting when we realise that the sequence of oPT4 corresponds exactly to the first 25 amino acids of oPT7 (Table 2), suggesting that the 7 last positions of this peptide are important for the observed haemolytic activity. Furthermore, oPT7 differs from oPT8 in just one amino acid position: while the former has a histidine in position 16 (His^{16}), the latter has an arginine (Arg^{16}), and this substitution accounts for a decrease in human RBC haemolysis of nearly 6%.

In this project, we measured the haemolysis induced by oPT9 in human erythrocytes, and the results are displayed in Fig. 11. It is clear that this peptide is not haemolytic, as no RBC lysis was detected for any peptide concentration (3-200 µM). Considering the physicochemical properties of oPT9, these results were expected, due to its low negative charge that prevents it from establishing electrostatic interactions with the erythrocytic cell membrane and causing toxicity. Additionally, ocellatins-L1 and -L2, that shared a sequence similarity of 87.5% with oPT9, had previously demonstrated no haemolytic properties against human erythrocytes as well [62, 71].

These findings also support the idea that the mechanism of toxicity of oPT9 in microglial cells, if confirmed, is probably independent from membrane destabilisation, since this peptide did not have any detectable effect on the cell membrane of RBCs. Nevertheless, it is possible to conclude that both oPT4 and oPT9 are safe against human erythrocytes, favouring their application in a therapeutic context.

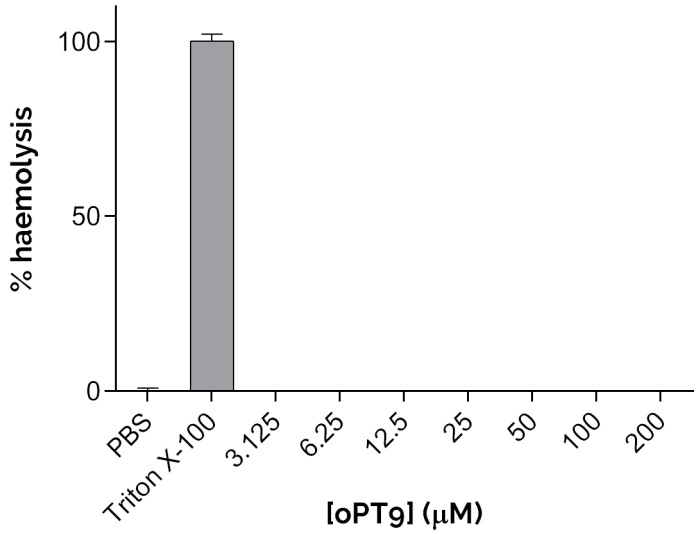

Figure 11 – Haemolytic activity of oPT9 in human erythrocytes. Treatment with PBS and 0.1% Triton X-100 were used as negative and positive controls, respectively. Results are presented as mean ± SD from triplicate measurements (N = 1).

C.3. oPT4 and oPT9 antimicrobial activity in *E. coli* and *S. aureus*

While the antimicrobial activity of oPT4 has already been assessed in several species, there is no information concerning the antimicrobial potential of oPT9. To fill in this gap, both peptides were tested on reference Gram-negative and Gram-positive bacterial strains – *E. coli* and *S. aureus*, respectively. The respective MIC and MBC values are displayed on Table 8.

Table 8 – Minimum inhibitory concentration (MIC) and minimum bactericidal concentration (MBC) of oPT4 and oPT9 against two reference strains.

Peptide	*E. coli* ATCC 25922		*S. aureus* ATCC 29213	
	MIC (μg/mL)	MBC (μg/mL)	MIC (μg/mL)	MBC (μg/mL)
oPT4	32	32	256	256
oPT9	> 1024	-	> 1024	-

oPT4 was active against both bacterial species, even though it was considerably more effective against *E. coli*. We previously demonstrated that the structure of this peptide is

modulated in the presence of LPS, suggesting an interaction between these molecules; nevertheless, its bactericidal effect in *S. aureus* is probably related to other structural characteristics. The ability to interfere with the cell wall and membrane of Gram-positive bacteria depends, among other factors, on peptide amphipathicity and hydrophobicity [243]. Importantly, oPT4 has an amidated C-terminus (-$CONH_2$), and this alteration is thought to stabilise the α-helix structure; in several studies, carboxyamidated peptides were found to have a greater antimicrobial activity than their carboxylated (C-terminus -COOH) counterparts [244-247]. This may explain why the C-terminal amidation appears to be conserved in several peptides from the *Leptodactylus* genus (Table 2) [77].

oPT9, however, was not active against any of the bacterial species up to a concentration of 1024 µg/mL. This was expected, since it did not show any interaction with LPS in the presented CD studies, presumably due to its negative charge. The absence of haemolytic activity and toxicity towards the Gram-positive species supports a low peptide amphipathicity. Of note, oPT9 does not contain a C-terminal amidation, which may also contribute for its lack of antibacterial potential.

Curiously, the MIC values obtained for oPT4 are very disparate from those determined previously. Of note, the *S. aureus* strains used in both studies are different, but the *E. coli* strain is the same. In this work, we determined that oPT4 has a MIC and MBC of 32 µg/mL in *E. coli* and 256 µg/mL in *S. aureus*, while in the study developed by Marani *et al.* [83] this peptide had a MIC of 200 µg/mL in *E. coli* and was not active against *S. aureus*. Therefore, in the present work, oPT4 demonstrated a more potent antimicrobial effect. These differences may originate from intrinsic variability between the bacterial cultures used, mainly in the case of *S. aureus*, where the strains differed. Furthermore, the peptide stocks used in both studies were also distinct, which may have contributed for such a discrepancy in the results. Nevertheless, the results obtained in this work are in accordance with what was observed for other peptides of this class, with a higher antimicrobial activity against the Gram-negative species than the Gram-positive ones.

C.4. Antileishmanial activity of oPT4 and oPT9

C.4.1. Effect of oPT4 and oPT9 treatment on *L. infantum* and *L. amazonensis* cell viability

Although ocellatin peptides were first investigated mainly as antibacterial agents, their potential application in other areas has already been explored. Accordingly, the activity of ocellatins PT1-PT8 against *Leishmania* parasites has already been assessed, namely in promastigotes and amastigotes of *L. infantum* [147]. oPT4 had the most noticeable effect in *L. infantum* promastigotes, with an IC_{50} of 25.6 µg/mL (9.8 µM). The IC_{50} for oPT4 in *L. infantum* amastigotes was 75 µg/mL (28.9 µM), indicating that the inhibitory effect of this

peptide is different for distinct stages of the parasite's lifecycle. A recent study performed by Messaoud *et al*. [248] showed that the total lipid composition of *L. infantum* parasites changes during the metamorphosis from promastigote to amastigote stages, suggesting that the cell membrane constitution might also vary during this process. Moreover, the leishmanial promastigote form has a dense glycocalyx with a high content in lipophosphoglycan (LPG) and glycoproteins, whereas the amastigotes downregulate the expression of LPG and other components [249, 250]. Accordingly, the effect of antileishmanial peptides, like oPT4, may be affected by such membrane- and surface-composition alterations.

In order to check if oPT4 leishmanicidal activity was species-specific and evaluate the antileishmanial potential of oPT9, *L. infantum* and *L. amazonensis* promastigotes were treated with both peptides in a concentration range of 0-512 µg/mL for 24h, after which their metabolic activity was measured *via* an Alamar Blue assay. The obtained IC_{50} values are displayed in Table 9 and the respective dose-response curves can be visualized in Fig. 12 (see **Appendix D** for the mean values obtained from all independent experiments).

Table 9 – IC_{50} concentrations of oPT4 and oPT9 in *L. infantum* and *L. amazonensis* promastigotes.

Peptide	IC_{50}			
	L. infantum		***L. amazonensis***	
	µg/mL	µM	µg/mL	µM
oPT4	59.8	23.1	272.56	104.9
oPT9	> 512	> 327	> 512	> 327

The difference between the effects of both peptides can be immediately distinguished, following the same tendency observed in the antimicrobial assays: while oPT4 inhibited the growth of promastigotes in both *Leishmania* species, oPT9 did not have any deleterious effect on parasitic metabolic activity in the concentrations tested. Furthermore, the two species used in this assay respond differently to oPT4 treatment. This peptide demonstrated more toxicity in *L. infantum* parasites, with an IC_{50} of 59.8 µg/mL (23.1 µM), than in *L. amazonensis* promastigotes, where the IC_{50} was 272.56 µg/mL (104.9 µM). Of note, the IC_{50} value for oPT4 in *L. infantum* obtained in this work is superior to that determined by Oliveira *et al*. [147] by more than two-fold, but these results correspond to a single independent experiment (N = 1), and, therefore, do not have the appropriate statistical strength. However, since this variability between different studies was also observed in the previous

experiments, it is likely that they really originate from differences between the peptide stocks and the parasite/bacterial cultures.

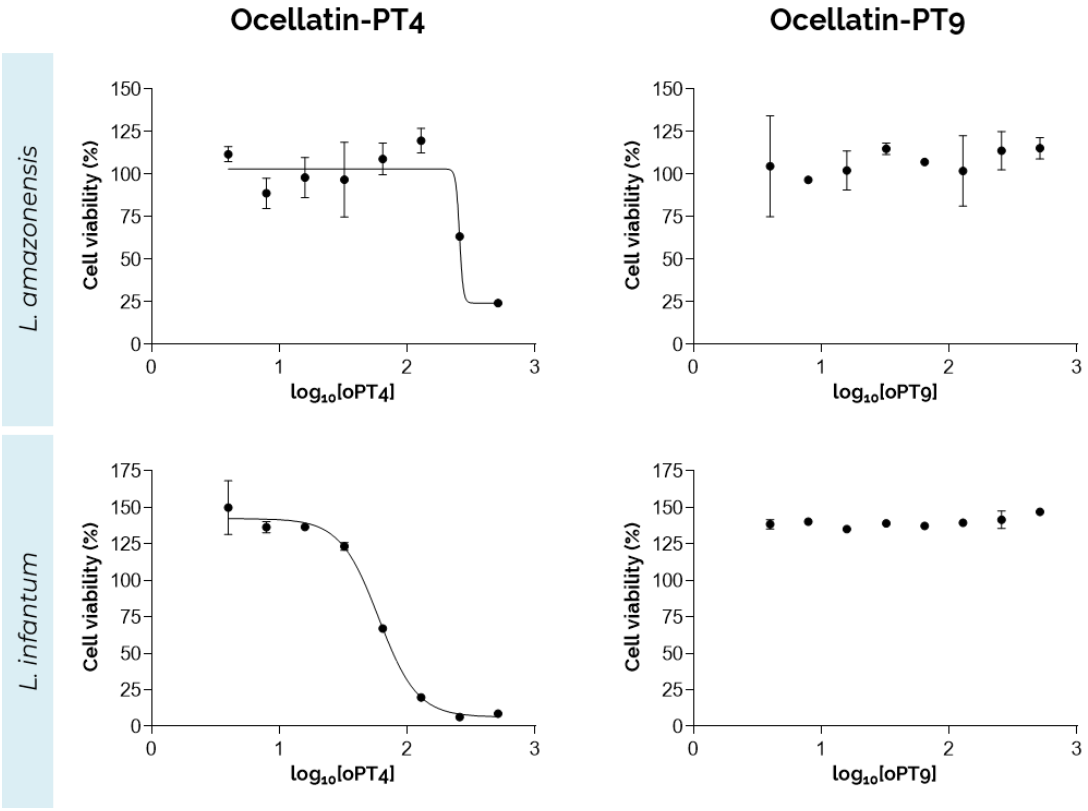

Figure 12 – Representative dose-response curves for *L. amazonensis* and *L. infantum* promastigotes treated with oPT4 and oPT9. Cell viability values are presented as mean ± SD from triplicate measurements.

Given the lack of information on *Leishmania* membrane composition and metabolism, it is difficult to explain these results with more than speculations. Nonetheless, it is interesting that oPT9, which tends to be more toxic for human macrophages and microglia than oPT4, did not have an antileishmanial effect in either of the species tested, since both human and leishmanial cells are eukaryotic and, therefore, more similar in terms of structure and chemical composition than the prokaryotic bacterial cells. Naturally, *Leishmania* parasites are unicellular, while mammalian cells compose much more complex, multicellular organisms (such as human beings), and this may reflect in different defence mechanisms to external threats. Furthermore, the lipid composition of *Leishmania* cell membranes differs from that of mammalian cells, namely in terms of phospholipid and sphingolipid content. Since these lipids modulate membrane properties like permeability and fluidity, as well as nutrient internalisation and vesicle trafficking, it seems reasonable to assume that they account, at least in part, for the observed differences between the responses of mammalian and leishmanial cells [251]. Perhaps the higher cationicity of oPT4, as well as its α-helix structure

stabilised by a C-terminal amidation, plays a more important role in the interaction with bacterial and leishmanial membranes than what was observed with human cells.

Intriguingly, oPT4 had distinct effects not only between mammalian and leishmanial cells, but also between both *Leishmania* species. *L. infantum* and *L. amazonensis* both belong to the *L. Leishmania* subgenus, but species like *L. braziliensis*, *L. guyanensis*, and *L. panamensis* fall under the *L. Viannia* subgenus [252]. While a few studies have shown that the membrane composition of *L. Leishmania* and *L. Viannia* species may be quite distinct [253-255], there is not a lot of information available on the differences between species of the same subgenera. However, it is known that *L. infantum* and *L. amazonensis* have very different pathological mechanisms, considering that the former causes VL and an infection with the latter results mainly in CL. Therefore, the disparate responses to the presence of oPT4 between both species may be owed to factors like distinct membrane chemistry and dynamics, metabolic pathways, and defence mechanisms.

Observing the dose-response curves in Fig. 12, it is also possible to conclude that, in *L. infantum*, cell viability levels tend to exceed 100% for low concentrations of oPT4 and for all concentrations of oPT9. This is in accordance with the idea, proposed after the macrophage biocompatibility assessment, that these peptides have a cellular metabolic effect that may be connected to their mechanism of action and toxicity. Interestingly, in *L. amazonensis*, this effect is less pronounced, accentuating the differences between the responses of both species to the presence of the peptides. Indeed, it is possible that the maintenance of cell metabolic activity levels in *L. amazonensis* is related to the lower susceptibility to oPT4 treatment.

As mentioned previously, the Alamar Blue assay is an indicator of the cellular reducing potential, and the reduction of resazurin to resorufin is carried by co-enzymes like NAD(P)H and FADH. Therefore, enhanced fluorescence levels may result from higher intracellular levels of these co-enzymes. Such an increase in the levels of reduced co-enzymes occurs during oxidative stress, where the presence of reactive species like ROS and RNS triggers metabolic and transcriptional adaptive responses to re-establish the redox balance within the cell [256]. Thus, the greater cell viability observed in *L. infantum* promastigotes treated with oPT4 and oPT9 may indicate that these peptides induce the parasitic production of reactive species, promoting an adaptive response that augments the cellular reducing potential. Higher peptide concentrations possibly result in the intensification of the oxidative stress, exhausting the cellular capability of maintaining the redox balance and ultimately resulting in cell death, as observed for oPT4.

A few AMPs have been shown to increase the cellular production of reactive species. Sampson *et al*. [257] demonstrated that polymyxin B and colistin, two cationic antimicrobial peptides, caused the production of higher levels of hydroxyl radicals (•OH) in *Acinetobacter*

baumannii and other Gram-negative bacterial species. Likewise, treatment of *Candida albicans* with pleurocidin, a broad-spectrum antimicrobial peptide isolated from *Pleuronectes americanus* [258], increased the production of ROS, resulting in mitochondrial membrane depolarisation and release of pro-apoptotic factors [259]. Naturally, a cell viability assay does not provide any direct information on oxidative stress, and there are several factors that could account for the observed increments in metabolic activity. Thus, measuring the levels of ROS and RNS, evaluating mitochondrial function, and assessing the expression levels of enzymes involved in the production of reduced co-enzymes (like glucose-6-phosphate dehydrogenase) [256] in *Leishmania* cells will be absolutely essential to verify this hypothesis.

Besides, as already observed for *L. infantum* parasites treated with oPT4, the effect of these peptides can vary for different stages of the *Leishmania* lifecycle. It should be taken into account that the amastigotes are clinically more relevant, since this is the intracellular form of the parasites, the one responsible for surviving and proliferating inside macrophages [146]. As such, even though studies with axenic amastigotes provide valuable insights on the direct impact of AMPs on this stage of the *Leishmania* lifecycle, it would be more advantageous to test these peptides on infected macrophages and evaluate their effect *via* microscopy techniques, for example. A bioluminescence method has also been developed, where *L. amazonensis* parasites were transfected with the firefly luciferase coding sequence, allowing the monitoring of the infection load in macrophages *in vitro* and *in vivo* [260].

C.4.2. Atomic force microscopy of *L. amazonensis* promastigotes treated with oPT4

It is thought that the most common mechanism of action used by AMPs arises from the interaction with the microbial plasma membrane, resulting in the leakage of intracellular components and nutrients, loss of ionic gradients, disruption of bioenergetic pathways, and ultimately cell lysis [146]. A high amphipathic α-helical content and cationicity generally favour this process, but other aspects like peptide volume and structure within the membrane also influence their antimicrobial potential [261, 262]. In order to shed some light on the mechanism of action of oPT4 and determine whether it affects the parasitic cell membrane, *L. amazonensis* promastigotes treated with this peptide were imaged by AFM. This is a high-resolution microscopy technique with a great sensibility to modifications in cell surface textures, making it an excellent approach to study drug-induced membrane alterations in several organisms, including protozoa [263, 264]. Importantly, it does not require sample coating with a conductive metal neither does it involve vacuum during the imaging process, unlike other microscopy techniques like scanning electron microscopy (SEM) [265].

AFM and SEM images of *L. infantum* promastigotes treated with oPT1 and oPT8 have already been published [147]. In this study, the parasites were treated with sub-lethal (16

µg/mL) and lethal (64 µg/mL) concentrations of each peptide. Concerning the SEM images, the differences between control (untreated) cells and peptide-treated parasites are clear: at a concentration of 16 µg/mL, oPT1 and oPT8 caused elevated circular features that appear to be membrane vesicles; at 64 µg/mL, these vesicles were replaced by holes in the cell body. Such effects were confirmed by AFM imaging, which was only performed for the lowest peptide concentration (16 µg/mL). Collectively, these results demonstrated that the morphology of *L. infantum* cell membrane was altered and its integrity compromised after treatment with oPT1 and oPT8.

However, to the best of our knowledge, AFM imaging of *L. amazonensis* parasites treated with ocellatins-PT had not been performed before. As such, Fig. 13 and **Appendix D** (Fig. D.1) show representative images of control and oPT4-treated *L. amazonensis* promastigotes. Control (untreated) promastigotes presented the classical elongated shape with an anterior flagellum, in accordance with previous microscopy studies [266, 267]. After a 24h treatment with 512 µg/mL of oPT4 (above the IC_{50}), changes on parasite surface texture can be observed: the cell surfaces are more irregular, in contrast with the smooth appearance of control cells, displaying several depressions and elevations on the parasitic plasma membrane. Furthermore, many cells treated with oPT4 were less elongated, which is represented in Fig. D.1B). This rounder morphology has also been observed for *L. infantum* [265] after treatment with other AMPs, as well as for *L. amazonensis* after treatment with 4-nitrobenzaldehyde thiosemicarbazone (BZTS), an antileishmanial molecule [267]. Hence, this indicates that oPT4 treatment affects the cell membrane and morphology of *L. amazonensis* promastigotes.

Conversely, the effects of oPT4 on *L. amazonensis* are not as drastic as those seen in publications with other *Leishmania* species, namely *L. infantum*. As a matter of fact, *L. amazonensis* promastigotes treated with 256 µg/mL of this peptide, a concentration just below the IC_{50} previously determined, generally had a normal morphology and surface texture (data not shown). Even in the samples where promastigotes were treated with 512 µg/mL of oPT4, cells with minor or no surface alterations could still be observed (Fig. D.1C)). These weaker effects on the plasma membrane of *L. amazonensis* may reflect structural differences between this species and *L. infantum* and explain the higher resistance of the former to oPT4 treatment. Furthermore, these results suggest that the mechanism of action of oPT4 in *L. amazonensis* does not rely, at least exclusively, on cell membrane destabilisation. It is possible that the peptide acts on an extracellular or intracellular target, activating a cellular pathway that culminates in cell death and, thus, exerting its toxic effect.

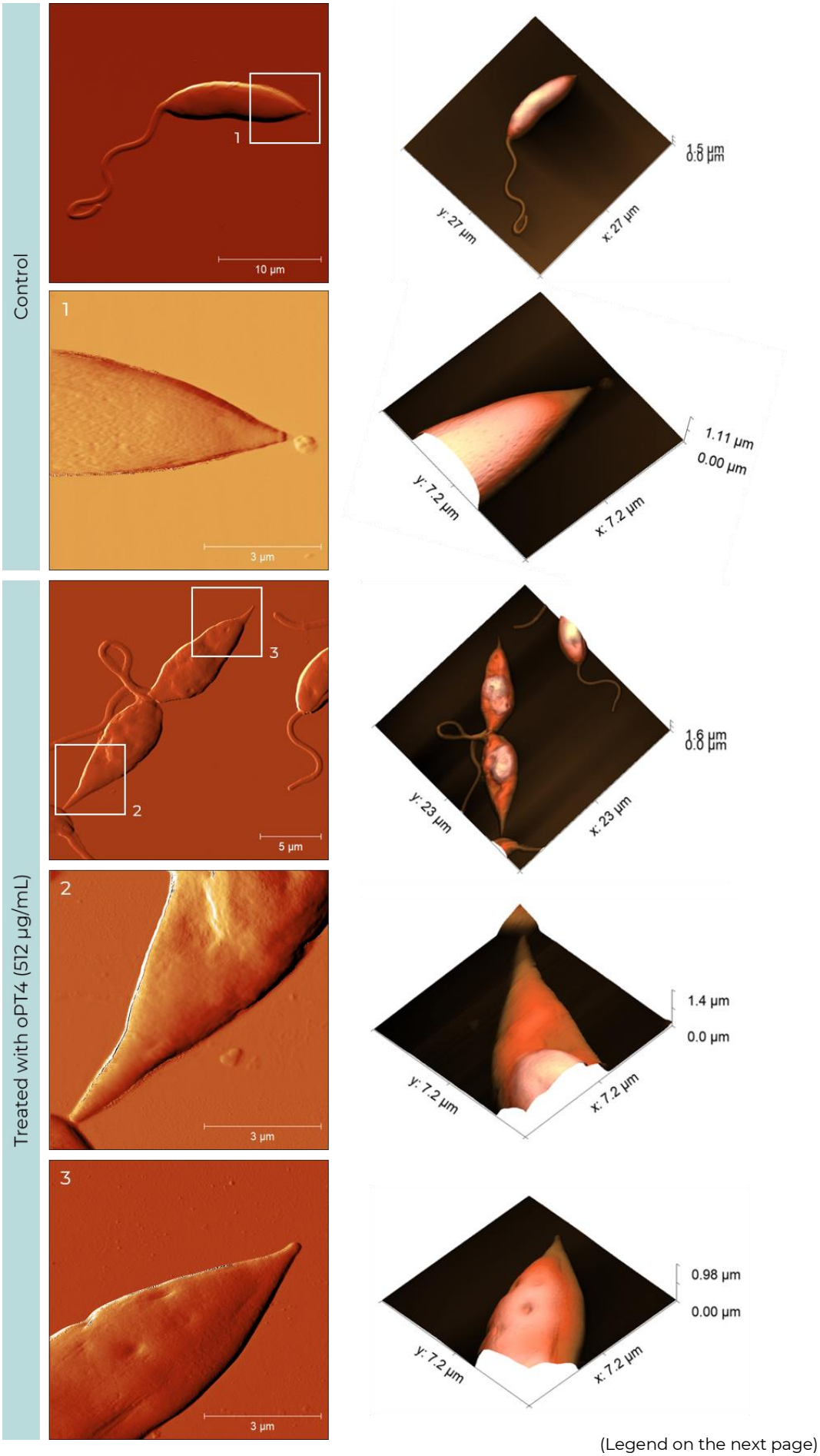

(Legend on the next page)

Figure 13 – Representative AFM images of *Leishmania amazonensis* parasites after treatment with oPT4 (512 µg/mL). Untreated cells were used as control.

In the abovementioned study carried by Britta *et al.* [267], where *L. amazonensis* parasites were treated with BZTS, this molecule did not affect membrane integrity, but it induced the production of ROS and marked alterations on mitochondrial membrane potential and morphology. The authors suggest these effects are related: the synthesis of reactive species can be the cause of the mitochondrial damage. Although BZTS is chemically and structurally very distinct from oPT4, this strengthens the previously postulated hypothesis that this peptide may induce oxidative stress in *L. amazonensis* parasites.

Altogether, these results perfectly demonstrate that the cytotoxicity of a given molecule or compound relies not only on its chemical and structural properties, but also on the characteristics of the target organism.

C.5. Antioxidant and immunomodulatory properties of oPT4 and oPT9 in human microglial cells

C.5.1. FRET and fluorescence live cell imaging

Even though LCI has been available for decades, progressive advances in microscopy techniques, computational analysis, and biosensors with improved sensitivity and stability have made it an increasingly attractive approach to monitor cellular dynamics and processes [268]. The isolation of the infamous green fluorescent protein (GFP) from the jellyfish *Aequorea victoria* and its subsequent application as a fluorescent probe paved the way for the development of versatile fluorescent sensors, which can be used as genetically encoded markers or labels for cellular proteins and organelles [269]. Accordingly, in this project, the responses of human microglial cells treated with oPT4 and oPT9 in the presence of LPS were monitored using LCI and two different types of fluorescent probes: a ratiometric, redox-sensitive FRET probe for the measurement of microglial ROS production [206, 207], and a monomeric near-infrared fluorescent protein (miRFP) to monitor the activation of the NF-kB signalling pathway [208].

HSP-FRET probe: effect of oPT4 and oPT9 on microglial LPS-induced ROS production

FRET (also referred to as Förster resonance energy transfer) is a non-radiative process that occurs between two fluorophores, a donor and an acceptor. Basically, the donor fluorophore is excited at an appropriate wavelength, and the energy it subsequently emits is absorbed by an acceptor molecule. This phenomenon can be intra- or intermolecular [270]. In order for this to occur, there has to exist a significant overlap (> 30%) between the emission spectrum of the donor and the excitation spectrum of the acceptor, and both molecules

should be separated by no more than 10 nm, implying that this technique has a very high resolution [271].

The FRET probe used in this work consists of CFP (donor) and YFP (acceptor) fluorescent domains linked by a redox-sensitive region of a bacterial heat shock protein (HSP-33) (Fig. 14). In a reducing environment, the distance between CFP and YFP domains is short, allowing the occurrence of FRET. In such conditions, the emission of fluorescence by CFP will be low, since a great part of the emitted energy will be absorbed by YFP. When there is a shift to a more oxidative milieu (*i.e.*, production of reactive species), the thiol (-SH) groups in the HSP-33 domain are oxidised, moving the two fluorophore regions apart and decreasing FRET intensity. The energy emitted by CFP is no longer transferred to YFP, and it is released in the form of fluorescence at 470 nm. As such, this effect can be quantified by the ratio between the donor (CFP) fluorescence signal and the FRET signal (CFP/FRET ratio), measured at 535 nm: the CFP/FRET ratio increases with a higher production of reactive species.

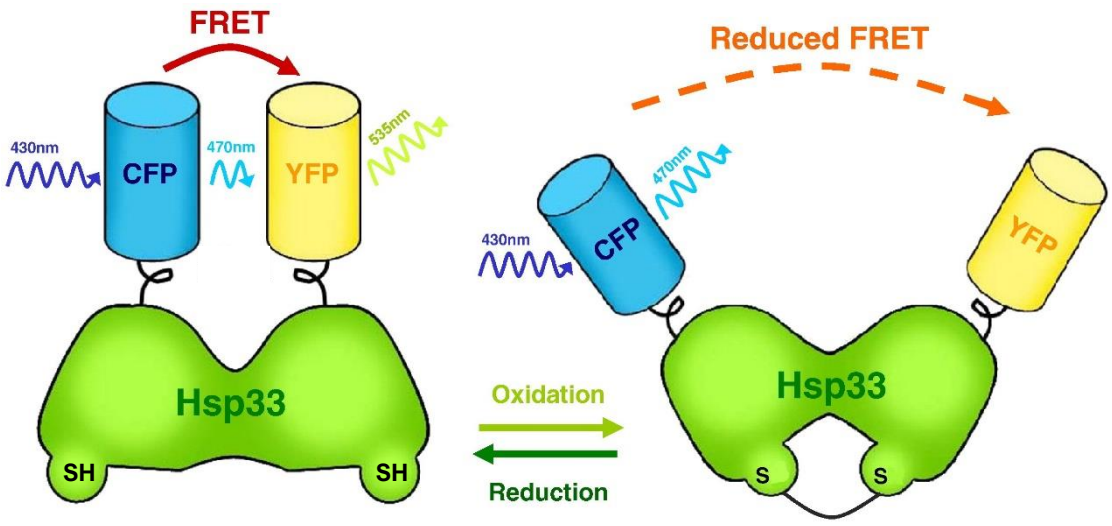

Figure 14 – Redox-dependent change of conformation in HSP-FRET probe. Adapted from [272].

The HSP-FRET probe is sensitive to the production of hydrogen peroxide (H_2O_2), but it does not appear to respond to superoxide [206]. Nevertheless, it is known that the HSP-33 domain reacts with other oxidant species, including nitric oxide (NO) and hypochlorous acid (HOCl) [273], making it an efficient tool for the measurement of intracellular reactive species, mainly ROS.

Previously (**section B.2** of the **Introduction**), it was emphasised how an exacerbated microglial reactivity and inflammatory response can be highly detrimental. ROS (*e.g.* superoxide, H_2O_2, $^{\bullet}OH$) are important players in such pro-inflammatory processes.

Furthermore, the elevated oxygen consumption in the brain and its high lipid content makes it more prone to oxidative damage. In fact, oxidative stress has been implicated in several neurological diseases [274]. To evaluate if oPT4 and oPT9 have a protective effect in microglial cells regarding the production of ROS, HMC3 microglia were transfected with a plasmid encoding the HSP-FRET probe and subsequently treated with each ocellatin peptide. The response to the peptides alone was imaged for 5 minutes, after which LPS was added as a pro-inflammatory stimulus. The results can be visualised in Figs. 15 and 16.

It is possible to conclude that the LPS stimulation resulted in a marked increase in the production of ROS by HMC3 microglial cells, as expected from previous studies [209]. However, in the presence of oPT4, this was completely prevented, and treatment with oPT9 actually decreased the production of ROS triggered by LPS. According to the histogram displayed in Fig. 16B, the differences between the levels of ROS in control and oPT9-treated cells are already statistically significant at 10 minutes ($P = 0.0022$). At 30 minutes, both peptides significantly impaired microglial ROS release after LPS stimulation, suggesting that oPT4 and oPT9 are capable of protecting microglia from LPS-induced oxidative stress. Considering that the peptides demonstrated no direct radical-scavenging activity on the ABTS and DPPH assay, there should be another mechanism by which oPT4 and oPT9 exert the observed antioxidant effect in living microglial cells.

IκBα-miRFP703 probe: effect of oPT4 and oPT9 on microglial LPS-induced NF-κB pathway activation

Monitoring the microglial LPS-induced pro-inflammatory responses was also carried with an indirect measurement of the NF-κB signalling pathway canonical activation. To this end, HMC3 cells were transfected with a plasmid encoding the IκBα-miRFP703 fluorescent probe. As the name implies, this biosensor consists of a fusion protein between the NF-κB inhibitor α (IκBα) and a near-infrared fluorescent protein (miRFP703). The principle behind this experiment is explained in detail in Fig. 17.

Briefly, in the absence of a pro-inflammatory signal, IκBα is located in the cytoplasm, where it binds the transcription factor NF-κB and prevents its translocation to the nucleus. Upon LPS recognition, which is mediated by TLR4, IκBα is phosphorylated by IκB kinase (IKK), ubiquitinated, and degraded in the proteasome, releasing NF-κB and allowing the transcription of pro-inflammatory target genes (*e.g.* TNFα, IL-6). This signalling cascade is known as the classical or canonical activation of the NF-κB pathway [275].

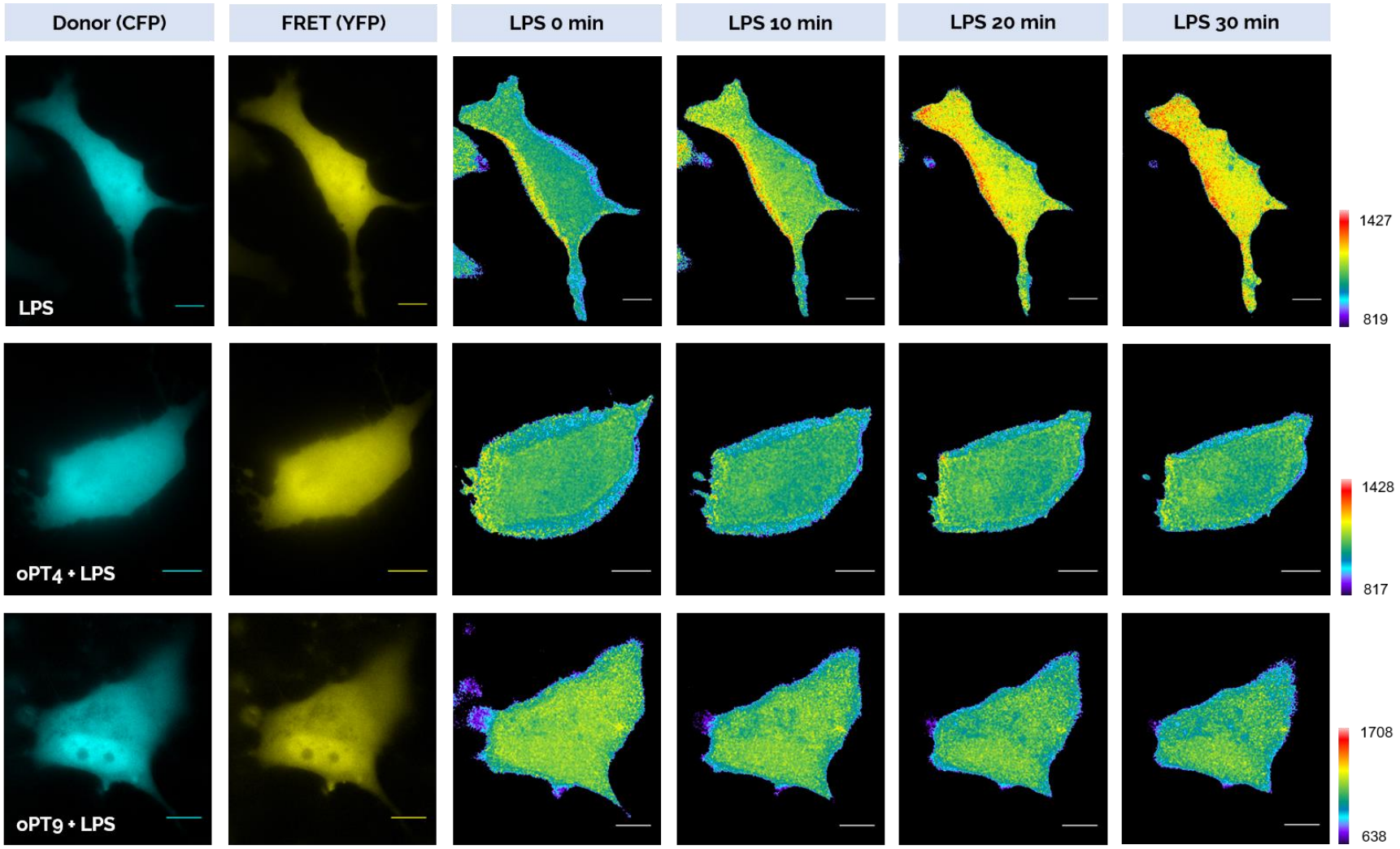

Figure 15 – ROS production after LPS stimulation in microglial cells treated with 100 μM of oPT4 and oPT9 (representative images). Cells treated with LPS alone were used as positive control. Scale bars – 10 μm.

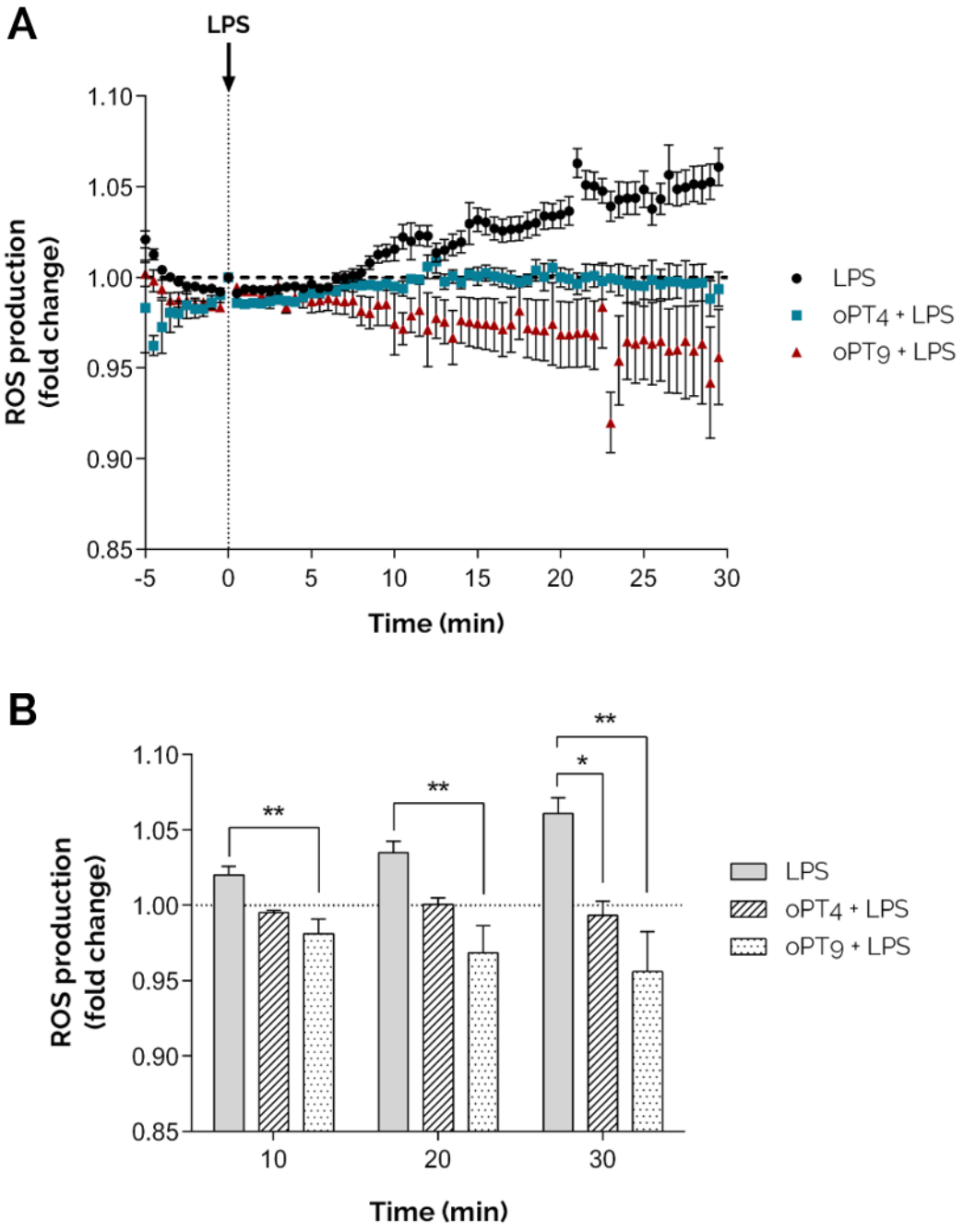

Figure 16 – ROS production by microglial cells after LPS stimulation and treatment with 100 µM of oPT4 and oPT9 (normalised donor/FRET ratios). **A)** Time-course measurements of microglial ROS release. The values at 10, 20, and 30 min. are represented in the histogram (**B**). The donor/FRET ratio at t = 0 min in each condition was used for the normalisation. Values corresponding to the measurements from 17 (LPS), 5 (oPT4 + LPS), and 13 (oPT9 + LPS) cells are represented as mean ± SEM. *P < 0.05; **P < 0.01.

Hence, the use of the IκBα-miRFP703 fusion protein allows the real-time (or near real-time) monitoring of IκBα degradation, which translates into a decrease of the fluorescence signal intensity that can be monitored and quantified [208]. Therefore, a more intense NF-κB pathway activation corresponds to a lower fluorescence signal.

The results of this experiment are available on Figs. 18 and 19. Expectedly, LPS induced NF-κB pathway activation in HMC3 cells, as demonstrated by the reduction in IκBα fluorescence levels. However, the two peptides had distinct effects: observing the time-course graph (Fig. 19A), it appears that oPT4 failed to protect microglia from the LPS-induced NF-κB activation, while incubation with oPT9 tends to delay the degradation of IκBα. Indeed, the fluorescence signals in oPT9-treated cells are consistently higher than those of control or oPT4-treated cells, although they still decrease over time. Similarly to the HSP-FRET analysis, the timepoints of 10, 20, and 30 minutes after LPS stimulation were chosen for the statistical analysis (Fig. 19B). Conversely, the differences between oPT9 and the remaining groups are only significant at the 10 minutes timepoint ($P = 0.0005$), albeit both the histogram and the time-course graph, as well as the heatmaps (Fig. 18), suggest that cells incubated with this peptide tend to maintain higher levels of IκBα activity. Relevantly, in this case, fewer cells were analysed than in the HSP-FRET probe experiment, because the transfection efficiency for the IκBα-miRFP703 biosensor was lower. Moreover, the intercellular variability appears to increase for later timepoints, as represented by the higher SEMs in the graphs. Possibly, repeating this experiment and analysing a greater number of cells will return a more statistically robust effect.

Nevertheless, oPT9-treated microglial cells clearly tend to yield higher fluorescence intensities, implying that this peptide may have an anti-inflammatory effect. Additionally, the greater antioxidant effect of oPT9 observed in the previous experiment could be related to this capacity of hampering NF-κB activation: NF-κB is involved in the transcription of genes that code proteins like the NADPH oxidase NOX2, iNOS and neuronal NOS (nNOS), cyclooxygenase-2 (COX-2), and cytochrome p450 enzymes, all of which participate in the production of ROS or RNS [276]. Hence, it is plausible that the reduced ROS levels in cells incubated with oPT9 are due to a lower activation of the NF-κB signalling pathway. The same hypothesis was postulated by Sousa *et al*. (submitted), where ocellatins-K1(1-16) and -K1(1-21), which are truncated forms of ocellatin-K1, also demonstrated antioxidant and anti-inflammatory activity in microglia. Interestingly, both ocellatin-K1(1-16) and oPT9 have 16 amino acids, and their sequences differ in only two positions: the amino acids Leu^5 and Gln^7 in oPT9 become Ile^5 and Lys^7 in ocellatin-K1(1-16). Such amino acid composition and sequence may, therefore, be important for the anti-inflammatory properties of these ocellatin peptides.

Focusing on oPT4, it is interesting that, despite having demonstrated an antioxidant activity in living microglia, this peptide does not seem to impair NF-κB pathway activation *via* IκBα. Thus, it is likely that its protective effect on the production of reactive species arises from another mechanism.

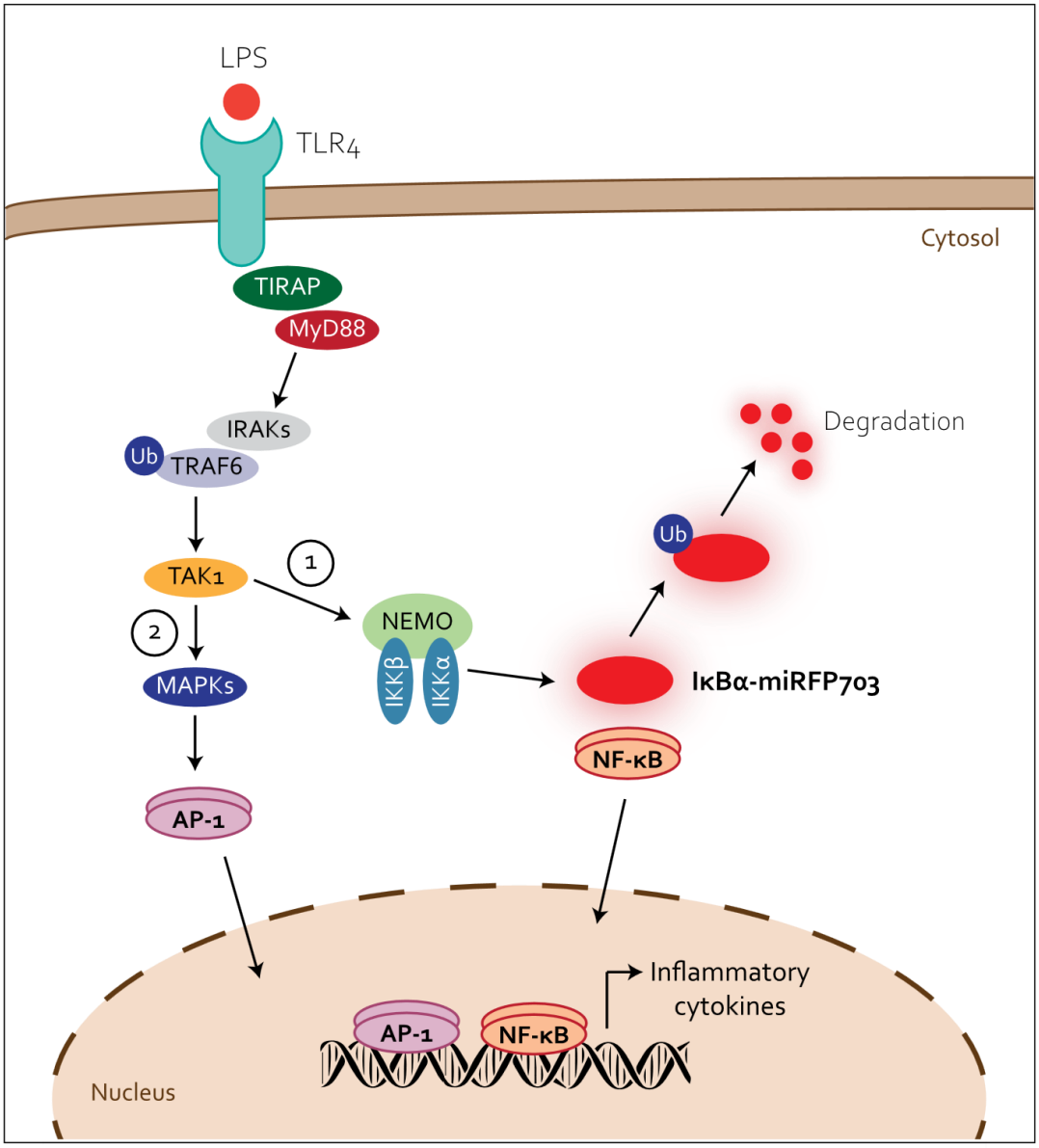

Figure 17 – Principle of the IκBα-miRFP703 fluorescent probe (adapted and redrawn from [277]). The engagement of LPS by TLR4 activates a MyD88-dependent pathway, which requires the presence of TIRAP. This results in the recruitment of TRAF6 and IRAKs, which activate the TAK1 complex *via* ubiquitination (Ub). In turn, TAK1 triggers two distinct pathways. **1) NF-κB canonical activation:** TAK1 activates the IKK complex, constituted by NEMO, IKKα, and IKKβ, that phosphorylates IκBα, which is then ubiquitinated and degraded in the proteasome. Because IκBα is coupled to a miRFP fluorescent protein, this degradation is monitored by a decrease in the fluorescence signal. The NF-κB dimer is then released and translocated to the nucleus. Therefore, the IκBα-miRFP703 probe is an indirect measurement of the NF-κB pathway canonical activation. **2)** The TAK1 complex is also capable of activating the MAPK pathway, which activates AP-1, another transcription factor. **Abbreviations:** AP-1 – activator protein 1; IκBα – NF-κB inhibitor α; IKK – IκB kinase; IRAK – interleukin-1 receptor (IL-1R) associated kinase; LPS – lipopolysaccharide; MAPK – mitogen-activated protein kinase; miRFP – monomeric near-infrared fluorescent protein; NEMO – NF-κB essential modifier; NF-κB – nuclear factor κ-light-chain-enhancer of activated B cells; TAK – transforming growth factor-β (TGFβ)-activated kinase-1; TIRAP – Toll/IL-1R (TIR)-containing adaptor protein; TLR4 – Toll-like receptor 4; TRAF – tumour necrosis factor receptor (TNFR)-associated factor.

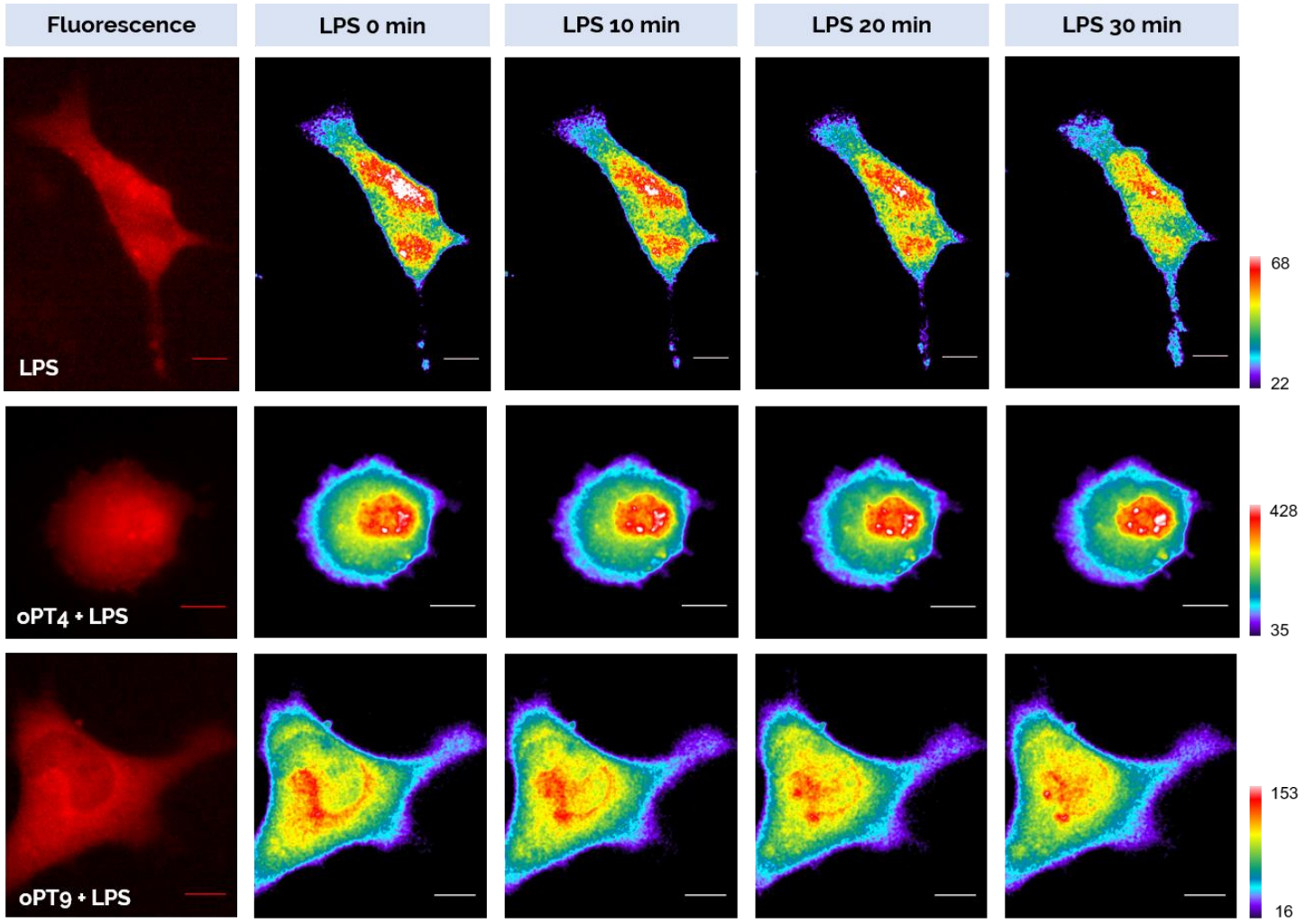

Figure 18 – IκBα expression after LPS stimulation in microglial cells treated with 100 μM of oPT4 and oPT9 (representative images). Untreated cells were used as control. Scale bars – 10 μm.

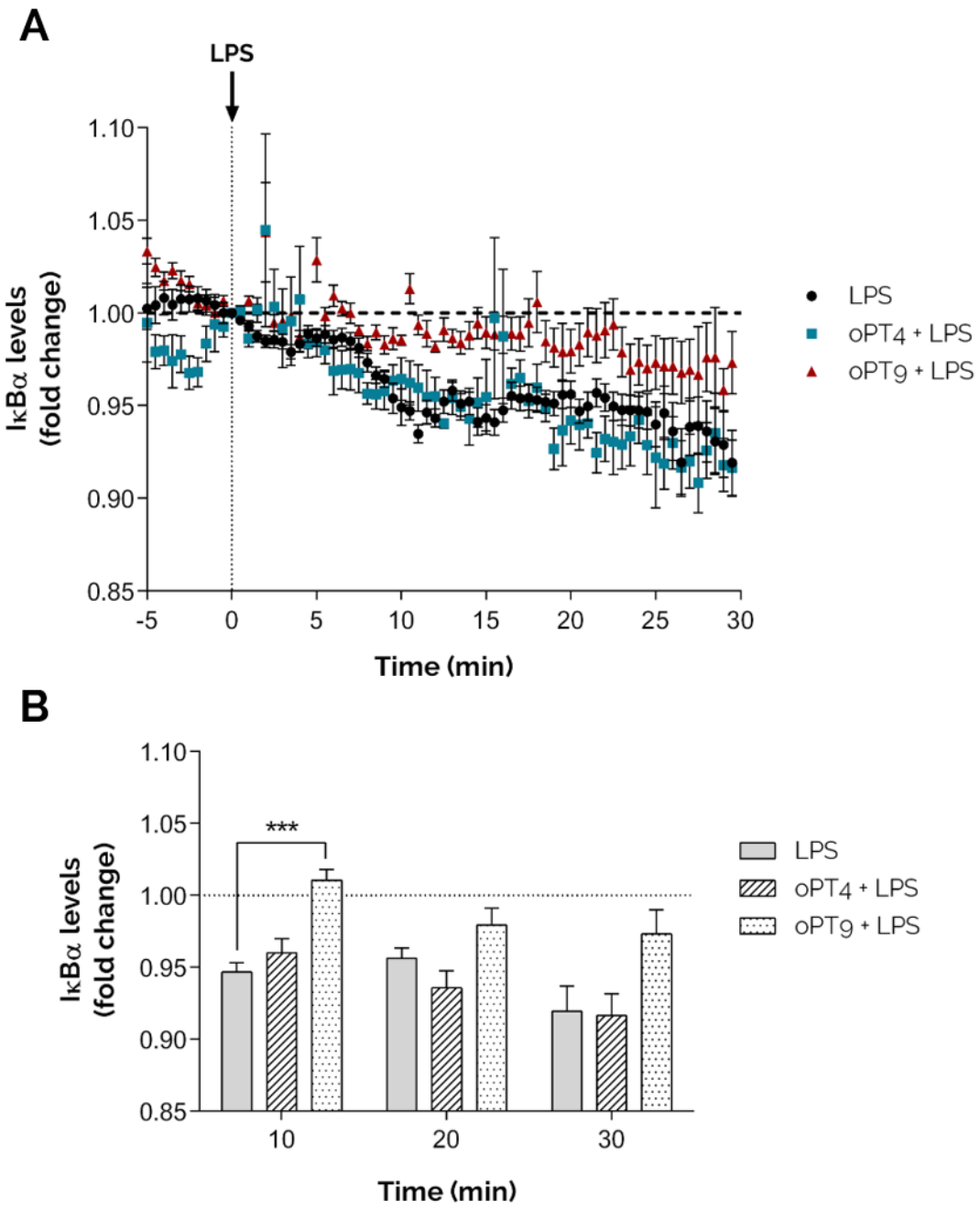

Figure 19 – NF-κB pathway activation in oPT4- and oPT9-treated microglia (100 μM) after LPS stimulation (normalised fluorescence signals). **A)** Time-course measurements of microglial NF-κB pathway activation. The values at 10, 20, and 30 min. are represented in the histogram (**B**). Fluorescence intensity at t = 0 min was used for the normalisation. Values corresponding to the measurements from 9 (LPS), 5 (oPT4 + LPS), and 8 (oPT9 + LPS) cells are represented as mean ± SEM. ***P < 0.001.

Observing, once again, Fig. 17, it is possible to conclude that TLR4 signalling results not only on IκBα degradation and consequent NF-κB translocation to the nucleus, but also on the activation of another transcription factor, activator protein 1 (AP-1). Like NF-κB, AP-1 has as target genes those that code for various cytokines, chemokines, and respective receptors,

among others [278]. Accordingly, oPT4 may have an inhibitory effect on the activation of this transcription factor that is not reported by the fluorescent probe used herein.

Otherwise, instead of decreasing ROS production, oPT4 may act by stimulating the activity of enzymes involved in the synthesis of intracellular antioxidants, like glutathione, that contribute to the reported stabilisation of the ROS levels and maintain the redox balance in microglial cells. In fact, several well-known antioxidants from natural sources like broccoli, green tea, turmeric, among others, act by modulating the expression of enzymes that participate in glutathione metabolism, including glutathione peroxidase (GPx), glutathione-S-transferase (GST), and γ-glutamylcysteine synthetase (γGCL) [279]. Uncovering whether this is also the case for oPT4 will implicate further experiments to measure the levels of oxidised (GSSG) and reduced (GSH) glutathione, as well as the expression and activity of said enzymes.

Cathelicidin-PY, an AMP isolated from the skin secretions of the frog *Paa yunnanensis*, inhibited macrophage pro-inflammatory cytokine and NO production, as well as TLR4 expression, after LPS stimulation. In nuclear magnetic resonance (NMR) studies, it was demonstrated that this peptide binds LPS, leading the authors to suggest that the anti-inflammatory effect of cathelicidin-PY may be owed to a direct blocking of LPS [280]. Accordingly, in the **CD structural studies**, we demonstrated that the structure of oPT4 was modulated by the presence of different LPS concentrations, indicating an interaction between the peptide and the bacterial cell wall component that was not observed for oPT9. Ergo, one could also propose that oPT4 is capable of binding LPS, consequently impairing its engagement by TLR4 receptors in microglia and inhibiting its pro-inflammatory action. This would explain why the levels of ROS production in microglial cells remained relatively unaltered, but it is inconsistent with the described activation of the NF-κB pathway.

These results highlighted, once more, the differences between the biological effects of oPT4 and oPT9. While both showed antioxidant activity in living microglial cells, only oPT9 tended to delay IκBα degradation and consequent NF-κB pathway canonical activation. It is possible that the shorter length of oPT9 favours its internalisation, whereby the peptide can interact with specific targets in the cytosol, but, as exposed previously in this dissertation, confirming this hypothesis will require additional studies. In fact, even though several other amphibian peptides have demonstrated both pro- and anti-inflammatory properties, their mechanism of action has yet to be precisely elucidated. Pantic *et al.* [59] suggested that these immunomodulatory effects may support the participation of skin peptides on the innate immune responses of amphibians. They further hypothesized that a balance between these pro- and anti-inflammatory effects helps maintain amphibian skin homeostasis, activating immune cells when a pathogen is detected and promoting an immunosuppressive environment when no such threat is present.

It would be interesting to repeat the reported LCI experiments in the presence of each peptide alone. It is possible to see that, in the five minutes that preceded the LPS addition to the cells, the fluorescence signals fluctuate, possibly revealing that an effect on microglial responses is elicited just by the presence of oPT4 and oPT9. Alternatively, a longer baseline imaging should be performed (10-30 min), in order to clarify whether those fluctuations stabilise over time or if they might influence the result interpretation when LPS is added. In addition, the presented results can be complemented with the analysis of the gene and protein expression profiles of microglia before and after the described treatments, using techniques like quantitative reverse transcription polymerase chain reaction (RT-qPCR), western blotting, and ELISA. The evaluation of the expression of mediators like IL-1β, IL-6, IL-10, TNFα, pro-oxidant and antioxidant enzymes, among others, will allow a more in-depth characterisation of the effects of oPT4 and oPT9 on microglial inflammatory responses. This drove us to carry out the next, and final, experiments.

C.5.2. TNFα expression by LPS-stimulated microglial cells in the presence of oPT4 and oPT9

To evaluate the effect of oPT4 and oPT9 on the expression of pro-inflammatory mediators, we started by performing an ELISA for the detection of TNFα. HMC3 microglial cells were treated with each peptide in the absence or presence of LPS, and the conditioned cell medium was collected for TNFα quantification. However, as we can see in Table 10, no detectable levels of this cytokine were present in nearly any of the experimental conditions. The lowest and highest TNFα concentrations used in the calibration curve (Appendix E, Fig. E.1.) were 4 and 500 pg/mL, respectively, meaning that even in the conditions where a low concentration of this cytokine was detected, it was outside of this range. Of note, it was not possible to perform the analysis for the cells treated with 50 µM of oPT4, due to a problem in the wells containing these cells that precluded MCM collection.

Studies have indicated that the concentrations of TNFα secreted by HMC3 microglial cells under basal conditions range between 4 and 28 pg/mL [281, 282], implying that they should have been detected by this assay. Furthermore, the LPS stimulus was expected to increase the production of this pro-inflammatory cytokine, but that is not what we observed. It is unlikely that the experimental ELISA procedure itself had any issue, since it responded to the pure TNFα solutions used to build the calibration curve. Nonetheless, there are several hypotheses that may explain these results. On one hand, the used cellular density may have been inappropriate, and a small number of cells may have accounted for the production of very low amounts of TNFα. On the other hand, it is possible that the concentration of LPS (500 ng/mL) was not sufficient to induce any alterations in cytokine expression. This is, however, improbable. In a study where a range of 10 to 5000 ng/mL of LPS was used, even the lowest concentration was enough to significantly increase IL-6 secretion [283], although

the production of TNFα was not measured. Of note, the release of both these cytokines is often differential, and a stimulus that enhances the production of IL-6 may not result in the secretion of TNFα. Lindberg *et al*. [284] demonstrated that treatment of HMC3 cells with Aβ peptides markedly increased IL-6 secretion, but the levels of TNFα, IL-1α, and IL-1β were undetectable even after incubation with Aβ. As such, to uncover the effect of oPT4 and oPT9 in the pro-inflammatory response elicited by LPS in microglia, it could prove more effective to quantify IL-6 secretion rather than that of TNFα.

Table 10 – TNFα production by LPS-stimulated microglia treated with oPT4 and oPT9. Untreated cells were used as negative control. Cells treated with LPS only were used as positive control. Results are presented as mean ± SD (25 µM, N = 1, triplicate measurements) or mean ± SEM (50 µM, N = 2).

Treatment	[TNFα] (pg/mL)	
	[Peptide] = 25 µM	[Peptide] = 50 µM
Untreated	0.00 ± 0.00	0.00 ± 0.00
LPS	0.00 ± 0.00	3.76 ± 3.76
oPT4	0.00 ± 0.00	-
oPT4 + LPS	0.00 ± 0.00	-
oPT9	0.86 ± 1.49	0.00 ± 0.00
oPT9 + LPS	0.00 ± 0.00	0.00 ± 0.00

C.5.3. Nitrite production by LPS-stimulated microglia treated with oPT4 and oPT9

NO is an important mediator of numerous biological processes, including the maintenance of vascular homeostasis, neurotransmission, and immune responses [285]. Its synthesis can be triggered by several pro-inflammatory stimuli and it is carried by various NOS enzymes, including iNOS, nNOS, and endothelial NOS. Like the excessive production of ROS results in the highly detrimental oxidative stress, an exacerbated synthesis of NO may culminate in nitrosative stress, potentially causing cellular and tissue damage [286]. Additionally, NO is capable of reacting with ROS like superoxide, originating aggressive oxidants like peroxynitrite ($ONOO^-$) that further aggravate these nefarious effects [287]. Within the CNS, perturbances in NO signalling have been implicated in the process of neuroinflammation and pathogenesis of neurodegenerative diseases like AD, PD, amyotrophic lateral sclerosis, and multiple sclerosis [288].

Because the half-life time of NO in biological systems is very short (1 to 30 seconds), techniques for its indirect measurement based on nitrite (NO_2^-) and nitrate (NO_3^-), products of its oxidation by O_2, have been developed. One such method is that of the Griess nitrite colorimetric assay [286]. It is based on a reaction between sulphanilamide, N-1-napthylethylenediamine, and nitrite, which forms a stable azo compound that has an absorbance maximum at approximately 550 nm [289]. This method was used to quantify the production of NO metabolites by LPS-stimulated microglia after treatment with both peptides. The results can be visualised in Fig. 20.

Similarly to what was observed for the TNFα quantification, the levels of nitrite produced by microglial cells were very low in every experimental condition. Despite being quantifiable, the concentrations in every sample were very close to the inferior limit of detection of the standard curve (Fig. E.2., concentration range: 0.4 – 50 µM). As such, none of the treatments (LPS and each peptide alone or in combination) significantly affected the production of nitrite by HMC3 microglia comparing to the control levels. Of note, only in one of the two independent experiments we performed did LPS stimulation result in the detection of higher levels of nitrite, which translates into an elevated average concentration, but a very high variation between both experiments.

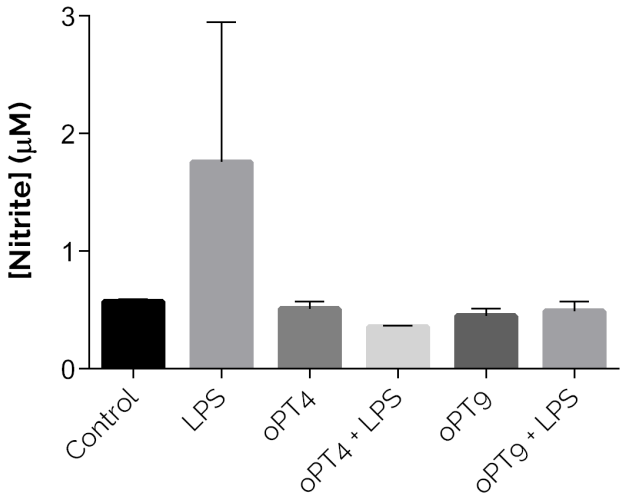

Figure 20 – Nitrite production by LPS-stimulated microglia treated with oPT4 and oPT9. Untreated cells were used as negative control. Cells treated with LPS only were used as positive control. Results are expressed as mean ± SEM (N = 2).

The rationale behind the presented TNFα and NO metabolite quantification assays is that the expression of genes that code said cytokine and NOS enzymes is controlled by the NF-kB pathway [288, 290]. Since oPT4 and oPT9 demonstrated a differential activation of this signalling cascade, we wanted to assess whether this had a measurable effect in terms of effector pro-inflammatory molecules. Therefore, it was expected that oPT9 would decrease

TNFα and NO secretion by microglia induced by LPS, while the effect of oPT4 in the inflammatory response of these cells could be further uncovered. Alas, it appears that LPS failed to elicit the intended pro-inflammatory response, which may raise the question as to whether it is a proper stimulus for these analyses. As a matter of fact, it has been demonstrated that this immortalised cell line is less responsive to LPS than primary microglia [204]. It should, however, be kept in mind that LPS successfully induced the production of ROS and NF-κB pathway activation in living microglial cells, even though it was present at twice the concentration used in these last studies (1 µg/mL vs. 500 ng/mL).

It is also possible that the HMC3 microglial cell line is not adequate for such assays. According to a recent review [212], «there are no available evidence that the CHME3/HMC3 cells release NO under basal conditions or in response to inflammatory activators», although the expression of iNOS has been described at mRNA and protein levels. In order to shed some light on the pro-inflammatory profile of HMC3 cells and determine if they are suitable for further testing with oPT4 and oPT9, it would be advantageous to use other activators of their inflammatory response. Rajalakshmy *et al*. [291] showed that a strong pro-inflammatory response is induced in HMC3 cells by the NS3 protein of the hepatitis C virus, *via* activation of the NF-κB pathway through TLR2 or TLR6 signalling. This resulted in the production of several pro-inflammatory cytokines, including IL-1β, IL-6, IL-8, and TNFα. Thus, stimulation of HMC3 microglia with this protein could be used as a more potent pro-inflammatory trigger.

Naturally, the use of the HMC3 cells presents numerous advantages: i) they are easy to maintain and have high proliferation rates; ii) the transfection efficiencies are higher than those of primary cells, which was relevant for the present study; iii) they are an easily accessible human microglial model, contrarily to human primary microglia. Nevertheless, testing oPT4 and oPT9 in microglial primary cell cultures will be imperative. It is well-established that the use of immortalised cell lines is associated with various issues, and the HMC3 cell line is not an exception. It has been demonstrated that the microglial phenotype can suffer modifications upon viral immortalisation [292]. A number of recent studies compared microglial cell lines with primary microglia, further accentuating the differences between these models. In one of these publications [293], the authors proved that the response of the murine microglial cell line BV2 to LPS poorly represents that of primary cells. Research by Melief *et al.* [294] showed considerable differences between the transcriptional profiles of HMC3 cells and human primary microglia, isolated from post-mortem brain tissue. Moreover, the HMC3 cell line was developed from embryonic microglial cells, which may not be an accurate representation of adult microglia [292].

Hence, the available evidence suggests that the use of primary cell cultures may represent the next step to study the effects of oPT4 and oPT9 on microglial gene and protein expression.

oPT4 and oPT9 as Therapeutic Agents: Where Do We Stand?

In the last decade, several antimicrobial peptides have been isolated from a wide variety of bacterial, plant, and animal species with the objective of combating the current antibiotic resistance crisis. Versatile research on this field has uncovered other potential applications for such peptides, as it has been shown by the present work as well. Accordingly, oPT4 and oPT9 demonstrated very interesting properties, and, albeit belonging to the same peptide class, quite distinct biological activities. Their structural and physicochemical differences partly explain these results, providing valuable information that can be used on the development and refinement of novel therapeutic molecules.

Starting with oPT4, this peptide is a promising antimicrobial agent. Not only was it effective against Gram-negative and Gram-positive bacterial species, posing as a peptide antibiotic candidate, but also against two *Leishmania* species, *L. infantum* and *L. amazonensis*, even though with distinct potencies. The potential for application on leishmaniasis increases even further considering that this peptide was not cytotoxic for human macrophages, target cells for *Leishmania* parasites, demonstrating selectivity against parasitic cells. Nevertheless, there are several challenges that hamper the development of effective antileishmanial agents. It should be kept in mind that oPT4 was only tested against promastigotes, in the case of *L. infantum* and *L. amazonensis*, and axenic amastigotes, only for *L. infantum*. In their natural, infective state, however, *Leishmania* amastigotes replicate inside macrophages, implying that the therapeutic agent must be internalised by host cells in order to reach the infecting *Leishmania* cells [145]. Thus, the action of oPT4 against axenic amastigotes is not a sufficient indicator of its effectiveness in the treatment of leishmaniasis. *In vitro* studies with infected macrophages, but, more importantly, *in vivo* research with leishmaniasis animal models will be pivotal to confirm this hypothesis.

Besides, when one of the biggest hurdles in fighting leishmaniasis is the poor financial resources in the countries with the highest incidence of the disease, it is important to have in mind the high costs associated with peptide synthesis. Even if ocellatins-PT, particularly oPT4, can effectively treat the infection and eradicate the disease in *in vivo* models, it will be difficult to make this therapy reach most of the people in need. A possible solution brought up by Rivas *et al*. [146] is determining the shortest peptide that still retains the antileishmanial activity, in order to reduce both the production costs and immunogenicity. Relevantly, it is also possible to test for amino acid substitutions that can potentiate the therapeutic effect while maintaining a shorter peptide length and a low cytotoxicity against host cells.

Moreover, several other strategies can be used to improve this peptide and increase the chances of applying it as a therapeutic agent. The substitution of L-amino acids for D-amino acids, for instance, can decrease its susceptibility to proteases and extend its half-life time when administered. This modification has already been tested and it has not resulted in a

loss of action of the AMPs, implying that the microbial growth inhibitory effect does not require a specific molecular chirality [295]. The combination of oPT4 with other well-established antileishmanial agents may also result in a more effective treatment [146]. Additionally, instead of being administered intravenously or intramuscularly, which requires special facility resources and medical/technical staff, oPT4 can be included in an ointment for the treatment of lesions caused by *L. amazonensis* or even *L. infantum*, since the aggravation of visceral leishmaniasis often results in the skin lesions that characterise post kala-azar dermal leishmaniasis. Perhaps the combination of this peptide with other components that accelerate skin wound healing will minimise scarring and pain.

oPT9, in turn, did not show any inhibitory activity against *E. coli*, *S. aureus*, *L. infantum* or *L. amazonensis*. We attribute this lack of antimicrobial potential mainly to a negative peptide charge that does not favour its interaction with the bacterial and leishmanial membranes. In addition, it is possible that the peptide's length, despite having an α-helix secondary structure, is too short to effectively destabilise the plasma membrane of these organisms at the concentrations tested. However, oPT9 may have interesting antioxidant and anti-inflammatory properties in microglia, since it was capable of decreasing ROS production and NF-κB pathway activation *via* IκBα induced by LPS in these cells. It is important to repeat the biocompatibility assays, in order to uncover potential toxic effects of the peptide and determine the maximum concentration tolerated by microglial cells that still provides protection against inflammation. It will also be interesting to test the effect of this peptide on other CNS components, including neuronal and astrocytic cells, and verify if a protective effect is also observable. Because the human life expectancy continues to grow and the population is ageing further each day, it is important to develop new strategies to prevent and treat chronic inflammatory and neurodegenerative diseases.

Final Remarks

Conclusion

This project brought into light the relevance of bioprospecting as a method to isolate and identify new versatile molecules with therapeutic potential. Particularly in amphibian skin secretions, a multitude of compounds with proven beneficial effects and low toxicity is available, of which oPT4 and oPT9 are only two examples. The presented research aimed at characterising these two peptides and evaluating, on one hand, their antiparasitic effect in *Leishmania*, and, on the other hand, their antioxidant and immunomodulatory potential in microglia. It was interesting to observe how the structural and chemical differences between these two peptides conditioned their action on the several biological models used in the present work.

oPT4 had the highest antibacterial and antiparasitic potential. It was effective, albeit with variable potency, against *E. coli* and *S. aureus*, which are, respectively, Gram-negative and Gram-positive bacteria, and *Leishmania infantum* and *L. amazonensis*. These results demonstrated this peptide's capability of interacting with diverse types of cell membranes, each organised in a particular structure and constructed with distinct "building blocks". It is curious that, while this peptide is toxic to all these unicellular live forms, it showed favourable safety profiles in human erythrocytes, macrophages, and microglia, having even exerted a protective effect in this last cell type against the production of reactive species. Such a selective action opens the road even further for the therapeutic application of oPT4. Conversely, oPT9 did not present any antimicrobial activity, but it showed an antioxidant and anti-inflammatory potential in living microglial cells that raises the possibility of application in a distinct field, namely that of neuroinflammation. Even though there is still a long way to go before these peptides can be used as valid treatment options, these are promising indicators of their bioactivity, that should be confirmed and strengthened by additional research.

Finally, it is pivotal to have in mind that «with great power, comes great responsibility», and the idea of exploring nature for therapeutic solutions should only be put into practice if done consciously. Our natural environment is undoubtedly a valuable source of active compounds that can be used to address various clinical issues, but only as long as its biodiversity and ecosystems are preserved. Therefore, it is essential to prioritise and keep developing non-invasive techniques that allow the extraction and isolation of new substances with minimal animal sacrifice, as well as sustainable practices that will guarantee the maintenance and preservation of these natural resources.

Future Work

Despite promising, the presented results represent the first step of a long journey that must be completed until oPT4 and oPT9 can be used as therapeutic agents. Accordingly, a few experiments are already on-going or will be performed on a short-term:

i. Assessment of the neuroprotective effect of oPT4 and oPT9: the conditioned medium from LPS-activated microglial cells treated with both peptides will be collected and used to treat primary neuronal cells and subsequently evaluate neuronal cell death;
ii. Gene and protein expression analysis of LPS-activated microglia treated with oPT4 and oPT9, using RT-qPCR and ELISA techniques;
iii. Evaluation of the effect of both peptides on microglial release of glutamate and consequent neuronal excitotoxicity, using a glutamate-responsive FRET probe.

As emphasized during the present thesis, on a longer run, it will be important to perform further experiments in order to clarify the mechanism of action of oPT4 and oPT9. In the case of oPT4, it is also essential to test its antileishmanial activity *in vitro*, in amastigote-infected macrophages, and *in vivo*, in an animal model of the disease. Furthermore, if the antioxidant/anti-inflammatory properties of oPT9 and/or oPT4 and their protective effect on microglia and neurons are confirmed, it will be necessary to test these peptides on other cell types, mainly astrocytes, which also contribute for the inflammatory response in the CNS. Once robust *in vitro* information on these protective actions is gathered, oPT4 and oPT9 can be tested on animal models of neuroinflammation and neurodegeneration.

Glossary

Amyloid β (Aβ)	Peptide that results from the proteolytic cleavage of a transmembrane protein, amyloid precursor protein (APP), and is associated with the pathogenesis of Alzheimer's disease **[**296**]**.
Anthroponotic disease	Disease that is transmitted from human to animal hosts.
Axenic culture	Constituted by a single type of cell or organism.
α-synuclein	Presynaptic neuronal protein involved in the pathogenesis of Parkinson's disease [297].
Bioprospecting	Searching nature for valuable products in the fields of pharmaceuticals, cosmetics, and industry.
Bufotoxins	Family of toxins produced by toads of the *Bufo* generus.
Cartogram	Type of representation where the geography of given regions is deformed to convey a numerical variable. These regions may be enlarged or shrunk depending on the value of this variable [298].
Chirality	Geometric property of certain molecules or ions, whose real and mirrored images are not superimposable.
Concanavalin A	Lectin isolated from the plant *Canavalia ensiformis* commonly used as a pro-inflammatory stimulus [299].
Holocrine secretion	«A secretion in which the entire cell and its contents are extruded as a part of the secretory product» [300].
Molar ellipticity	Ellipticity (θ) is the unit (in degrees, deg) defined for circular dichroism that quantifies the differential absorption of left-handed and right-handed polarised light by a given molecule. Molar ellipticity, [θ], is corrected for concentration, and its units are $deg.cm^2.dmol^{-1}$ [220].
Monoisotopic mass	The monoisotopic mass of a given molecule is calculated using the masses of the most abundant isotopes of each element in its constitution [301].
Neuroinflammation	Inflammation in the central nervous system.
Nociceptors	Specialised peripheral sensory neurons responsible for pain perception upon potentially damaging conditions (alterations in temperature, pressure, presence of an injury) [302].
Proboscis	«The long nose of some animals, or the long tube-like mouth of some insects» [303].
Reactive gliosis	Non-specific response of glial cells (astrocytes, microglia, and others) to an injury or threat [304].
Synaptic stripping	Removal of non-functional synapses [163].
Zoonotic disease	Disease that is transmitted from animal to human hosts.
Zwitterionic	Property of a molecule or structure that is composed of both positive and negative charges, but has a neutral net charge.

References

1. Vishnuprasad, C.N. and C.P. Unnikannan, *Bioprospecting Traditional Medicine*, in *Bioresources and Bioprocess in Biotechnology: Volume 1: Status and Strategies for Exploration*, S. Abdulhameed, N.S. Pradeep, and S. Sugathan, Editors. 2017, Springer Singapore: Singapore. p. 375-395.
2. Strobel, G. and B. Daisy, *Bioprospecting for microbial endophytes and their natural products.* Microbiology and Molecular Biology Reviews (MMBR), 2003. **67**(4): p. 491-502.
3. Fleming, A., *On the Antibacterial Action of Cultures of a Penicillium, with Special Reference to their Use in the Isolation of B. influenzæ.* British Journal of Experimental Pathology, 1929. **10**(3): p. 226-236.
4. Wani, M.C., et al., *Plant antitumor agents. VI. Isolation and structure of taxol, a novel antileukemic and antitumor agent from Taxus brevifolia.* Journal of the American Chemical Society, 1971. **93**(9): p. 2325-2327.
5. Thrithamarassery Gangadharan, N., A.B. Venkatachalam, and S. Sugathan, *High-Throughput and In Silico Screening in Drug Discovery*, in *Bioresources and Bioprocess in Biotechnology: Volume 1: Status and Strategies for Exploration*, S. Abdulhameed, N.S. Pradeep, and S. Sugathan, Editors. 2017, Springer Singapore: Singapore. p. 247-273.
6. Agatonovic-Kustrin, S. and D. Morton, *Data Mining in Drug Discovery and Design*, in *Artificial Neural Network for Drug Design, Delivery and Disposition*, M. Puri, et al., Editors. 2016, Academic Press: Boston. p. 181-193.
7. Borris, R.P., *Bioprospecting: An Industrial Perspective*, in *Bioprospecting: Success, Potential and Constraints*, R. Paterson and N. Lima, Editors. 2017, Springer International Publishing: Cham. p. 1-14.
8. Davies, J. and D. Davies, *Origins and Evolution of Antibiotic Resistance.* Microbiology and Molecular Biology Reviews, 2010. **74**(3): p. 417-433.
9. Clarke, B.T., *The Natural History of Amphibian Skin Secretions, Their Normal Functioning and Potential Medical Applications.* Biological Reviews, 1997. **72**(3): p. 365-379.
10. Xu, X. and R. Lai, *The Chemistry and Biological Activities of Peptides from Amphibian Skin Secretions.* Chemical Reviews, 2015. **115**(4): p. 1760-1846.
11. Koo, M.S., et al. *Visualizing AmphibiaWeb Data with Continuous Cartograms*. 2013. Retrieved June 23, 2019, from https://amphibiaweb.org/amphibian/cartograms/.
12. Duellman, W.E., L. Trueb, and C.M. Bogert, *Biology of Amphibians*. 1986: McGraw Hill.
13. Gomes, A., et al., *Bioactive molecules from amphibian skin: Their biological activities with reference to therapeutic potentials for possible drug development*. Vol. 45. 2007. 579-93.
14. Conlon, J.M., et al., *Potential therapeutic applications of multifunctional host-defense peptides from frog skin as anti-cancer, anti-viral, immunomodulatory, and anti-diabetic agents.* Peptides, 2014. **57**: p. 67-77.
15. Demori, I., et al., *Peptides for Skin Protection and Healing in Amphibians.* Molecules (Basel, Switzerland), 2019. **24**(2): p. 347.
16. Giovannini, M.G., et al., *Biosynthesis and degradation of peptides derived from Xenopus laevis prohormones.* Biochemical Journal, 1987. **243**(1): p. 113-120.
17. Zasloff, M., *Magainins, a class of antimicrobial peptides from Xenopus skin: isolation, characterization of two active forms, and partial cDNA sequence of a precursor.* Proceedings of the National Academy of Sciences, 1987. **84**(15): p. 5449-5453.
18. Bocchinfuso, G., et al., *Different mechanisms of action of antimicrobial peptides: insights from fluorescence spectroscopy experiments and molecular dynamics simulations.* Journal of Peptide Science, 2009. **15**(9): p. 550-558.

19. Almeida, P.F. and A. Pokorny, *Mechanisms of Antimicrobial, Cytolytic, and Cell-Penetrating Peptides: From Kinetics to Thermodynamics.* Biochemistry, 2009. **48**(34): p. 8083-8093.

20. Segrest, J.P., et al., *Amphipathic helix motif: Classes and properties.* Proteins: Structure, Function, and Bioinformatics, 1990. **8**(2): p. 103-117.

21. Oren, Z., J. Hong, and Y. Shai, *A comparative study on the structure and function of a cytolytic α-helical peptide and its antimicrobial β-sheet diastereomer.* European Journal of Biochemistry, 1999. **259**(1-2): p. 360-369.

22. Jiri, P., et al., *Antimicrobial Peptides: Amphibian Host Defense Peptides.* Current Medicinal Chemistry, 2018. **25**: p. 1-21.

23. Bessalle, R., et al., *Augmentation of the antibacterial activity of magainin by positive-charge chain extension.* Antimicrobial Agents and Chemotherapy, 1992. **36**(2): p. 313-317.

24. Sitaram, N., et al., *Change of glutamic acid to lysine in a 13-residue antibacterial and hemolytic peptide results in enhanced antibacterial activity without increase in hemolytic activity.* Antimicrobial Agents and Chemotherapy, 1992. **36**(11): p. 2468-2472.

25. Andreu, D., et al., *N-Terminal analogs of cecropin A: synthesis, antibacterial activity, and conformational properties.* Biochemistry, 1985. **24**(7): p. 1683-1688.

26. Chen, H.-C., et al., *Synthetic magainin analogues with improved antimicrobial activity.* FEBS Letters, 1988. **236**(2): p. 462-466.

27. Tyler, M.J., D.J.M. Stone, and J.H. Bowie, *A novel method for the release and collection of dermal, glandular secretions from the skin of frogs.* Journal of Pharmacological and Toxicological Methods, 1992. **28**(4): p. 199-200.

28. König, E., O.R.P. Bininda-Emonds, and C. Shaw, *The diversity and evolution of anuran skin peptides.* Peptides, 2015. **63**: p. 96-117.

29. Chen, T., et al., *Elements of the granular gland peptidome and transcriptome persist in air-dried skin of the South American orange-legged leaf frog, Phyllomedusa hypocondrialis.* Peptides, 2006. **27**(9): p. 2129-2136.

30. Nakajima, T., *Active peptides in amphibian skin.* Trends in Pharmacological Sciences, 1981. **2**(C): p. 202-205.

31. Gibson, B.W., et al., *Novel peptide fragments originating from PGLa and the caerulein and xenopsin percursors from Xenopus laevis.* Journal of Biological Chemistry, 1986. **261**(12): p. 5341-5349.

32. Gibson, B.W., et al., *Bombinin-like peptides with antimicrobial activity from skin secretions of the Asian toad, Bombina orientalis.* Journal of Biological Chemistry, 1991. **266**(34): p. 23103-23111.

33. Michl, H., *Isolation and structure of an hemolytic polypeptide from the defensive secretion of European Bombina species*. Vol. 101. 1970. 182-189.

34. Mor, A., et al., *Isolation, amino acid sequence and synthesis of dermaseptin, a novel antimicrobial peptide of amphibian skin.* Biochemistry, 1991. **30**(36): p. 8824-8830.

35. Morikawa, N., K.i. Hagiwara, and T. Nakajima, *Brevinin-1 and -2, unique antimicrobial peptides from the skin of the frog, Rana brevipoda porsa.* Biochemical and Biophysical Research Communications, 1992. **189**(1): p. 184-190.

36. Goraya, J., F.C. Knoop, and J.M. Conlon, *Ranatuerins: Antimicrobial Peptides Isolated from the Skin of the American Bullfrog,Rana catesbeiana.* Biochemical and Biophysical Research Communications, 1998. **250**(3): p. 589-592.

37. Simmaco, M., et al., *Novel antimicrobial peptides from skin secretion of the European frog Rana esculenta.* FEBS Letters, 1993. **324**(2): p. 159-161.

38. Yasin, B., et al., *Evaluation of the Inactivation of Infectious Herpes Simplex Virus by Host-Defense Peptides*. Vol. 19. 2000. 187-94.

39. VanCompernolle, S.E., et al., *Antimicrobial peptides from amphibian skin potently inhibit human immunodeficiency virus infection and transfer of virus from dendritic cells to T cells.* Journal of virology, 2005. **79**(18): p. 11598-11606.

40. Waugh, R.J., et al., *Peptides from australian frogs. Structures of the caeridins from Litoria caerulea.* Journal of the Chemical Society, Perkin Transactions 1, 1993(5): p. 573-576.

41. Stone, D.J.M., et al., *Peptides From Australian Frogs - The Structures of the Caerins From Litoria Caerulea.* Journal of Chemical Research-S, 1993(4): p. 138-138.

42. Steinborner, S.T., et al., *New antibiotic caerin 1 peptides from the skin secretion of the Australian tree frog Litoria chloris. Comparison of the activities of the caerin 1 peptides from the genus Litoria.* The Journal of Peptide Research, 1998. **51**(2): p. 121-126.

43. Rozek, T., et al., *The Maculatin peptides from the skin glands of the tree frog Litoria genimaculata: a comparison of the structures and antibacterial activities of Maculatin 1.1 and Caerin 1.1.* Journal of Peptide Science, 1998. **4**(2): p. 111-115.

44. Holthausen, D.J., et al., *An Amphibian Host Defense Peptide Is Virucidal for Human H1 Hemagglutinin-Bearing Influenza Viruses.* Immunity, 2017. **46**(4): p. 587-595.

45. Ohsaki, Y., et al., *Antitumor Activity of Magainin Analogues against Human Lung Cancer Cell Lines.* Cancer Research, 1992. **52**(13): p. 3534-3538.

46. Lehmann, J., et al., *Antitumor Activity of the Antimicrobial Peptide Magainin II against Bladder Cancer Cell Lines.* European Urology, 2006. **50**(1): p. 141-147.

47. van Zoggel, H., et al., *Antitumor and angiostatic peptides from frog skin secretions.* Amino Acids, 2012. **42**(1): p. 385-395.

48. Shi, D., et al., *Two Novel Dermaseptin-Like Antimicrobial Peptides with Anticancer Activities from the Skin Secretion of Pachymedusa dacnicolor.* Toxins, 2016. **8**(5): p. 144.

49. Libério, M.S., et al., *Anti-proliferative and cytotoxic activity of pentadactylin isolated from Leptodactylus labyrinthicus on melanoma cells.* Amino Acids, 2011. **40**(1): p. 51-59.

50. Michael Conlon, J., et al., *Design of Potent, Non-Toxic Antimicrobial Agents Based Upon the Naturally Occurring Frog Skin Peptides, Ascaphin-8 and Peptide XT-7.* Chemical Biology & Drug Design, 2008. **72**(1): p. 58-64.

51. Edelstein, M.C., et al., *Studies on the in vitro spermicidal activity of synthetic magainins.* Fertility and Sterility, 1991. **55**(3): p. 647-649.

52. Reddy, K.V.R., S.K. Shahani, and P.K. Meherji, *Spermicidal activity of Magainins: in vitro and in vivo studies.* Contraception, 1996. **53**(4): p. 205-210.

53. Reddy, V.R.K. and D.D. Manjramkar, *Evaluation of the antifertility effect of magainin-A in rabbits: in vitro and in vivo studies.* Fertility and Sterility, 2000. **73**(2): p. 353-358.

54. Zairi, A., et al., *Spermicidal activity of dermaseptins.* Contraception, 2005. **72**(6): p. 447-453.

55. Zairi, A., et al., *In vitro spermicidal activity of peptides from amphibian skin: Dermaseptin S4 and derivatives.* Bioorganic & Medicinal Chemistry, 2008. **16**(1): p. 266-275.

56. Mor, A., et al., *Natural and synthetic dermaseptins: in vitro large spectrum antimicrobial peptides.* Journal de mycologie médicale, 1993. **3**(3): p. 137-143.

57. Conlon, J.M., et al., *A family of antimicrobial and immunomodulatory peptides related to the frenatins from skin secretions of the Orinoco lime frog Sphaenorhynchus lacteus (Hylidae).* Peptides, 2014. **56**: p. 132-140.

58. Ojo, O.O., et al., *Tigerinin-1R: a potent, non-toxic insulin-releasing peptide isolated from the skin of the Asian frog, Hoplobatrachus rugulosus.* Diabetes, Obesity and Metabolism, 2011. **13**(12): p. 1114-1122.

59. Pantic, J.M., et al., *Effects of tigerinin peptides on cytokine production by mouse peritoneal macrophages and spleen cells and by human peripheral blood mononuclear cells.* Biochimie, 2014. **101**: p. 83-92.

60. Conlon, J.M., et al., *Purification of peptides with differential cytolytic activities from the skin secretions of the Central American frog, Lithobates vaillanti (Ranidae).* Comparative Biochemistry and Physiology Part C: Toxicology & Pharmacology, 2009. **150**(2): p. 150-154.

61. Mechkarska, M., et al., *Peptidomic analysis of skin secretions demonstrates that the allopatric populations of Xenopus muelleri (Pipidae) are not conspecific.* Peptides, 2011. **32**(7): p. 1502-1508.

62. Conlon, J.M., et al., *A glycine-leucine-rich peptide structurally related to the plasticins from skin secretions of the frog Leptodactylus laticeps (Leptodactylidae).* Peptides, 2009. **30**(5): p. 888-892.

63. Scorciapino, M.A., et al., *Conformational Analysis of the Frog Skin Peptide, Plasticin-L1, and Its Effects on Production of Proinflammatory Cytokines by Macrophages.* Biochemistry, 2013. **52**(41): p. 7231-7241.

64. Mo, G.-X., et al., *A Novel Insulinotropic Peptide from the Skin Secretions of Amolops loloensis Frog.* Natural products and bioprospecting, 2014. **4**(5): p. 309-313.

65. Mechkarska, M., et al., *The hymenochirins: A family of host-defense peptides from the Congo dwarf clawed frog Hymenochirus boettgeri (Pipidae).* Peptides, 2012. **35**(2): p. 269-275.

66. Owolabi, B.O., et al., *In vitro and in vivo insulinotropic properties of the multifunctional frog skin peptide hymenochirin-1B: a structure–activity study.* Amino Acids, 2016. **48**(2): p. 535-547.

67. Marenah, L., et al., *Skin secretions of Rana saharica frogs reveal antimicrobial peptides esculentins-1 and -1B and brevinins-1E and -2EC with novel insulin releasing activity.* **188**(1): p. 1-9.

68. Nascimento, A., et al., *Ocellatins: New Antimicrobial Peptides from the Skin Secretion of the South American Frog Leptodactylus ocellatus (Anura: Leptodactylidae)*. Vol. 23. 2004. 501-8.

69. Rollins-Smith, L.A., et al., *An antimicrobial peptide from the skin secretions of the mountain chicken frog Leptodactylus fallax (Anura:Leptodactylidae).* Regulatory Peptides, 2005. **124**(1): p. 173-178.

70. King, J.D., et al., *Pentadactylin: An antimicrobial peptide from the skin secretions of the South American bullfrog Leptodactylus pentadactylus.* Comparative Biochemistry and Physiology Part C: Toxicology & Pharmacology, 2005. **141**(4): p. 393-397.

71. Conlon, J.M., et al., *Purification and Properties of Laticeptin, an Antimicrobial Peptide from Skin Secretions of the South American Frog Leptodactylus laticeps.* Protein & Peptide Letters, 2006. **13**(4): p. 411-415.

72. Dourado, F.S., et al., *Antimicrobial peptide from the skin secretion of the frog Leptodactylus syphax.* Toxicon, 2007. **50**(4): p. 572-580.

73. Giangaspero, A., L. Sandri, and A. Tossi, *Amphipathic α helical antimicrobial peptides: A systematic study of the effects of structural and physical properties on biological activity.* European Journal of Biochemistry, 2001. **268**(21): p. 5589–5600.

74. Conlon, J.M., *A proposed nomenclature for antimicrobial peptides from frogs of the genus Leptodactylus.* Peptides, 2008. **29**(9): p. 1631-1632.

75. Nascimento, A., et al., *Purification, characterization and homology analysis of ocellatin 4, a cytolytic peptide from the skin secretion of the frog Leptodactylus ocellatus*. Vol. 50. 2008. 1095-104.

76. King, J.D., et al., *Purification and characterization of antimicrobial peptides from the Caribbean frog, Leptodactylus validus (Anura: Leptodactylidae).* Peptides, 2008. **29**(8): p. 1287-1292.

77. Leite Jr, J.M.A., et al., *Leptodactylus ocellatus (Amphibia): mechanism of defense in the skin and molecular phylogenetic relationships.* Journal of Experimental Zoology Part A: Ecological Genetics and Physiology, 2010. **313A**(1): p. 1-8.

78. Abdel-Wahab, Y.H.A., et al., *A peptide of the phylloseptin family from the skin of the frog Hylomantis lemur (Phyllomedusinae) with potent in vitro and in vivo insulin-releasing activity.* Peptides, 2008. **29**(12): p. 2136-2143.

79. Olson, L., et al., *Pseudin-2: An Antimicrobial Peptide with Low Hemolytic Activity from the Skin of the Paradoxical Frog.* Biochemical and Biophysical Research Communications, 2001. **288**(4): p. 1001-1005.

80. Abdel-Wahab Yasser, H.A., et al., *Insulin-releasing properties of the frog skin peptide pseudin-2 and its [Lys18]-substituted analogue*, in *Biological Chemistry*. 2008. p. 143.

81. Conlon, J.M., S. Patterson, and P.R. Flatt, *Major contributions of comparative endocrinology to the development and exploitation of the incretin concept.* Journal of Experimental Zoology Part A: Comparative Experimental Biology, 2006. **305A**(9): p. 781-786.

82. Nascimento, A., et al., *Purification, characterization and homology analysis of ocellatin 4, a cytolytic peptide from the skin secretion of the frog Leptodactylus ocellatus.* Toxicon, 2007. **50**(8): p. 1095-1104.

83. Marani, M.M., et al., *Characterization and Biological Activities of Ocellatin Peptides from the Skin Secretion of the Frog Leptodactylus pustulatus.* Journal of Natural Products, 2015. **78**(7): p. 1495-1504.

84. Cardozo-Filho, J.L., et al. *Identification of peptides from Amazonian Leptodactylus knudseni skin secretion by MALDI TOF/TOF.* Retrieved July 04, 2019, from https://www.uniprot.org/uniprot/P86711.

85. Gusmão, K.A.G., et al., *Ocellatin peptides from the skin secretion of the South American frog Leptodactylus labyrinthicus (Leptodactylidae): characterization, antimicrobial activities and membrane interactions.* Journal of Venomous Animals and Toxins including Tropical Diseases, 2017. **23**.

86. Tan, L.T.-H., et al., *Targeting Membrane Lipid a Potential Cancer Cure?* Frontiers in pharmacology, 2017. **8**: p. 12-12.

87. Zwaal, R.F.A., P. Comfurius, and E.M. Bevers, *Surface exposure of phosphatidylserine in pathological cells.* Cellular and Molecular Life Sciences CMLS, 2005. **62**(9): p. 971-988.

88. Gillies, R.J., et al., *MRI of the tumor microenvironment.* Journal of Magnetic Resonance Imaging, 2002. **16**(4): p. 430-450.

89. Gallagher, F.A., et al., *Magnetic resonance imaging of pH in vivo using hyperpolarized 13C-labelled bicarbonate.* Nature, 2008. **453**: p. 940.

90. Chiche, J., M.C. Brahimi-Horn, and J. Pouysségur, *Tumour hypoxia induces a metabolic shift causing acidosis: a common feature in cancer.* Journal of Cellular and Molecular Medicine, 2010. **14**(4): p. 771-794.

91. Conlon, J.M., *Structural diversity and species distribution of host-defense peptides in frog skin secretions.* Cellular and Molecular Life Sciences, 2011. **68**(13): p. 2303-2315.

92. Bessa, L.J., et al., *Synergistic and antibiofilm properties of ocellatin peptides against multidrug-resistant Pseudomonas aeruginosa.* Future Microbiology, 2018. **13**(2): p. 151-163.

93. Georgiadou, S.P., K.P. Makaritsis, and G.N. Dalekos, *Leishmaniasis revisited: Current aspects on epidemiology, diagnosis and treatment.* Journal of translational internal medicine, 2015. **3**(2): p. 43-50.

94. Kevric, I., M.A. Cappel, and J.H. Keeling, *New World and Old World Leishmania Infections: A Practical Review.* Dermatologic Clinics, 2015. **33**(3): p. 579-593.

95. WHO. *Leishmaniasis*. 2019. Retrieved July 28, 2019, from https://www.who.int/news-room/fact-sheets/detail/leishmaniasis.

96. Burza, S., S.L. Croft, and M. Boelaert, *Leishmaniasis.* The Lancet, 2018. **392**(10151): p. 951-970.

97. WHO. *Neglected tropical diseases*. Retrieved July 29, 2019, from https://www.who.int/neglected_diseases/diseases/en/.

98. WHO. *Leishmaniasis - Epidemiological Situation*. Retrieved July 28, 2019, from https://www.who.int/leishmaniasis/burden/en/.

99. Sutherst, R.W., *Global Change and Human Vulnerability to Vector-Borne Diseases.* Clinical Microbiology Reviews, 2004. **17**(1): p. 136-173.

100. Dey, A. and S. Singh, *Transfusion transmitted leishmaniasis: A case report and review of literature.* Indian Journal of Medical Microbiology, 2006. **24**(3): p. 165-170.

101. Basset, D., et al., *Visceral leishmaniasis in organ transplant recipients: 11 new cases and a review of the literature.* Microbes and Infection, 2005. **7**(13): p. 1370-1375.

102. Antinori, S., et al., *Leishmaniasis among organ transplant recipients.* The Lancet Infectious Diseases, 2008. **8**(3): p. 191-199.

103. Alvar, J., et al., *Leishmania and human immunodeficiency virus coinfection: the first 10 years.* Clinical Microbiology Reviews, 1997. **10**(2): p. 298-319.

104. Herwaldt, B.L., *Laboratory-Acquired Parasitic Infections from Accidental Exposures.* Clinical Microbiology Reviews, 2001. **14**(4): p. 659-688.

105. Meinecke, C.K., et al., *Congenital Transmission of Visceral Leishmaniasis (Kala Azar) From an Asymptomatic Mother to Her Child.* Pediatrics, 1999. **104**(5): p. e65-e65.

106. Akilov, O.E., A. Khachemoune, and T. Hasan, *Clinical manifestations and classification of Old World cutaneous leishmaniasis.* International Journal of Dermatology, 2007. **46**(2): p. 132-142.

107. Schwartz, E., C. Hatz, and J. Blum, *New world cutaneous leishmaniasis in travellers.* The Lancet Infectious Diseases, 2006. **6**(6): p. 342-349.

108. Bogdan, C., *Leishmaniasis in rheumatology, haematology and oncology: epidemiological, immunological and clinical aspects and caveats.* Annals of the Rheumatic Diseases, 2012. **71**(Suppl 2): p. i60-i66.

109. Torres-Guerrero, E., et al., *Leishmaniasis: a review.* F1000Research, 2017. **6**: p. 750-750.

110. Alemayehu, B. and M. Alemayehu, *Leishmaniasis: A Review on Parasite, Vector and Reservoir Host.* Health Science Journal, 2017. **11**.

111. Bi, K., et al., *Current Visceral Leishmaniasis Research: A Research Review to Inspire Future Study.* BioMed Research International, 2018. **2018**: p. 13.

112. Takken, W.A.K., Constantianus J.M., *Ecology of parasite-vector interactions*. Ecology of parasite-vector interactions.

113. Michel, G., et al., *Importance of worldwide asymptomatic carriers of Leishmania infantum (L. chagasi) in human.* Acta Tropica, 2011. **119**(2): p. 69-75.

114. van Griensven, J., et al., *Leishmaniasis in immunosuppressed individuals.* Clinical Microbiology and Infection, 2014. **20**(4): p. 286-299.

115. Alvar, J., et al., *The Relationship between Leishmaniasis and AIDS: the Second 10 Years.* Clinical Microbiology Reviews, 2008. **21**(2): p. 334-359.

116. Andreani, G., et al., *Mechanisms of interaction between protozoan parasites and HIV.* Current opinion in HIV and AIDS, 2012. **7**: p. 276-82.

117. WHO. *Guidelines for diagnosis, treatment and prevention of visceral leishmaniasis in South Sudan*. Retrieved July 29, 2019, from https://www.who.int/leishmaniasis/burden/Guidelines_for_diagnosis_treatment_and_prevention_of_VL_in_South_Sudan.pdf?ua=1.

118. Sunyoto, T., J. Potet, and M. Boelaert, *Why miltefosine - a life-saving drug for leishmaniasis - is unavailable to people who need it the most.* BMJ global health, 2018. **3**(3): p. e000709-e000709.

119. den Boer, M. and R.N. Davidson, *Treatment options for visceral leishmaniasis.* Expert Review of Anti-infective Therapy, 2006. **4**(2): p. 187-197.

120. Sundar, S., et al., *Failure of Pentavalent Antimony in Visceral Leishmaniasis in India: Report from the Center of the Indian Epidemic.* Clinical Infectious Diseases, 2000. **31**(4): p. 1104-1107.

121. Rijal, S., et al., *Treatment of visceral leishmaniasis in south-eastern Nepal: decreasing efficacy of sodium stibogluconate and need for a policy to limit further decline.* Transactions of The Royal Society of Tropical Medicine and Hygiene, 2003. **97**(3): p. 350-354.

122. Sundar, S., *Drug resistance in Indian visceral leishmaniasis.* Tropical Medicine & International Health, 2001. **6**(11): p. 849-854.

123. Sindermann, H. and J. Engel, *Development of miltefosine as an oral treatment for leishmaniasis.* Transactions of The Royal Society of Tropical Medicine and Hygiene, 2006. **100**(Supplement_1): p. S17-S20.

124. Bhattacharya, S.K., et al., *Phase 4 Trial of Miltefosine for the Treatment of Indian Visceral Leishmaniasis.* The Journal of Infectious Diseases, 2007. **196**(4): p. 591-598.

125. Dorlo, T.P.C., et al., *Optimal Dosing of Miltefosine in Children and Adults with Visceral Leishmaniasis.* Antimicrobial Agents and Chemotherapy, 2012. **56**(7): p. 3864-3872.

126. Seaman, J., et al., *Epidemic Visceral Leishmaniasis in Sudan: A Randomized Trial of Aminosidine plus Sodium Stibogluconate versus Sodium Stibogluconate Alone.* The Journal of Infectious Diseases, 1993. **168**(3): p. 715-720.

127. Thakur, C.P., et al., *A prospective randomized, comparative, open-label trial of the safety and efficacy of paromomycin (aminosidine) plus sodium stibogluconate versus sodium stibogluconate alone for the treatment of visceral leishmaniasis.* Transactions of the Royal Society of Tropical Medicine and Hygiene, 2000. **94**(4): p. 429-431.

128. Chunge, C.N., et al., *Treatment of visceral leishmaniasis in Kenya by aminosidine alone or combined with sodium stibogluconate.* Transactions of The Royal Society of Tropical Medicine and Hygiene, 1990. **84**(2): p. 221-225.

129. Thomaidou, E., et al., *Lymphatic Dissemination in Cutaneous Leishmaniasis Following Local Treatment.* The American journal of tropical medicine and hygiene, 2015. **93**(4): p. 770-773.

130. Hofstraat, K. and W.H. van Brakel, *Social stigma towards neglected tropical diseases: a systematic review.* International Health, 2016. **8**(suppl_1): p. i53-i70.

131. David, C.V. and N. Craft, *Cutaneous and mucocutaneous leishmaniasis.* Dermatologic Therapy, 2009. **22**(6): p. 491-502.

132. Aronson, N., et al., *Diagnosis and Treatment of Leishmaniasis: Clinical Practice Guidelines by the Infectious Diseases Society of America (IDSA) and the American Society of Tropical Medicine and Hygiene (ASTMH).* The American journal of tropical medicine and hygiene, 2017. **96**(1): p. 24-45.

133. Asilian, A., et al., *Comparative study of the efficacy of combined cryotherapy and intralesional meglumine antimoniate (Glucantime®) vs. cryotherapy and intralesional meglumine antimoniate (Glucantime®) alone for the treatment of cutaneous leishmaniasis.* International Journal of Dermatology, 2004. **43**(4): p. 281-283.

134. Salmanpour, R., M.R. Razmavar, and N. Abtahi, *Comparison of intralesional meglumine antimoniate, cryotherapy and their combination in the treatment of cutaneous leishmaniasis.* International Journal of Dermatology, 2006. **45**(9): p. 1115-1116.

135. El Darouti, M.A. and S.M. Al Rubaie, *Cutaneous Leishmaniasis.* International Journal of Dermatology, 1990. **29**(1): p. 56-59.

136. Heras-Mosteiro, J., et al., *Interventions for Old World cutaneous leishmaniasis.* Cochrane Database of Systematic Reviews, 2017(11).

137. Mosimann, V., et al., *Miltefosine for Mucosal and Complicated Cutaneous Old World Leishmaniasis: A Case Series and Review of the Literature.* Open forum infectious diseases, 2016. **3**(1): p. ofw008-ofw008.

138. Solomon, M., et al., *Liposomal amphotericin B in comparison to sodium stibogluconate for Leishmania braziliensis cutaneous leishmaniasis in travelers.* Journal of the American Academy of Dermatology, 2013. **68**(2): p. 284-289.

139. Wortmann, G., et al., *Lipsosomal amphotericin B for treatment of cutaneous leishmaniasis.* The American journal of tropical medicine and hygiene, 2010. **83**(5): p. 1028-1033.

140. Solomon, M., et al., *Liposomal amphotericin B treatment of cutaneous leishmaniasis due to Leishmania tropica.* Journal of the European Academy of Dermatology and Venereology, 2011. **25**(8): p. 973-977.

141. Ghorbani, M. and R. Farhoudi, *Leishmaniasis in humans: drug or vaccine therapy?* Drug design, development and therapy, 2017. **12**: p. 25-40.

142. Bern, C., et al., *Factors associated with visceral leishmaniasis in Nepal: Bed-net use is strongly protective.* The American journal of tropical medicine and hygiene, 2000. **63**: p. 184-8.

143. Campbell-Lendrum, D., et al., *Domestic and peridomestic transmission of American cutaneous leishmaniasis: changing epidemiological patterns present new control opportunities.* Memórias do Instituto Oswaldo Cruz, 2001. **96**: p. 159-162.

144. Grech, V., et al., *Visceral leishmaniasis in Malta—an 18 year paediatric, population based study.* Archives of Disease in Childhood, 2000. **82**(5): p. 381-385.

145. Cobb, S.L. and P.W. Denny, *Antimicrobial peptides for leishmaniasis.* Current Opinion in Investigational Drugs (London, England: 2000), 2010. **11**: p. 868-75.

146. Rivas, L., J.R. Luque-Ortega, and D. Andreu, *Amphibian antimicrobial peptides and Protozoa: Lessons from parasites.* Biochimica et Biophysica Acta (BBA) - Biomembranes, 2009. **1788**(8): p. 1570-1581.

147. Oliveira, M., et al., *Ocellatin-PT antimicrobial peptides: High-resolution microscopy studies in antileishmania models and interactions with mimetic membrane systems.* Biopolymers, 2016. **105**(12): p. 873-886.

148. Bernard, C., *Leçons sur les phénomènes de la vie communs aux animaux et aux végétaux: cours de physiologie générale du Museum d'histoire naturelle*. 1879: Billière.

149. Cannon, W.B., *Organization for Physiological Homeostasis.* Physiological Reviews, 1929. **9**(3): p. 399-431.

150. Kotas, Maya E. and R. Medzhitov, *Homeostasis, Inflammation, and Disease Susceptibility.* Cell, 2015. **160**(5): p. 816-827.

151. Chovatiya, R. and R. Medzhitov, *Stress, inflammation, and defense of homeostasis.* Molecular cell, 2014. **54**(2): p. 281-288.

152. Medzhitov, R., *Inflammation 2010: New Adventures of an Old Flame.* Cell, 2010. **140**(6): p. 771-776.

153. R, P. and J. I., *Chronic Inflammation. In: StatPearls [Internet]*. 2019, Treasure Island (FL): StatPearls Publishing.

154. Amor, S., et al., *Inflammation in neurodegenerative diseases.* Immunology, 2010. **129**(2): p. 154-169.

155. Verkhratsky, A., et al., *Neurological diseases as primary gliopathies: a reassessment of neurocentrism.* ASN neuro, 2012. **4**(3): p. e00082.

156. Ransom, B., T. Behar, and M. Nedergaard, *New roles for astrocytes (stars at last).* Trends in Neurosciences, 2003. **26**(10): p. 520-522.

157. ElAli, A. and S. Rivest, *Microglia in Alzheimer's disease: A multifaceted relationship.* Brain, Behavior, and Immunity, 2016. **55**: p. 138-150.

158. Ginhoux, F., et al., *Fate Mapping Analysis Reveals That Adult Microglia Derive from Primitive Macrophages.* Science, 2010. **330**(6005): p. 841-845.

159. Ginhoux, F. and M. Guilliams, *Tissue-Resident Macrophage Ontogeny and Homeostasis.* Immunity, 2016. **44**(3): p. 439-449.

160. Li, Q. and B.A. Barres, *Microglia and macrophages in brain homeostasis and disease.* Nature Reviews Immunology, 2017. **18**: p. 225.

161. Kierdorf, K., et al., *Microglia emerge from erythromyeloid precursors via Pu.1- and Irf8-dependent pathways.* Nature Neuroscience, 2013. **16**: p. 273.

162. Schafer, D.P. and B. Stevens, *Microglia Function in Central Nervous System Development and Plasticity.* Cold Spring Harbor Perspectives in Biology, 2015. **7**(10).

163. Kettenmann, H., F. Kirchhoff, and A. Verkhratsky, *Microglia: New Roles for the Synaptic Stripper.* Neuron, 2013. **77**(1): p. 10-18.

164. Fetler, L. and S. Amigorena, *Brain Under Surveillance: The Microglia Patrol.* Science, 2005. **309**(5733): p. 392-393.

165. Neumann, H., M.R. Kotter, and R.J.M. Franklin, *Debris clearance by microglia: an essential link between degeneration and regeneration.* Brain, 2008. **132**(2): p. 288-295.

166. Nimmerjahn, A., F. Kirchhoff, and F. Helmchen, *Resting Microglial Cells Are Highly Dynamic Surveillants of Brain Parenchyma in Vivo.* Science, 2005. **308**(5726): p. 1314-1318.

167. Colton, C.A., *Heterogeneity of Microglial Activation in the Innate Immune Response in the Brain.* Journal of Neuroimmune Pharmacology, 2009. **4**(4): p. 399-418.

168. Burda, Joshua E. and Michael V. Sofroniew, *Reactive Gliosis and the Multicellular Response to CNS Damage and Disease.* Neuron, 2014. **81**(2): p. 229-248.

169. Voet, S., M. Prinz, and G. van Loo, *Microglia in Central Nervous System Inflammation and Multiple Sclerosis Pathology.* Trends in Molecular Medicine, 2019. **25**(2): p. 112-123.

170. Saijo, K. and C.K. Glass, *Microglial cell origin and phenotypes in health and disease.* Nature Reviews Immunology, 2011. **11**: p. 775.

171. Sarlus, H. and M.T. Heneka, *Microglia in Alzheimer's disease.* The Journal of Clinical Investigation, 2017. **127**(9): p. 3240-3249.

172. Clayton, K.A., A.A. Van Enoo, and T. Ikezu, *Alzheimer's Disease: The Role of Microglia in Brain Homeostasis and Proteopathy.* Frontiers in Neuroscience, 2017. **11**(680).

173. Cameron, B. and G.E. Landreth, *Inflammation, microglia, and Alzheimer's disease.* Neurobiology of Disease, 2010. **37**(3): p. 503-509.

174. Russo, M.V. and D.B. McGavern, *Immune Surveillance of the CNS following Infection and Injury.* Trends in Immunology, 2015. **36**(10): p. 637-650.

175. DiSabato, D.J., N. Quan, and J.P. Godbout, *Neuroinflammation: the devil is in the details.* Journal of Neurochemistry, 2016. **139**(S2): p. 136-153.

176. Oeckinghaus, A. and S. Ghosh, *The NF-kappaB family of transcription factors and its regulation.* Cold Spring Harbor perspectives in biology, 2009. **1**(4): p. a000034-a000034.

177. Davalos, D., et al., *ATP mediates rapid microglial response to local brain injury in vivo.* Nature Neuroscience, 2005. **8**(6): p. 752-758.

178. Skaper, S.D., et al., *An Inflammation-Centric View of Neurological Disease: Beyond the Neuron.* Frontiers in Cellular Neuroscience, 2018. **12**(72).

179. Balducci, C. and G. Forloni, *Novel targets in Alzheimer's disease: A special focus on microglia.* Pharmacological Research, 2018. **130**: p. 402-413.

180. Simon, E., J. Obst, and D. Gomez-Nicola, *The Evolving Dialogue of Microglia and Neurons in Alzheimer's Disease: Microglia as Necessary Transducers of Pathology.* Neuroscience, 2019. **405**: p. 24-34.

181. Zhang, Q.-S., et al., *Pathological α-synuclein exacerbates the progression of Parkinson's disease through microglial activation.* Toxicology Letters, 2017. **265**: p. 30-37.

182. Brites, D. and A. Fernandes, *Neuroinflammation and Depression: Microglia Activation, Extracellular Microvesicles and microRNA Dysregulation.* Frontiers in Cellular Neuroscience, 2015. **9**(476).

183. Yirmiya, R., N. Rimmerman, and R. Reshef, *Depression as a Microglial Disease.* Trends in Neurosciences, 2015. **38**(10): p. 637-658.

184. Kern, J.K., et al., *Relevance of Neuroinflammation and Encephalitis in Autism.* Frontiers in Cellular Neuroscience, 2016. **9**(519).

185. Morgan, J.T., et al., *Microglial Activation and Increased Microglial Density Observed in the Dorsolateral Prefrontal Cortex in Autism.* Biological Psychiatry, 2010. **68**(4): p. 368-376.

186. Vargas, D.L., et al., *Neuroglial activation and neuroinflammation in the brain of patients with autism.* Annals of Neurology, 2005. **57**(1): p. 67-81.

187. Möller, T. and H.W.G.M. Boddeke, *Glial cells as drug targets: What does it take?* Glia, 2016. **64**(10): p. 1742-1754.

188. Popovic, S., et al., *Peptides with antimicrobial and anti-inflammatory activities that have therapeutic potential for treatment of acne vulgaris.* Peptides, 2012. **34**(2): p. 275-282.

189. AH, S. and S. J, *Acne Vulgaris. In: StatPearls [Internet].* Treasure Island (FL): StatPearls Publishing.

190. Mechkarska, M., et al., *An analog of the host-defense peptide hymenochirin-1B with potent broad-spectrum activity against multidrug-resistant bacteria and immunomodulatory properties.* Peptides, 2013. **50**: p. 153-159.

191. Cao, X., et al., *Cathelicidin-OA1, a novel antioxidant peptide identified from an amphibian, accelerates skin wound healing.* Scientific Reports, 2018. **8**(1): p. 943.

192. Barbosa, E.A., et al., *Structure and function of a novel antioxidant peptide from the skin of tropical frogs.* Free Radical Biology and Medicine, 2018. **115**: p. 68-79.

193. WHO. *Dementia - Key facts*. 2019. Retrieved August 12, 2019, from https://www.who.int/news-room/fact-sheets/detail/dementia.

194. Scholtes, F., G. Brook, and D. Martin, *Spinal cord injury and its treatment: current management and experimental perspective.* Advances and Technical Standards in Neurosurgery, 2012. **38**: p. 29-56.

195. Fields, G.B. and R.L. Noble, *Solid phase peptide synthesis utilizing 9-fluorenylmethoxycarbonyl amino acids.* International Journal of Peptide and Protein Research, 1990. **35**(3): p. 161-214.

196. Subirós-Funosas, R., et al., *Oxyma: An Efficient Additive for Peptide Synthesis to Replace the Benzotriazole-Based HOBt and HOAt with a Lower Risk of Explosion.* Chemistry – A European Journal, 2009. **15**(37): p. 9394-9403.

197. Chan, W. and P. White, *Fmoc Solid Phase Peptide Synthesis: A Practical Approach*. 2000: OUP Oxford.

198. Friedman, M., *Applications of the Ninhydrin Reaction for Analysis of Amino Acids, Peptides, and Proteins to Agricultural and Biomedical Sciences.* Journal of Agricultural and Food Chemistry, 2004. **52**(3): p. 385-406.

199. Kumar, S., et al., *MEGA X: Molecular Evolutionary Genetics Analysis across Computing Platforms.* Molecular Biology and Evolution, 2018. **35**(6): p. 1547-1549.

200. Lamiable, A., et al., *PEP-FOLD3: faster de novo structure prediction for linear peptides in solution and in complex.* Nucleic Acids Research, 2016. **44**(W1): p. W449-W454.

201. Schiffer, M. and A.B. Edmundson, *Use of helical wheels to represent the structures of proteins and to identify segments with helical potential.* Biophysical journal, 1967. **7**(2): p. 121-135.

202. Gautier, R., et al., *HELIQUEST: a web server to screen sequences with specific α-helical properties.* Bioinformatics, 2008. **24**(18): p. 2101-2102.

203. *PepCalc.com - Peptide Property Calculator*. Innovagen, from https://pepcalc.com/.

204. Janabi, N., et al., *Establishment of human microglial cell lines after transfection of primary cultures of embryonic microglial cells with the SV40 large T antigen.* Neuroscience Letters, 1995. **195**(2): p. 105-108.

205. Dello Russo, C., et al., *The human microglial HMC3 cell line: where do we stand? A systematic literature review.* Journal of Neuroinflammation, 2018. **15**(1): p. 259.

206. Waypa, G., B., et al., *Increases in Mitochondrial Reactive Oxygen Species Trigger Hypoxia-Induced Calcium Responses in Pulmonary Artery Smooth Muscle Cells.* Circulation Research, 2006. **99**(9): p. 970-978.

207. Guzy, R.D., et al., *Mitochondrial complex III is required for hypoxia-induced ROS production and cellular oxygen sensing.* Cell Metabolism, 2005. **1**(6): p. 401-408.

208. Shcherbakova, D.M., et al., *Bright monomeric near-infrared fluorescent proteins as tags and biosensors for multiscale imaging.* Nature Communications, 2016. **7**: p. 12405.

209. Portugal, C.C., et al., *Caveolin-1–mediated internalization of the vitamin C transporter SVCT2 in microglia triggers an inflammatory phenotype.* Science Signaling, 2017. **10**(472): p. eaal2005.

210. Socodato, R., et al., *c-Src deactivation by the polyphenol 3-O-caffeoylquinic acid abrogates reactive oxygen species-mediated glutamate release from microglia and neuronal excitotoxicity.* Free Radical Biology and Medicine, 2015. **79**: p. 45-55.

211. Socodato, R., et al., *Dopamine promotes NMDA receptor hypofunction in the retina through D1 receptor-mediated Csk activation, Src inhibition and decrease of GluN2B phosphorylation.* Scientific Reports, 2017. **7**: p. 40912.

212. *ProteinProspector - Proteomics tools for mining sequence databases in conjunction with Mass Spectrometry experiments.* University of California, San Francisco, from http://prospector.ucsf.edu.

213. Pinkse, M., et al., *MS approaches to select peptides with post-translational modifications from amphibian defense secretions prior to full sequence elucidation.* EuPA Open Proteomics, 2014. **5**: p. 32-40.

214. Loo, J.A., H.R. Udseth, and R.D. Smith, *Peptide and protein analysis by electrospray ionization-mass spectrometry and capillary electrophoresis-mass spectrometry.* Analytical Biochemistry, 1989. **179**(2): p. 404-412.

215. Liu, H., et al., *The Prediction of Peptide Charge States for Electrospray Ionization in Mass Spectrometry.* Procedia Environmental Sciences, 2011. **8**: p. 483-491.

216. Behrendt, R., P. White, and J. Offer, *Advances in Fmoc solid-phase peptide synthesis.* Journal of Peptide Science, 2016. **22**(1): p. 4-27.

217. D'Hondt, M., et al., *Related impurities in peptide medicines.* Journal of Pharmaceutical and Biomedical Analysis, 2014. **101**: p. 2-30.

218. Mól, A., M. S. Castro, and W. Fontes, *NetWheels: A web application to create high quality peptide helical wheel and net projections*. 2018.

219. Venyaminov, S.Y., et al., *Circular Dichroic Analysis of Denatured Proteins: Inclusion of Denatured Proteins in the Reference Set.* Analytical Biochemistry, 1993. **214**(1): p. 17-24.

220. Greenfield, N.J., *Using circular dichroism spectra to estimate protein secondary structure.* Nature Protocols, 2006. **1**(6): p. 2876-2890.

221. Holzwarth, G. and P. Doty, *The Ultraviolet Circular Dichroism of Polypeptides.* Journal of the American Chemical Society, 1965. **87**(2): p. 218-228.

222. Silhavy, T.J., D. Kahne, and S. Walker, *The bacterial cell envelope.* Cold Spring Harbor Perspectives in Biology, 2010. **2**(5): p. a000414-a000414.

223. David, D.K. and W. Katie, *Bioactive Proteins and Peptides from Food Sources. Applications of Bioprocesses used in Isolation and Recovery.* Current Pharmaceutical Design, 2003. **9**(16): p. 1309-1323.

224. Rajapakse, N., et al., *Purification of a radical scavenging peptide from fermented mussel sauce and its antioxidant properties.* Food Research International, 2005. **38**(2): p. 175-182.

225. Girgih, A.T., et al., *Structural and functional characterization of hemp seed (Cannabis sativa L.) protein-derived antioxidant and antihypertensive peptides.* Journal of Functional Foods, 2014. **6**: p. 384-394.

226. Esfandi, R., M.E. Walters, and A. Tsopmo, *Antioxidant properties and potential mechanisms of hydrolyzed proteins and peptides from cereals.* Heliyon, 2019. **5**(4): p. e01538.

227. Mendis, E., et al., *Investigation of jumbo squid (Dosidicus gigas) skin gelatin peptides for their in vitro antioxidant effects.* Life Sciences, 2005. **77**(17): p. 2166-2178.

228. Chen, H.-M., et al., *Antioxidant Activity of Designed Peptides Based on the Antioxidative Peptide Isolated from Digests of a Soybean Protein.* Journal of Agricultural and Food Chemistry, 1996. **44**(9): p. 2619-2623.

229. Brand-Williams, W., M.E. Cuvelier, and C. Berset, *Use of a free radical method to evaluate antioxidant activity.* LWT - Food Science and Technology, 1995. **28**(1): p. 25-30.

230. Re, R., et al., *Antioxidant activity applying an improved ABTS radical cation decolorization assay.* Free Radical Biology and Medicine, 1999. **26**(9): p. 1231-1237.

231. Espinosa-Diez, C., et al., *Antioxidant responses and cellular adjustments to oxidative stress.* Redox biology, 2015. **6**: p. 183-197.

232. McGaw, L.J., E.E. Elgorashi, and J.N. Eloff, *8 - Cytotoxicity of African Medicinal Plants Against Normal Animal and Human Cells*, in *Toxicological Survey of African Medicinal Plants*, V. Kuete, Editor. 2014, Elsevier. p. 181-233.

233. Aslantürk, Ö.S., *In Vitro Cytotoxicity and Cell Viability Assays: Principles, Advantages, and Disadvantages*, in *Genotoxicity - A Predictable Risk to Our Actual World*. 2017, IntechOpen.

234. Rampersad, S.N., *Multiple applications of Alamar Blue as an indicator of metabolic function and cellular health in cell viability bioassays.* Sensors (Basel, Switzerland), 2012. **12**(9): p. 12347-12360.

235. O'Brien, J., et al., *Investigation of the Alamar Blue (resazurin) fluorescent dye for the assessment of mammalian cell cytotoxicity.* European Journal of Biochemistry, 2000. **267**(17): p. 5421-5426.

236. Riss, T.L., et al., *Cell Viability Assays*, in *Assay Guidance Manual [Internet]*. 2013, Bethesda (MD): Eli Lilly & Company and the National Center for Advancing Translational Sciences.

237. Korzeniewski, C. and D.M. Callewaert, *An enzyme-release assay for natural cytotoxicity.* Journal of Immunological Methods, 1983. **64**(3): p. 313-320.

238. Decker, T. and M.-L. Lohmann-Matthes, *A quick and simple method for the quantitation of lactate dehydrogenase release in measurements of cellular cytotoxicity and tumor necrosis factor (TNF) activity.* Journal of Immunological Methods, 1988. **115**(1): p. 61-69.

239. Riss, T.L. and R.A. Moravec, *Use of Multiple Assay Endpoints to Investigate the Effects of Incubation Time, Dose of Toxin, and Plating Density in Cell-Based Cytotoxicity Assays.* ASSAY and Drug Development Technologies, 2004. **2**(1): p. 51-62.

240. Stoddart, M.J., *Cell Viability Assays: Introduction*, in *Mammalian Cell Viability: Methods and Protocols*, M.J. Stoddart, Editor. 2011, Humana Press: Totowa, NJ. p. 1-6.

241. Patel, L.N., J.L. Zaro, and W.-C. Shen, *Cell Penetrating Peptides: Intracellular Pathways and Pharmaceutical Perspectives.* Pharmaceutical Research, 2007. **24**(11): p. 1977-1992.

242. Illien, F., et al., *Quantitative fluorescence spectroscopy and flow cytometry analyses of cell-penetrating peptides internalization pathways: optimization, pitfalls, comparison with mass spectrometry quantification.* Scientific Reports, 2016. **6**: p. 36938.

243. Malanovic, N. and K. Lohner, *Antimicrobial Peptides Targeting Gram-Positive Bacteria.* Pharmaceuticals, 2016. **9**(3): p. 59.

244. Strandberg, E., et al., *Influence of C-terminal amidation on the antimicrobial and hemolytic activities of cationic-helical peptides.* Pure Appl. Chem, 2007. **79**: p. 717-728.

245. Dennison, S.R. and D.A. Phoenix, *Influence of C-Terminal Amidation on the Efficacy of Modelin-5.* Biochemistry, 2011. **50**(9): p. 1514-1523.

246. Sarah, R.D., H.G.M. Leslie, and A.P. David, *Effect of Amidation on the Antimicrobial Peptide Aurein 2.5 from Australian Southern Bell Frogs.* Protein & Peptide Letters, 2012. **19**(6): p. 586-591.

247. Mura, M., et al., *The effect of amidation on the behaviour of antimicrobial peptides.* European biophysics journal : EBJ, 2016. **45**(3): p. 195-207.

248. Bouazizi-Ben Messaoud, H., et al., *Changes in Lipid and Fatty Acid Composition During Intramacrophagic Transformation of Leishmania donovani Complex Promastigotes into Amastigotes.* Lipids, 2017. **52**(5): p. 433-441.

249. McConville, M.J. and J.M. Blackwell, *Developmental changes in the glycosylated phosphatidylinositols of Leishmania donovani. Characterization of the promastigote and amastigote glycolipids.* Journal of Biological Chemistry, 1991. **266**(23): p. 15170-15179.

250. Pimenta, P.F.P., E.M.B. Saraiva, and D.L. Sacks, *The comparative fine structure and surface glycoconjugate expression of three life stages of Leishmania major.* Experimental Parasitology, 1991. **72**(2): p. 191-204.

251. Zhang, K. and S.M. Beverley, *Phospholipid and sphingolipid metabolism in Leishmania.* Molecular and Biochemical Parasitology, 2010. **170**(2): p. 55-64.

252. Akhoundi, M., et al., *A Historical Overview of the Classification, Evolution, and Dispersion of Leishmania Parasites and Sandflies.* PLoS neglected tropical diseases, 2016. **10**(3): p. e0004349-e0004349.

253. Muskus, C., et al., *Carbohydrate and LPG Expression in Leishmania viannia Subgenus.* The Journal of Parasitology, 1997. **83**(4): p. 671-678.

254. Soares, R.P.P., et al., *Leishmania braziliensis: a novel mechanism in the lipophosphoglycan regulation during metacyclogenesis.* International Journal for Parasitology, 2005. **35**(3): p. 245-253.

255. Yoneyama, K.A.G., et al., *Characterization of Leishmania (Viannia) braziliensis membrane microdomains, and their role in macrophage infectivity.* Journal of Lipid Research, 2006. **47**(10): p. 2171-2178.

256. Mullarky, E. and L.C. Cantley. *Diverting Glycolysis to Combat Oxidative Stress*. 2015. Tokyo: Springer Japan.

257. Sampson, T.R., et al., *Rapid Killing of Acinetobacter baumannii by Polymyxins Is Mediated by a Hydroxyl Radical Death Pathway.* Antimicrobial Agents and Chemotherapy, 2012. **56**(11): p. 5642-5649.

258. Cole, A.M., P. Weis, and G. Diamond, *Isolation and Characterization of Pleurocidin, an Antimicrobial Peptide in the Skin Secretions of Winter Flounder.* Journal of Biological Chemistry, 1997. **272**(18): p. 12008-12013.

259. Cho, J. and D.G. Lee, *Oxidative stress by antimicrobial peptide pleurocidin triggers apoptosis in Candida albicans.* Biochimie, 2011. **93**(10): p. 1873-1879.

260. Lang, T., et al., *Bioluminescent Leishmania expressing luciferase for rapid and high throughput screening of drugs acting on amastigote-harbouring macrophages and for quantitative real-time monitoring of parasitism features in living mice.* Cellular Microbiology, 2005. **7**(3): p. 383-392.

261. Shai, Y., *Mode of action of membrane active antimicrobial peptides.* Peptide Science, 2002. **66**(4): p. 236-248.

262. Dathe, M. and T. Wieprecht, *Structural features of helical antimicrobial peptides: their potential to modulate activity on model membranes and biological cells.* Biochimica et Biophysica Acta (BBA) - Biomembranes, 1999. **1462**(1): p. 71-87.

263. Eaton, P. and P. West, *Atomic Force Microscopy*. 2010: OUP Oxford.

264. de Souza, W. and G.M. Rocha, *Atomic force microscopy: a tool to analyze the structural organization of pathogenic protozoa.* Trends in Parasitology, 2011. **27**(4): p. 160-167.

265. Eaton, P., et al., *Anti-leishmanial activity of the antimicrobial peptide DRS 01 observed in Leishmania infantum (syn. Leishmania chagasi) cells.* Nanomedicine: Nanotechnology, Biology and Medicine, 2014. **10**(2): p. 483-490.

266. Akaki, M., et al., *Invasive forms of Toxoplasma gondii , Leishmania amazonensis and Trypanosoma cruzi have a positive charge at their contact site with host cells.* Parasitology Research, 2001. **87**: p. 193-197.

267. Britta, E., et al., *Cell death and ultrastructural alterations in Leishmania amazonensis caused by new compound 4-Nitrobenzaldehyde thiosemicarbazone derived from S-limonene.* BMC microbiology, 2014. **14**: p. 236.

268. Frigault, M.M., et al., *Live-cell microscopy – tips and tools.* Journal of Cell Science, 2009. **122**(6): p. 753-767.

269. Chudakov, D.M., et al., *Fluorescent Proteins and Their Applications in Imaging Living Cells and Tissues.* Physiological Reviews, 2010. **90**(3): p. 1103-1163.

270. Piston, D.W. and G.-J. Kremers, *Fluorescent protein FRET: the good, the bad and the ugly.* Trends in Biochemical Sciences, 2007. **32**(9): p. 407-414.

271. Sekar, R.B. and A. Periasamy, *Fluorescence resonance energy transfer (FRET) microscopy imaging of live cell protein localizations.* The Journal of cell biology, 2003. **160**(5): p. 629-633.

272. Fearon, I.M. and S.P. Faux, *Oxidative stress and cardiovascular disease: Novel tools give (free) radical insight.* Journal of Molecular and Cellular Cardiology, 2009. **47**(3): p. 372-381.

273. Jakob, U. and D. Reichmann, *Oxidative Stress and Redox Regulation*. 2013: Springer Netherlands.

274. Salim, S., *Oxidative Stress and the Central Nervous System.* Journal of Pharmacology and Experimental Therapeutics, 2017. **360**(1): p. 201-205.

275. Viatour, P., et al., *Phosphorylation of NF-κB and IκB proteins: implications in cancer and inflammation.* Trends in Biochemical Sciences, 2005. **30**(1): p. 43-52.

276. Morgan, M.J. and Z.-g. Liu, *Crosstalk of reactive oxygen species and NF-κB signaling.* Cell research, 2011. **21**(1): p. 103-115.

277. Kawai, T. and S. Akira, *Signaling to NF-kB by Toll-like receptors.* Trends in Molecular Medicine, 2007. **13**(11): p. 460-469.

278. Kaminska, B., M. Mota, and M. Pizzi, *Signal transduction and epigenetic mechanisms in the control of microglia activation during neuroinflammation.* Biochimica et Biophysica Acta (BBA) - Molecular Basis of Disease, 2016. **1862**(3): p. 339-351.

279. Lushchak, V.I., *Glutathione Homeostasis and Functions: Potential Targets for Medical Interventions.* Journal of Amino Acids, 2012. **2012**: p. 26.

280. Wei, L., et al., *Structure and Function of a Potent Lipopolysaccharide-Binding Antimicrobial and Anti-inflammatory Peptide.* Journal of Medicinal Chemistry, 2013. **56**(9): p. 3546-3556.

281. Zhu, M., et al., *Differential Regulation of Resolution in Inflammation induced by Amyloid-β42 and Lipopolysaccharides in Human Microglia.* Journal of Alzheimer's disease : JAD, 2014. **43**.

282. Hjorth, E., et al., *Omega-3 Fatty Acids Enhance Phagocytosis of Alzheimer's Disease-Related Amyloid-β 42 by Human Microglia and Decrease Inflammatory Markers.* Journal of Alzheimer's Disease, 2013. **35**(4): p. 697-713.

283. Lindberg, C., et al., *Effects of statins on microglia.* Journal of Neuroscience Research, 2005. **82**(1): p. 10-19.

284. Lindberg, C., et al., *Cytokine production by a human microglial cell line: Effects of ß-amyloid and α-melanocyte-stimulating hormone.* Neurotoxicity Research, 2005. **8**(3): p. 267-276.

285. Moncada, S., R.M. Palmer, and E.A. Higgs, *Nitric oxide: physiology, pathophysiology, and pharmacology.* Pharmacological Reviews, 1991. **43**(2): p. 109-142.

286. Sun, J., et al., *Measurement of Nitric Oxide Production in Biological Systems by Using Griess Reaction Assay.* Sensors, 2003. **3**(8): p. 276-284.

287. Beckman, J.S. and W.H. Koppenol, *Nitric oxide, superoxide, and peroxynitrite: the good, the bad, and ugly.* American Journal of Physiology-Cell Physiology, 1996. **271**(5): p. C1424-C1437.

288. Yuste, J.E., et al., *Implications of glial nitric oxide in neurodegenerative diseases.* Frontiers in cellular neuroscience, 2015. **9**: p. 322-322.

289. Bryan, N.S. and M.B. Grisham, *Methods to detect nitric oxide and its metabolites in biological samples.* Free radical biology & medicine, 2007. **43**(5): p. 645-657.

290. Liu, T., et al., *NF-κB signaling in inflammation.* Signal transduction and targeted therapy, 2017. **2**: p. 17023.

291. Rajalakshmy, A.R., J. Malathi, and H.N. Madhavan, *Hepatitis C Virus NS3 Mediated Microglial Inflammation via TLR2/TLR6 MyD88/NF-κB Pathway and Toll Like Receptor Ligand Treatment Furnished Immune Tolerance.* PLOS ONE, 2015. **10**(5): p. e0125419.

292. Timmerman, R., S.M. Burm, and J.J. Bajramovic, *An Overview of in vitro Methods to Study Microglia.* Frontiers in Cellular Neuroscience, 2018. **12**: p. 242-242.

293. Das, A., et al., *Transcriptome sequencing reveals that LPS-triggered transcriptional responses in established microglia BV2 cell lines are poorly representative of primary microglia.* Journal of Neuroinflammation, 2016. **13**(1): p. 182.

294. Melief, J., et al., *Characterizing primary human microglia: A comparative study with myeloid subsets and culture models.* Glia, 2016. **64**(11): p. 1857-1868.

295. Feder, R., A. Dagan, and A. Mor, *Structure-Activity Relationship Study of Antimicrobial Dermaseptin S4 Showing the Consequences of Peptide Oligomerization on Selective Cytotoxicity.* Journal of Biological Chemistry, 2000. **275**(6): p. 4230-4238.

296. Chen, G.-f., et al., *Amyloid beta: structure, biology and structure-based therapeutic development.* Acta Pharmacologica Sinica, 2017. **38**(9): p. 1205-1235.

297. Stefanis, L., *α-Synuclein in Parkinson's disease.* Cold Spring Harbor perspectives in medicine, 2012. **2**(2): p. a009399-a009399.

298. *Cartogram Maps: Data Visualization with Exaggeration*. February 23, 2018 Retrieved September 8, 2019, from https://gisgeography.com/cartogram-maps/.

299. Akla, N., J. Pratt, and B. Annabi, *Concanavalin-A triggers inflammatory response through JAK/STAT3 signalling and modulates MT1-MMP regulation of COX-2 in mesenchymal stromal cells.* Experimental cell research, 2012. **318**: p. 2498-506.

300. *"Holocrine secretion"*. Medical Dictionary 2009. Retrieved September 8, 2019, from https://medical-dictionary.thefreedictionary.com/holocrine+secretion.

301. Creasy, D.M. and J.S. Cottrell, *Unimod: Protein modifications for mass spectrometry.* PROTEOMICS, 2004. **4**(6): p. 1534-1536.

302. Dubin, A.E. and A. Patapoutian, *Nociceptors: the sensors of the pain pathway.* The Journal of clinical investigation, 2010. **120**(11): p. 3760-3772.

303. *"Proboscis"*. Cambridge Dictionary, Retrieved September 8, 2019, from https://dictionary.cambridge.org/dictionary/english/proboscis.

304. McKeever, P.E., *Chapter 20 - Immunohistology of the Nervous System*, in *Diagnostic Immunohistochemistry (Third Edition)*, D.J. Dabbs, Editor. 2010, W.B. Saunders: Philadelphia. p. 820-889.

Appendices

Appendix A – RP-HPLC chromatograms of oPT4 and oPT9

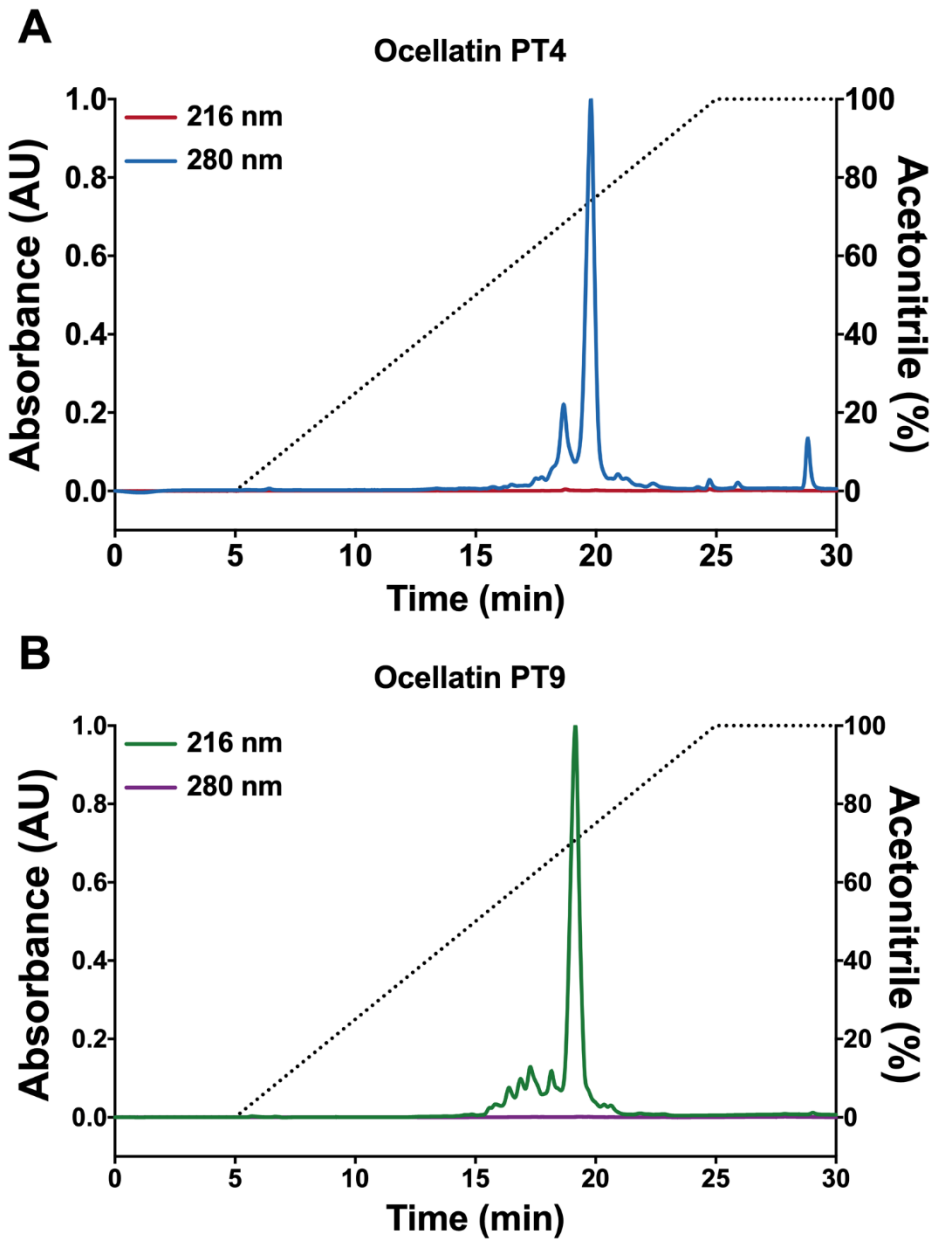

Appendix B – LC-MS and MS/MS data

Ocellatin-PT4

[-] **Parameters**

Distribution Type: **Peptide Sequence**
Sequence: **GVFDIIKGAGKQLIAHAMGKIAEKV-Amidated**
Parent Charge: **1**
Intensity: **1**
Profile Type: **Gaussian**
Resolution: **10000**

Elemental Composition: **C118 H202 N33 O30 S1**
Monoisotopic M/Z: **2593.50106**
Total Abundance: **100.00%**

Isotope Number	m/z	Percent Total	Percent Maximum
0	2593.50106	20.42	67.04
1	2594.50395	30.47	100.00
2	2595.50639	24.72	81.14
3	2596.50857	14.27	46.85
4	2597.51063	6.51	21.36
5	2598.51262	2.48	8.13
6	2599.51460	0.81	2.67
7	2600.51660	0.24	0.77
8	2601.51862	0.06	0.20
9	2602.52068	0.01	0.05
10	2603.52293	0.00	0.01
11	2604.52501	0.00	0.00
12	2605.52548	0.00	0.00

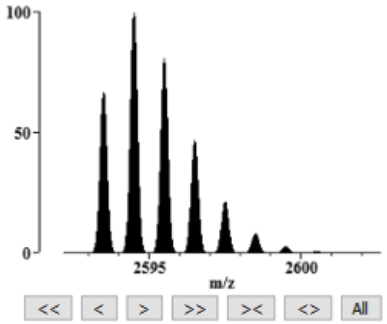

Ocellatin-PT9

[-] **Parameters**

Distribution Type: **Peptide Sequence**
Sequence: **GVVDLLQGAAKDLAGH**
Parent Charge: **1**
Intensity: **1**
Profile Type: **Gaussian**
Resolution: **10000**

Elemental Composition: **C68 H115 N20 O22**
Monoisotopic M/Z: **1563.84893**
Total Abundance: **100.00%**

Isotope Number	m/z	Percent Total	Percent Maximum
0	1563.84893	40.63	100.00
1	1564.85181	34.95	86.02
2	1565.85452	16.68	41.05
3	1566.85715	5.73	14.09
4	1567.85971	1.57	3.86
5	1568.86224	0.36	0.89
6	1569.86473	0.07	0.18
7	1570.86720	0.01	0.03
8	1571.86975	0.00	0.00
9	1572.87225	0.00	0.00

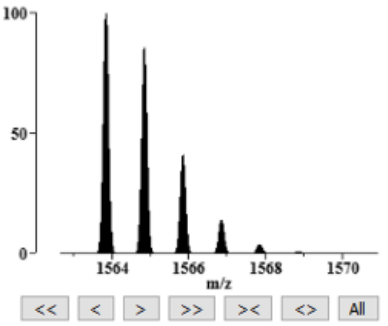

Figure B.1. – Theoretical predictions of oPT4 and oPT9 monoisotopic masses.

Ocellatin-PT4

[–] **Parameters**

Distribution Type: **Peptide Sequence**
Sequence: **GVFDIIKGAGKQLIAHAMGKIAEKV-Amidated**
Parent Charge: **3**
Intensity: **1**
Profile Type: **Gaussian**
Resolution: **10000**

Elemental Composition: **C118 H202 N33 O30 S1**
Monoisotopic M/Z: **865.17187**
Total Abundance: **100.00%**

Isotope Number	m/z	Percent Total	Percent Maximum
0	865.17187	20.42	67.04
1	865.50617	30.47	100.00
2	865.84031	24.72	81.14
3	866.17437	14.27	46.85
4	866.50839	6.51	21.36
5	866.84239	2.48	8.13
6	867.17639	0.81	2.67
7	867.51038	0.24	0.77
8	867.84439	0.06	0.20
9	868.17841	0.01	0.05
10	868.51249	0.00	0.01
11	868.84652	0.00	0.00
12	869.18001	0.00	0.00

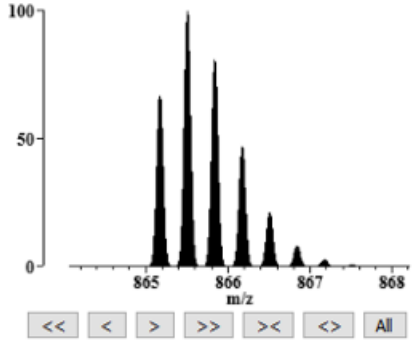

Ocellatin-PT9

[–] **Parameters**

Distribution Type: **Peptide Sequence**
Sequence: **GVVDLLQGAAKDLAGH**
Parent Charge: **3**
Intensity: **1**
Profile Type: **Gaussian**
Resolution: **10000**

Elemental Composition: **C68 H115 N20 O22**
Monoisotopic M/Z: **521.95449**
Total Abundance: **100.00%**

Isotope Number	m/z	Percent Total	Percent Maximum
0	521.95449	40.63	100.00
1	522.28879	34.95	86.02
2	522.62303	16.68	41.05
3	522.95723	5.73	14.09
4	523.29142	1.57	3.86
5	523.62560	0.36	0.89
6	523.95976	0.07	0.18
7	524.29392	0.01	0.03
8	524.62810	0.00	0.00
9	524.96227	0.00	0.00

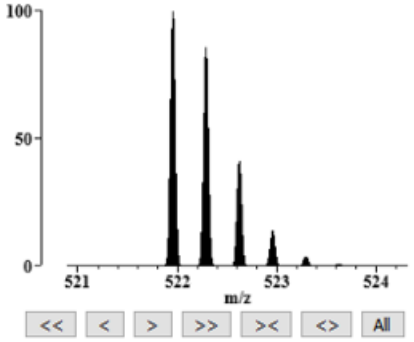

Figure B.2. – Theoretical predictions of oPT4 and oPT9 fragmentation (+3 charge).

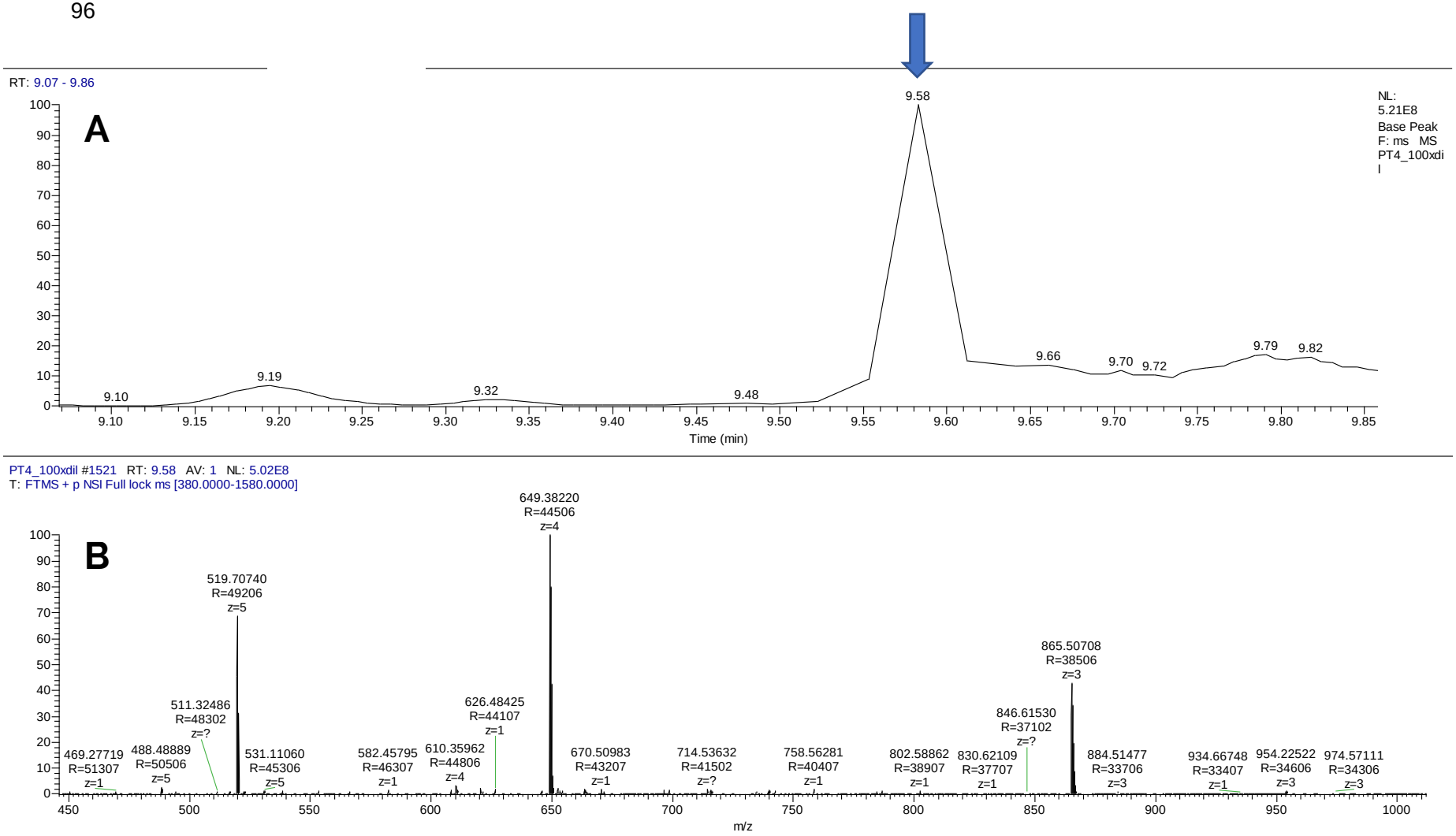

Figure B.3 – RP-HPLC chromatogram (**A**) and mass spectrum (**B**) of oPT4. The blue arrow indicates the fraction containing oPT4. The mass spectrum is referent to that fraction.

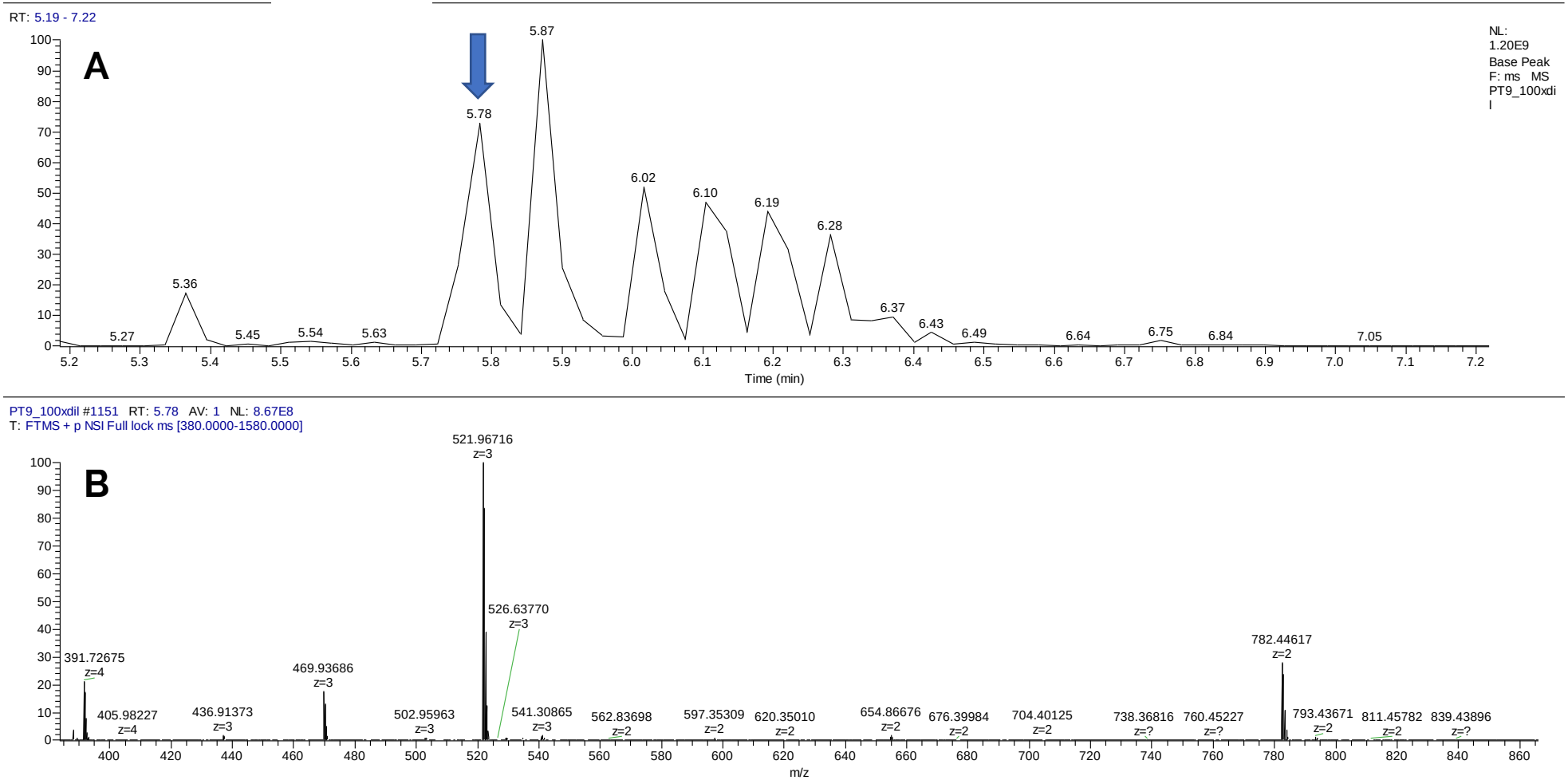

Figure B.4. – RP-HPLC chromatogram (**A**) and mass spectrum (**B**) of oPT9. The blue arrow indicates the fraction containing oPT9. The mass spectrum is referent to that fraction.

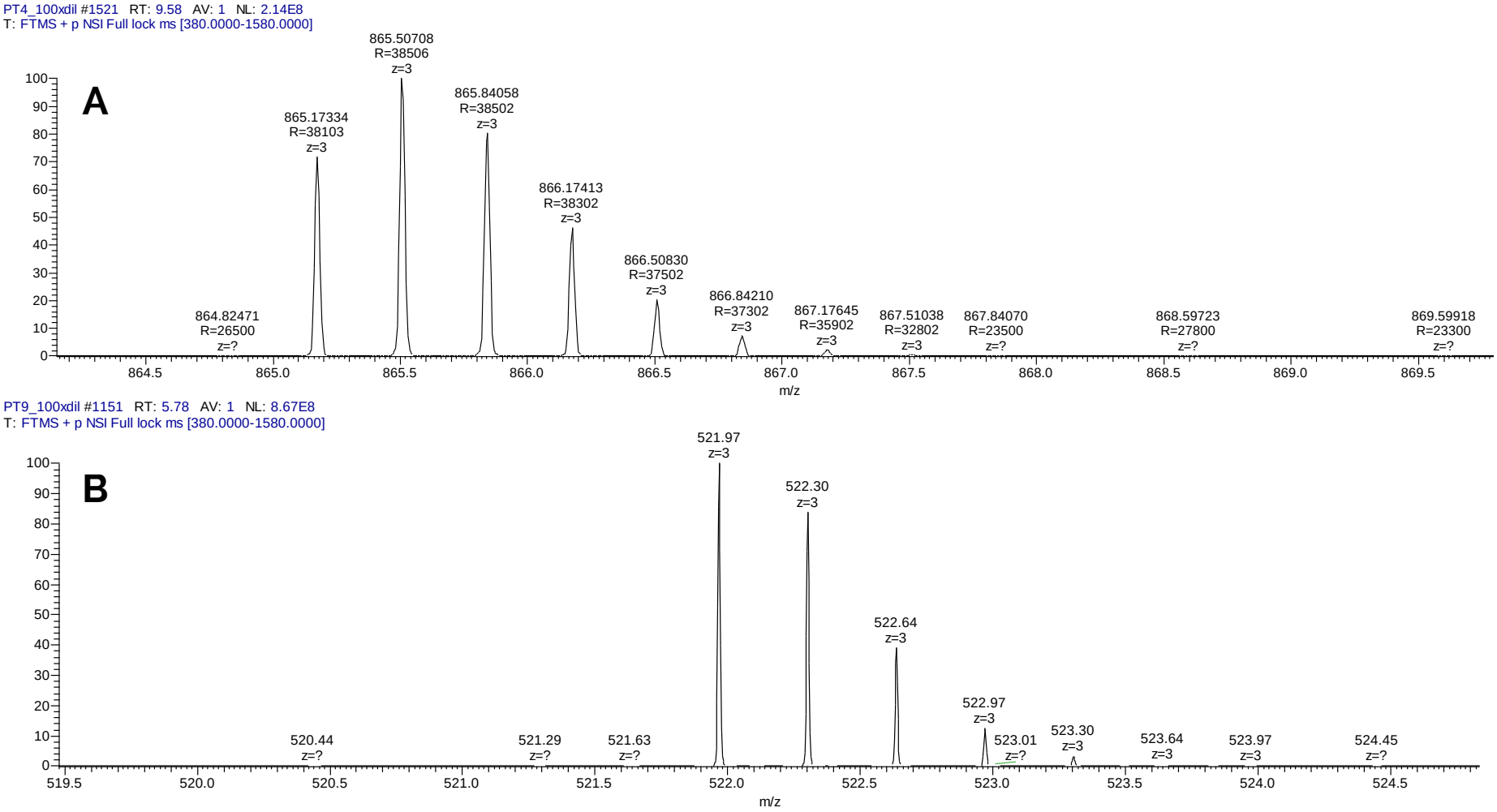

Figure B.5. – Fragmentation of oPT4 (**A**) and oPT9 (**B**) into ions with a +3 charge.

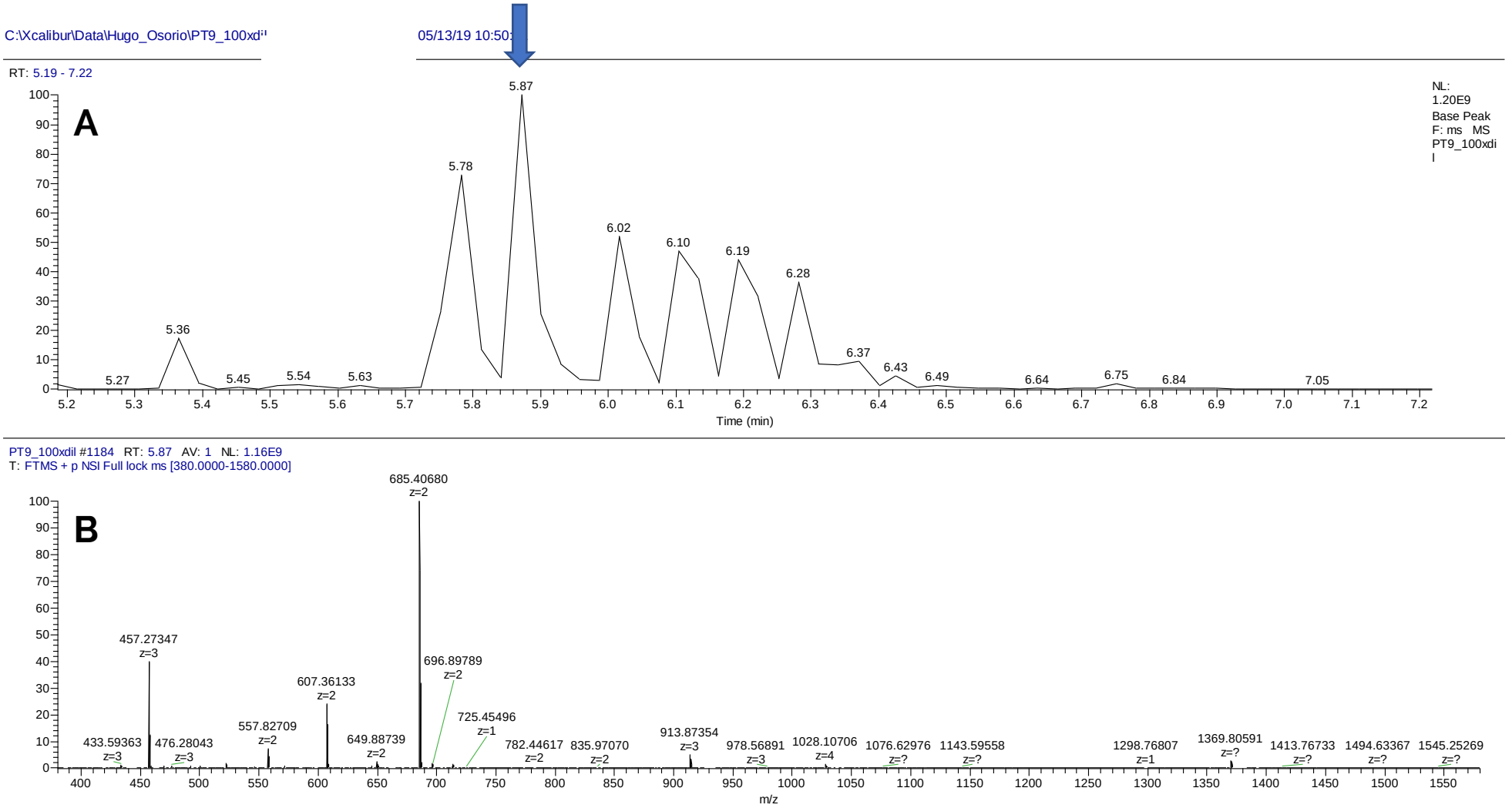

Figure B.6. – RP-HPLC chromatogram (**A**) and mass spectrum (**B**) of the fraction eluted at 5.87 min in oPT9 sample (blue arrow).

Peptide Summary

Sequence: GVFDIIKGAGKQLIAHAMGKIAEKV, V25-Amidated (-0.98402 Da)
Charge: +3, Monoisotopic m/z: 865.17114 Da (-0.73 mmu/-0.84 ppm), MH+: 2593.49887 Da, RT: 9.5523 min,
Identified with: Sequest HT (v1.17); XCorr:7.58, Ions matched by search engine: 0/0
Fragment match tolerance used for search: 0.02 Da

Fragment Matches

Value Type: Theo. Mass [Da]

Ion Series | Neutral Losses | Precursor Ions

#1	b^{+}	b^{2+}	b^{3+}	Seq.	y^{+}	y^{2+}	y^{3+}	#2
1	58.02874	29.51801	20.01443	G				25
2	157.09715	79.05222	53.03724	V	2536.47959	1268.74344	846.16472	24
3	304.16557	152.58642	102.06004	F	2437.41118	1219.20923	813.14191	23
4	419.19251	210.09989	140.40235	D	2290.34277	1145.67502	764.11911	22
5	532.27657	266.64193	178.09704	I	2175.31582	1088.16155	725.77679	21
6	645.36064	323.18396	215.79173	I	2062.23176	1031.61952	688.08210	20
7	773.45560	387.23144	258.49005	K	1949.14770	975.07749	650.38742	19
8	830.47707	415.74217	277.49721	G	1821.05273	911.03000	607.68910	18
9	901.51418	451.26073	301.17624	A	1764.03127	882.51927	588.68194	17
10	958.53564	479.77146	320.18340	G	1692.99416	847.00072	565.00290	16
11	1086.63061	543.81894	362.88172	K	1635.97269	818.48998	545.99575	15
12	1214.68918	607.84823	405.56791	Q	1507.87773	754.44250	503.29743	14
13	1327.77325	664.39026	443.26260	L	1379.81915	690.41321	460.61123	13
14	1440.85731	720.93229	480.95729	I	1266.73509	633.87118	422.91655	12
15	1511.89442	756.45085	504.63633	A	1153.65102	577.32915	385.22186	11
16	1648.95334	824.98031	550.32263	H	1082.61391	541.81059	361.54282	10
17	1719.99045	860.49886	574.00167	A	945.55500	473.28114	315.85652	9
18	1851.03094	926.01911	617.68183	M	874.51788	437.76258	292.17748	8
19	1908.05240	954.52984	636.68898	G	743.47740	372.24234	248.49732	7
20	2036.14736	1018.57732	679.38731	K	686.45594	343.73161	229.49016	6
21	2149.23143	1075.11935	717.08199	I	558.36097	279.68412	186.79184	5
22	2220.26854	1110.63791	740.76103	A	445.27691	223.14209	149.09715	4
23	2349.31113	1175.15920	783.77523	E	374.23980	187.62354	125.41812	3
24	2477.40610	1239.20669	826.47355	K	245.19720	123.10224	82.40392	2
25				V-Amidated	117.10224	59.05476	39.70560	1

Figure B.7. – oPT4 sequencing after MS/MS analysis.

Peptide Summary

Sequence: GVVDLLQGAAKDLAGH, Charge: +2, Monoisotopic m/z: 782.44653 Da (+18.44 mmu/+23.57 ppm), MH+: 1563.88579 Da, RT: 5.7635 min,
Identified with: Sequest HT (v1.17); XCorr:5.34,
Fragment match tolerance used for search: 0.2 Da
Fragments used for search: -H_2O; y; -NH_3; y; b; b; -H_2O; b; -NH_3; y

Fragment Matches

Value Type: Theo. Mass [Da]

Ion Series | Neutral Losses | Precursor Ions | Internal Fragments

#1	b^+	b^{2+}	Seq.	y^+	y^{2+}	#2
1	58.02874	29.51801	G			16
2	157.09715	79.05222	V	1506.82747	753.91737	15
3	256.16557	128.58642	V	1407.75905	704.38317	14
4	371.19251	186.09989	D	1308.69064	654.84896	13
5	484.27657	242.64193	L	1193.66370	597.33549	12
6	597.36064	299.18396	L	1080.57963	540.79345	11
7	725.41922	363.21325	Q	967.49557	484.25142	10
8	782.44068	391.72398	G	839.43699	420.22213	9
9	853.47779	427.24254	A	782.41553	391.71140	8
10	924.51491	462.76109	A	711.37841	356.19285	7
11	1052.60987	526.80857	K	640.34130	320.67429	6
12	1167.63681	584.32205	D	512.24634	256.62681	5
13	1280.72088	640.86408	L	397.21939	199.11334	4
14	1351.75799	676.38263	A	284.13533	142.57130	3
15	1408.77945	704.89337	G	213.09822	107.05275	2
16			H	156.07675	78.54201	1

Figure B.8. – oPT9 sequencing after MS/MS analysis.

Appendix C – CD data

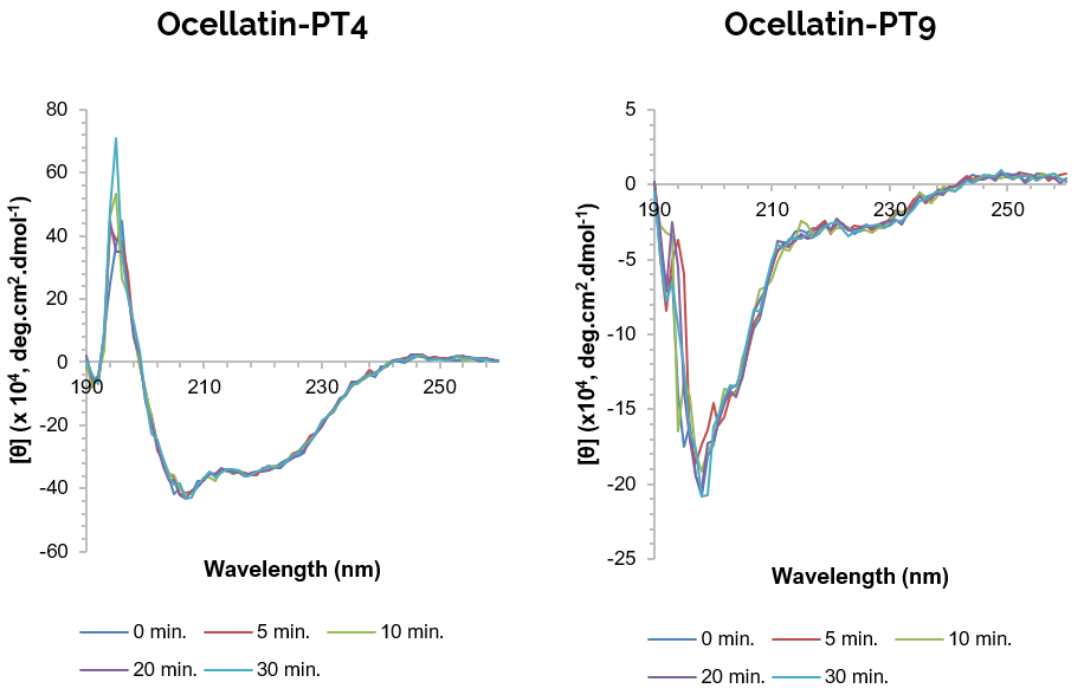

Figure C.1. – Circular dichroism time-course studies of oPT4 and oPT9 in the presence of LPS. Peptide concentration was 150 µg/mL. [θ] – molar ellipticity.

Appendix D – Antileishmanial activity assessment data

Initially, the antileishmanial assays were performed with a concentration range of 0-256 µg/mL. Because no major effects were observed in parasite cell viability for either of the peptides in any of these concentrations, we decided to perform additional assays with one extra concentration (512 µg/mL), explaining why the number of independent experiments is different between concentrations 4-256 and 512 µg/mL (Tables D.1. and D.2.). Furthermore, treatment of *L. infantum* parasites with oPT4 was only performed once, as a control of the sample, since these results had already been published by Oliveira *et al*. [147].

Table D.1. – Cell viability of *L. amazonensis* promastigotes treated with oPT4 and oPT9. SEM – standard error of the mean; N – number of independent experiments.

L. amazonensis

Peptide concentration (µg/mL)		**512**	**256**	**128**	**64**	**32**	**16**	**8**	**4**
oPT4	% Cell viability (mean)	39,9	88,2	111,7	103,2	104,0	106,7	102,9	102,5
	SEM	15,6	14,0	2,1	4,3	7,5	10,3	11,5	7,4
	N	2	3						
oPT9	% Cell viability (mean)	115,3	106,1	97,9	101,3	104,0	101,2	102,9	102,3
	SEM	-	7,7	4,0	5,9	11,0	1,0	0,9	2,4
	N	1	2						

Table D.2. – Cell viability of *L. infantum* promastigotes treated with oPT4 and oPT9. SD – standard deviation; SEM – standard error of the mean; N – number of independent experiments.

L. infantum

Peptide concentration (µg/mL)		**512**	**256**	**128**	**64**	**32**	**16**	**8**	**4**
oPT4	% Cell viability (mean)	8,7	6,3	19,2	67,0	123,3	136,6	136,4	149,8
	SD	0,4	0,9	0,9	1,1	2,7	2,1	3,8	18,4
	N	1							
oPT9	% Cell viability (mean)	146,9	122,6	120,1	108,0	119,7	117,0	121,6	120,2
	SEM	-	19,0	19,3	6,0	19,3	18,1	18,5	18,2
	N	1	2						

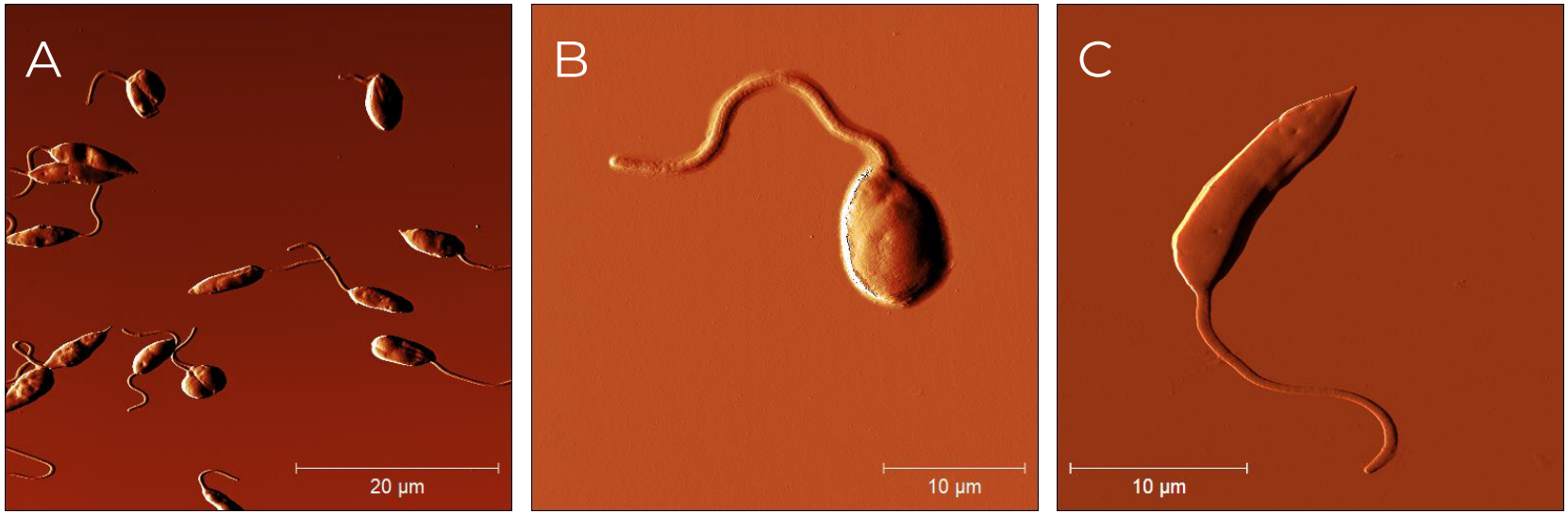

Fig. D.1. – AFM images of *L. amazonensis* promastigotes treated with 512 µg/mL of oPT4. **A)** Overview of oPT4-treated parasites. **B)** *L. amazonensis* promastigote with an altered, rounder cell-shape after oPT4 treatment. **C)** *L. amazonensis* promastigote with minor cavities on the cell body and an overall normal morphology after oPT4 treatment.

Appendix E – ELISA and Griess colorimetric assay calibration curves

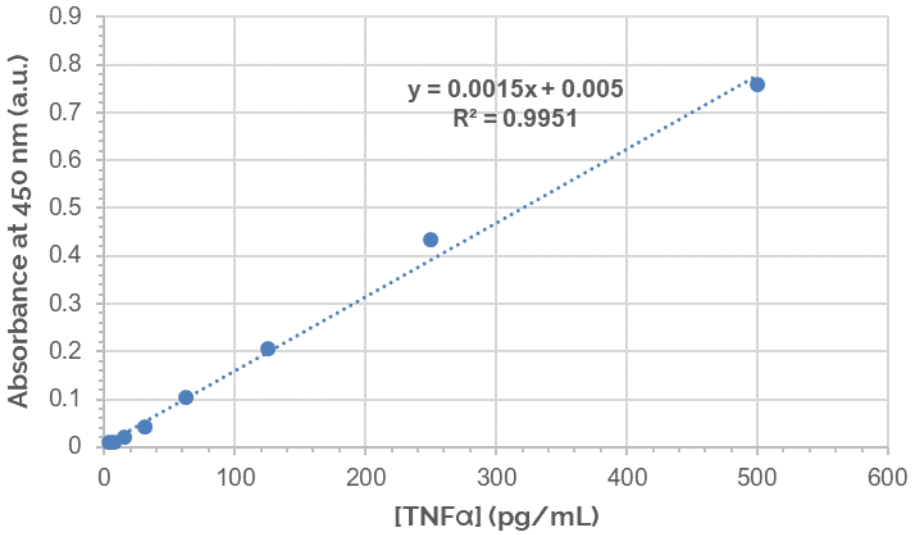

Fig. E.1. – TNFα calibration curve determined for the ELISA assay.

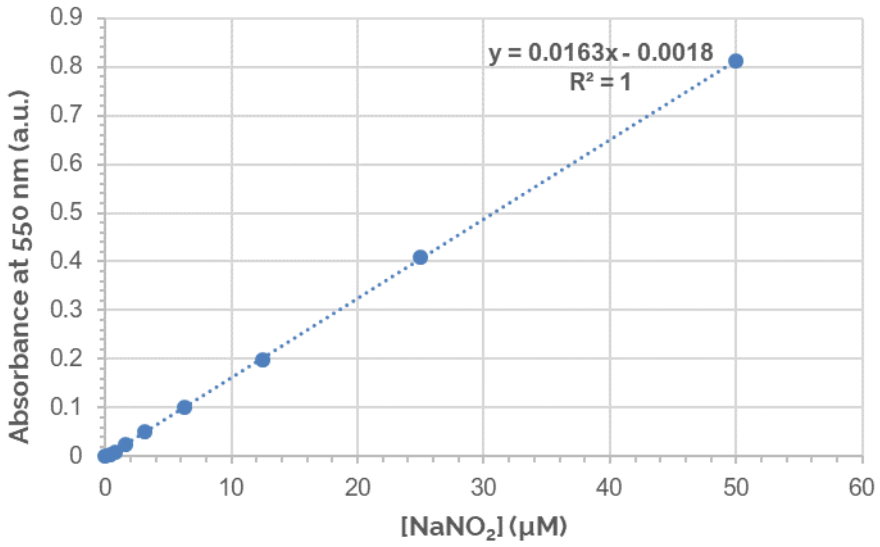

Fig. E.2. – $NaNO_2$ calibration curve determined for the Griess colorimetric assay.